2017

S-band Planar Antenna Designs for CubeSat Communications

Faisel Em Tubbal
University of Wollongong

S-band Planar Antenna Designs for CubeSat Communications

A thesis submitted in fulfilment of the requirements for the award of the degree

PhD

From

The University of Wollongong

By

Faisel Em M Tubbal
Masters of Engineering Management
Masters of Engineering (Telecommunication)
Bachelor of Electronic Engineering (Telecommunication)

SCHOOL OF ELECTRICAL, COMPUTER
AND TELECOMMUNICATIONS ENGINEERING
2017

In memory of my father and brother

Abstract

Cube satellites or CubeSats are attractive for use in space research and education programs. This is because of their low-cost, short development time, and ease of deployment. Moreover, CubeSats are able to communicate with each other, and assemble into swarms to carry out different functions such as wide area measurements and sensing. These capabilities require CubeSats to be equipped with an efficient, high gain, wideband and small antenna to facilitate communication links with each other and with ground stations. However, the limited real estate, power and communication opportunities of CubeSats pose real challenges to any antenna designs. Specifically, designs are required to meet the size and weight restrictions of CubeSats while yielding high gain and wide bandwidth. To date, CubeSats employ wrapped-up wire dipole antennas that require deployment after launch. However, this adds complexity and there is a risk they might not deploy, which increases the likelihood of mission failure. They also have low total gain and narrow bandwidth. One approach to avoid deployment failure is to use micro-strip patch or slot antennas. However, they have low gains and narrow bandwidth. Moreover, their performance on CubeSats is unknown.

This thesis, therefore, provides the first comprehensive study of existing planar antenna designs to determine their suitability for use on CubeSats. The study is focused on small size micro-strip patch and slot antennas that have the ability to achieve high gain, beam steering, and wide bandwidth. It shows that amongst all previous S-band planar antennas that are suitable for CubeSats, the best gain is only 5.96 dB and the smallest size is 38×38×3.2 mm^3 at 2.45 GHz. The qualitative comparison shows that only shorted patch, CPW-feed square slot and asymmetric E-shaped antennas have suitable designs for use on CubeSats. This is followed by a quantitative evaluation of their performance on a 2U CubeSat. The results show that only the performance of the CPW-feed square slot antenna is significantly affected by the 2U CubeSat body. In addition, all three designs are relatively small. However, their main limitation is that they do not operate at the desired CubeSat ISM operating

frequency of 2.4-2.5 GHz band. To this end, this thesis presents a repurposed shorted patch and CPW-fed square slot antennas that have operating frequency of 2.45 GHz. It also compares their performance in the presence of a CubeSat body. Although the repurposed shorted patch and CPW-fed square slot antennas have smaller size, they have low gains and bandwidths.

Henceforth, this thesis proposes a wideband S-band F-shaped patch antenna for a 3U CubeSat. The main idea is to use two arms of the upper patch with different lengths and feed them by a folded ramp-shaped patch to generate a second resonant frequency and hence broaden its bandwidth. The results show that the antenna achieves a wideband of 1121 MHz (1.606-2.727 GHz) and a high gain of 8.51 dB.

This thesis also presents a high gain coplanar waveguide (CPW)-fed slot antenna for use on 3U CubeSats. A key feature is the use of a Metasurface Superstrate Structure (MSS) to significantly improve gain and reduce back-lobe. This antenna has been evaluated comprehensively using the High Frequency Simulator Structure (HFSS) as well as on a 3U (10 x 10 x 30 cm^3) CubeSat platform. The results show that proposed antenna achieves a wide bandwidth of 730 MHz and a superior gain of 9.71 dB.

Finally, this thesis presents a low profile high gain CPW-fed slot antenna for CubeSats. The proposed antenna is backed with a low profile metallic reflector. The cavity reflector is utilized to significantly improve gain and reduce back lobe radiation. The antenna has a compact size of 36×36 mm^2, meaning it is compatible with any CubeSats standard structure. It occupies only 12.96% of a 1U CubeSat's surface and 6.48% of a 2U CubeSat's surface. The results show that the proposed antenna achieves a superior gain of 8.62 dB and a bandwidth of 109 MHz.

Statement of Originality

I, Faisel EM M Tubbal, declare that this thesis, submitted in partial fulfilment of the requirements for the award of Doctor of Philosophy, in the School of Electrical, Computer and Telecommunications Engineering, University of Wollongong, is wholly my own work unless otherwise referenced or acknowledged. The document has not been submitted for qualifications at any other academic institutions.

Signed

Faisel Em M Tubbal
16 March, 2017

Acknowledgements

This research has been conducted with the support of Ministry of Higher Education and Scientific Research in Libya and the Australian Government Research Training Program Scholarship.

I would like to express my deepest gratitude to my thesis supervisors: Dr Raad Raad and Associate Professor Kwan-Wu Chin. I am particularly thankful for their invaluable guidance, meticulous reviews and prompt feedbacks that have greatly enhanced the quality of my thesis. I thank them for their continuous, support, understanding, suggestions, and confidence in me. To both, their easy manner and sense of humour served to calm and motivate me when frustration and dismay had set in.

I am deeply indebted to my parents who nurtured me all the way long to the person I am today. I express my sincere respect and gratitude towards them.

Lastly, I would like to thank my wife and my kids for their patience, dedication and support, without your unwavering support I would never have made it

CONTENTS

1 Introduction 1

1.1 Satellite Communications 1

1.2 Pico satellites 2

1.3 Antennas for CubeSat Communications 8

1.4 Frequency Bands Allocation for CubeSats 10

1.5 Motivation 10

1.6 Thesis Aims and Contributions 11

1.7 Publications 12

1.8 Thesis Structure 13

2 Literature Review: Micro-strip patch and slot antennas 15

2.1 Micro-strip Patch and Slot Antennas 15

2.1.1 Micro-strip patch antennas 15

2.1.2 Slot antennas 28

2.2 Qualitative Evaluation 37

2.3 Summary 42

3 Micro-strip and Slot antennas for CubeSats 44

3.1 Quantitative Evaluation 44

3.1.1 CPW-feed square slot antenna [45] 44

3.1.2 Shorted patch antenna using folded-patch techniques [46] 45

3.1.3 Miniaturized asymmetric E-shaped micro-strip patch antenna with folded-patch feed [56] 45

3.2 Simulation Results 50

3.3 Comparison of All Three Designs 59

3.4 Conclusion 64

4 S-band planar antenna designs for cubesats 65

4.1 Evaluation and Improvements of Shorted Patch and CPW-fed Square Slot Antennas 65

4.1.1 New shorted patch antenna 65

4.1.2 New CPW-feed square slot antenna 67

4.1.3 Evaluation 68
4.2 Newly Designed Wideband High Gain F-shaped Patch Antenna 76
4.2.1 Antenna design and structure 77
4.2.2 Results and discussion 80
4.3 Conclusion 84
5 High Gain s-band CPW-fed slot antenna for CubeSats 86
5.1 Antenna Configuration 89
5.2 Results and Discussion 90
5.2.1 Parametric study 90
5.2.2 Experimental verification 101
5.3 Conclusion 106
6 A low profile high gain, CAVITY-backed cpw-fed slot antenna 107
6.1 Geometry of the Proposed Antenna 107
6.2 Analysis of the CPW-fed Slot Antenna 110
6.3 CPW-fed Slot Antenna array 116
6.4 Conclusion 117
7 Conclusions 118
Bibliography 121

LIST OF FIGURES

1.1. Satellite orbits: (a) geostationary, and (b) sun synchronous. 2
1.2. An example CubeSat (10cm×10cm×10cm) [9]..... 4
1.3. A poly-pico satellite orbital deployer [10]. 5
1.4. A swarm with seven small-sized 1U CubeSats. 7

2.1. A micro-strip patch antenna. 17
2.2. A rectangular slot antenna. 29

3.1. A CPW-feed square slot antenna: (a) installation on a 2U CubeSat face, and (b) geometry. 47
3.2. Geometry of a shorted patch antenna (a) with a CubeSat, and (b) without a CubeSat. 48
3.3. Geometry of an asymmetric E-shaped patch antenna (a) with a 2U CubeSat, and (b) without a 2U CubeSat. 49
3.4. Return losses (S_{11}) of a CPW-feed square slot antenna. 50
3.5. The axial ratio of the CPW-feed square slot antenna. 51
3.6. 2D gain of a CPW-feed square slot antenna. 52
3.7. 3D gain of a CPW-feed square slot antenna at 3.2 GHz: (a) without, and (b) with a CubeSat. 52
3.8. Return loss (S_{11}) of the tested shorted patch antenna. 53
3.9. The axial ratio of the shorted patch antenna. 54
3.10. 2D gain of tested shorted patch antenna. 55
3.11. 3D gain of the tested shorted patch antenna at 4.3 GHz: (a) without, and (b) with CubeSat. 55
3.12. Return losses (S_{11}) of the asymmetric E-shaped patch antenna. 56
3.13. The axial ratio of the tested asymmetric E-shaped patch antenna. 57
3.14. 2D gain of asymmetric E-shaped patch antenna. 58
3.15. 3D gains of asymmetric E-shaped patch antenna at 4.75 GHz: (a) without, and (b) with a CubeSat. 58
3.16. Return losses of the shorted patch, asymmetric E-shaped patch and CPW-feed square slot antennas on a 2U CubeSat body. 60

3.17. The axial ratio of the shorted patch, asymmetric E-shaped patch and CPW-feed square slot antennas on a 2U CubeSat body. 61

3.18. A comparison of gain of the tested shorted patch, asymmetric E-shaped patch and CPW-feed square slot antennas on a 2U CubeSat body..... 62

3.19. Simulated radiation patterns of an (a) E-shaped patch, (b) CPW-feed square slot, and (c) shorted patch antennas. 62

4.1. Geometry of the shorted patch antenna in [46]. 66

4.2. Geometry of CPW-feed square slot antenna in [45]. 68

4.3. Geometry of shorted patch antenna on a 2U CubeSat body..... 69

4.4. Geometry of CPW-feed square slot antenna on a 2U CubeSat body. 70

4.5. The simulated return loss of shorted patch and CPW-feed square slot antennas with and without a CubeSat. 70

4.6. The simulated 2D gain of shorted patch and CPW-feed slot antenna with and without a CubeSat body. 71

4.7. Simulated return losses of re-dimensioned shorted patch and CPW-fed slot antennas on 2U CubeSat. 72

4.8. The simulated 2D gain of the modified shorted patch and CPW-feed slot antenna. 73

4.9. Geometry of the re-dimensioned CPW-feed square slot antenna without F-shaped slits. 74

4.10. Total 3D gain of the re-dimensioned CPW-feed square slot antenna without F-shaped slits. 75

4.11. Simulated return loss against frequency for the various L_t values. 76

4.12. Configuration of the wideband F-shaped patch antenna. (a) a 3D view of the proposed antenna in HFSS on a 3U CubeSat, (b) top view, and (c) side view. 79

4.13. Simulated return loss against frequency for various L_1 values. 80

4.14. Simulated return loss against frequency for various W_2 values. 81

4.15. 3D gain at 2.45 GHz. 82

4.16. Simulated radiation pattern of the proposed F-shaped patch antenna at 2.45 GHz. 83

4.17. Input impedance of the proposed F-shaped patch antenna..... 84

5.1. Configuration of the proposed CPW-fed slot antenna with a MSS (a) the proposed CPW-fed slot antenna, (b) MSS, (c) a cross section view, and (d) the model in HFSS. 90

5.2. Simulated return loss against frequency for various (a) W_n, and (b) L_t values. 93

5.3. Simulated return loss against frequency for various values of L_n. 94

5.4. The effect of the starting edge of the MSS position on (a) the reflecting coefficient S_{11}, and (b) antenna gain. 95

5.5. The influence of MSS element sets over the return loss (S_{11}) of the proposed antenna. 96

5.6. The MSS height, i.e., h_a, as a function of (a) the return loss and (b) VSWR of the proposed antenna. 97

5.7. The total gain of the proposed CPW-fed slot antenna (a) without MSS, and (b) with the MSS. 98

5.8. A CPW-fed slot antenna on a 3U CubeSat. 99

5.9. Simulated results of proposed antenna on the CubeSat's body (a) return loss and (b) total gain at 2.45 GHz. 100

5.10. Simulated radiation pattern of the proposed antenna on a CubeSat's body at 2.45 GHz. 101

5.11. A photograph of the fabricated prototype CPW-fed slot antenna: (a) geometry, and (b) its installation on a 3U CubeSat model face. 102

5.12. Simulated and measured return losses (S_{11}) of the proposed antenna. 104

5.13. Simulated and measured input impedance of the proposed antenna. 104

5.14. Simulated and measured radiation pattern of the proposed antenna on a CubeSat's body at 2.45 GHz (inset: Antenna under measurement). 105

5.15. Simulated (continuous line) and measured (dashed line) gain of the proposed antenna with CubeSat……..……106

6.1. Configuration of the CPW-fed slot antenna with a cavity backed reflector. The (a) proposed cavity backed CPW-fed slot antenna, and (b) a 2U CubeSat with the proposed antenna as modelled in HFSS. 109

6.2. Comparison of radiation pattern at 2.45 GHz: (a) without cavity, and (b) with cavity. 111

6.3. Return loss for various depth values. 112

6.4. Radiation patterns for depths different h_2 values. 113
6.5. Return loss for various substrate thickness h_1. 114
6.6. Input impedance. 115
6.7. Axial ratio. 115
6.8. Proposed ACM antenna configuration. 116

LIST OF TABLES

1.1. Classifications of small satellites. 3
1.2. Pico- satellites system challenges and their importance 8
2.1. Antenna design challenges for pico-satellites. 16
2.2. Different micro-strip patch antenna designs and their performance 18
2.3. Different slot antenna designs and their performance 37
2.4. Comparison between all types of planar antennas 39
3.1. Evaluation of the most suitable planar antenna designs for inter CubeSat communications 63
4.1. Return loss, BW, gain and size of modified antennas 73
4.2. A comparison between S-band patch antennas for CubeSats and the proposed antenna 77
5.1. Comparison between antennas for CubeSat communications and proposed antenna 88
5.2. Optimal parameters of the proposed antenna 91

List of Abbreviations

CMR	Communication Moon Relay
PicoSats	Pico Satellites
COTS	Commercial Off-The-Shelf
ISS	International Space Station
LEO	Low Earth Orbit
UHF	Ultra High Frequency
DMC	Disaster Monitoring Constellation
ADCS	Attitude Determination and Control Systems
HFSS	High Frequency Structure Simulator
TTC	Telemetry, Tracking and Command
GPS	Global Positioning System
CP	Circular Polarization (CP)
RF	Radio Frequency
SHF	Super High Frequency
PBG	Photonic Band-Gap
LP	Linear Polarization
BW	Bandwidth
VSWR	Voltage Standing Wave Ratio
UWB	Ultra-Wideband
AMC	Artificial Magnetic Conductor
HMSIW	Half Mode Substrate Integrated Waveguide
QLQC	Quasi Lumped Quadrature Coupler

CPW	Coplanar Waveguide
CBSA	Cavity Backed Slot Antennas
RHCP	Right Hand Circular Polarization
LHCP	Left Hand Circular Polarization
AR	Axial Ratios
HPBW	Half Power Beam Width
ISM	Industrial, Scientific and Medical
MSS	Metasurface Superstrate Structure
DCSR	Double Closed-Square Resonator
VNA	Vector Network Analyser

Chapter 1

INTRODUCTION

1.1 Satellite Communications

Satellites communication was first demonstrated by the United States of America (USA) navy in 1954. The project, called Communication Moon Relay (CMR), used the moon as a natural communication satellite to reflect radio waves back to a ground station. In particular, the moon was used to relay operational and facsimile messages in the Medium Frequency/High Frequency (MF/HF) range [1].

To date, satellites have become an essential part of our everyday life. They have many advantages. Amongst them, they include enabling communication links between users located in different parts of the Earth; for example, in the CMR project, the moon was used to link Hawaii and Washington DC. Advantageously, they are able to cover large geographical areas. Apart from that, the cost of a satellite connection is not effected by increasing user numbers or the distance between communication points [2]. Moreover, satellites operate independently from terrestrial infrastructure. This means they are not affected by man-made and natural disasters.

Satellites are classified based on their orbits; namely, geostationary or sun synchronous. Geostationary satellites also known as Earth-synchronous satellites orbit the Earth's axis as fast as the Earth spins; see Figure 1.1 (a). These geostationary satellites operate at an altitude of about 36,000 km over a single point above the Earth and their path follows the equatorial plane of the Earth; examples are those used by video or TV communications systems [3].

Sun synchronous, aka polar orbiting, satellites operate at altitudes of 800 to 900 km. They cross the equator at the same local time every day with an orbital velocity of about 7.8 km/s; see Figure 1.1 (b). They are mainly used for (i) communications;

e.g., mobile telephony, or (ii) remote sensing; e.g., land imaging and weather forecasting. Another application is military, where they are used for spying, watching the borders of countries, and to enable secure communications [4]. As shown in Table 1.1, these conventional satellites are relatively large and heavy with most weighing in at above one tonne, and have high power consumption in the range of 1 kW. Moreover, they are able to carry high gain (usually parabolic) antennas for ground communications, and their typical life cycle exceeds 10 years. Lastly, they are very expensive, costing upwards of one billion dollars [5]. Compared with conventional and medium sized satellites, as set out in Table 1.1, small satellites cost less and easy to construct but have fewer capabilities.

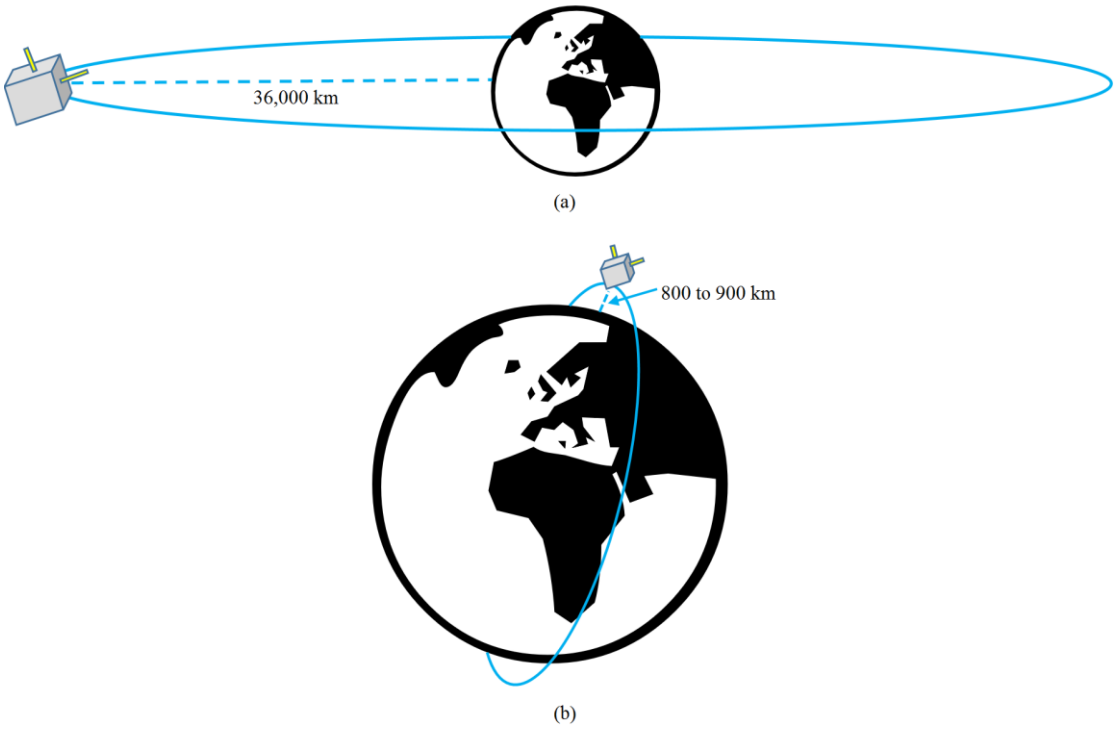

Figure 1.1. Satellite orbits: (a) geostationary, and (b) sun synchronous.

1.2 Pico satellites

Pico-satellites (picosats) are extremely small and lightweight. They have a wet mass between 0.1 and 1.33 kg. The most common type of picosats is CubeSat [4]. Advantageously, CubeSats can be constructed using Commercial Off-The-Shelf

(COTS) electronic components [6]. Figure 1.2 depicts a 10-cm CubeSat with a mass of no more than 1 kg. All CubeSats have a fixed size of 10cm×10cm with three different lengths: 10cm, 20cm, and 30cm. These lengths correspond to the requirement of the Poly-Pico satellite Orbital Deployer (P-POD) [7]; a standardized CubeSat deployment system developed by students at Cal Poly San Luis Obispo. As shown in Figure 1.3, P-POD is capable of carrying three standard CubeSats and can be released as secondary payloads on a wide range of launch vehicles. Consequently, they can be deployed from standard rockets or more recently from the International Space Station (ISS) [8]. Indeed, they can be placed in a single launcher/tube. A launch vehicle carrying such a tube can then simply release the satellites upon reaching their target orbit.

Table 1.1. Classifications of small satellites

	Type	**Mass (kg)**	**Cost (US $)**	**Time to Build (Year)**	**Antenna Gain**	**Power Consumption (W)**
	Conventional	>1000	0.1-2 B	>5	Very high	~ 1000
	Medium	500-1000	50-100 M	4	Very high	~ 800
Small Satellites	Mini	100-500	10-50 M	3	High	53.2
	Micro	10-100	2-10 M	~ 1	Medium	35
	Nano	1-10	0.2-2 M	~ 1	Medium	7
	Pico	1-1.3	20-200 K	<1	Low	2
	Femto	<0.1	0.1-20 K	<1	Low	0.006

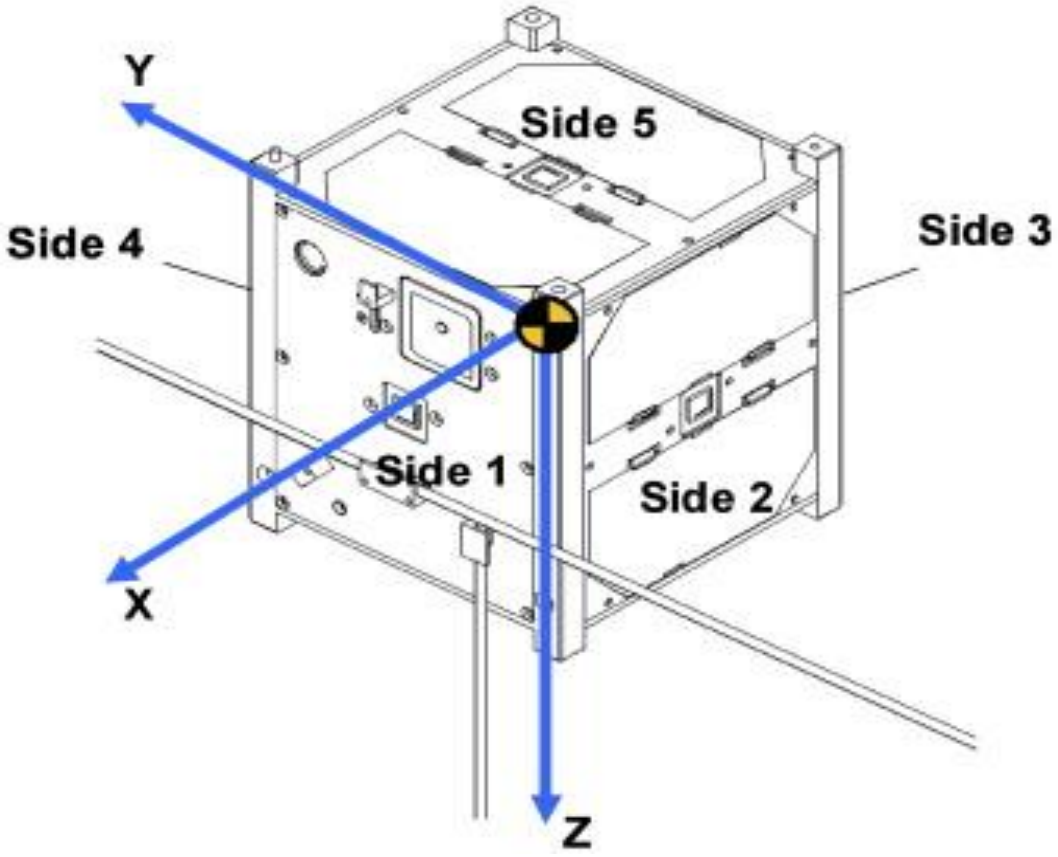

Figure 1.2. An example CubeSat (10cm×10cm×10cm) [9].

Figure 1.3. A poly-pico satellite orbital deployer [10].

Interestingly, CubeSats can be networked to form a swarm comprising of a constellation of satellites; see Figure 1.4. The resulting swarm allows CubeSats to have a longer contact time with ground stations and enables them to collectively take multiple measurements over a larger geographical area; consequently, they allow sensing missions to conduct comprehensive assessments of a given geographical region that otherwise would be impossible with a single conventional satellite [11, 12]. Moreover, CubeSats can jointly maintain a fixed or relative position with each other in a distributed manner [13]. An example CubeSat swarm is RapidEye. It is a commercial venture with a constellation of five mini-satellites deployed in 2008 and operate in the low earth orbit (LEO) (630 km) [5]. In another example, the authors of

[14] and [15] reported the launch of six aerospace pico-satellites by Stanford University using an orbiting automated pico-satellite launcher. Four of these pico-satellites have a dimension of 4×3×1 cubic inches, and the other two measure 8×3×1 cubic inches. Notably, the entire launch costs only USD $30,000 [16]. The Edison Demonstration of Smallsat Network (EDSN) is the first 1.5U CubeSat swarm project demonstrated by NASA [17]. The EDSN swarm consists of eight CubeSats. Each has a mass of about 1.7 kg. The mission goal is to conduct multi-point science and transfer collected data to a ground station. Hence, EDSN can be used as a platform for distributed space weather measurements or other experiments that require distributed and multi space radiation measurements in LEO. The pico-satellites in the swarm use the Ultra-high frequency (UHF) band at a data rate of 9.6 Kbits. It also provides a communication link between CubeSats and a ground station over S-band.

To date, CubeSats have found applications in fields such as education and scientific experiments. Specifically, CubeSats programs provide education and training to students, scientists and engineers in space related skills; e.g., design production, test, launch and orbital operations of satellites. Many universities and engineering schools in Europe, Japan, and the United States of America have already developed, launched and operated their own pico-satellites. For example, Picpot [18] is an educational pico-satellite built at the Politecnico di Torino University. In particular, pico-satellites are good examples of a complex system with specific constraints and requirements. Consequently, building one allows students to learn techniques and procedures related to pico-satellites development. Apart from that, CubeSats enable missions that cannot be accomplished by large satellites. For example, missions that require high temporal and spatial resolution. In this respect, CubeSats can be used to gather data from multiple points. For example, ocean altimetry measurements, remote sensing of sea ice, land and ocean temperature measurements, environmental disaster monitoring, atmospheric temperature and humidity measurements [19]. One example is the Disaster Monitoring Constellation (DMC) project [16, 20]. It consists of six micro satellites that are used to monitor and mitigate man-made and natural disasters; e.g., the Indian Ocean tsunami in 2004. Apart from that, the international community is working to form and launch swarms of pico-satellites. One example is the QB50 project, which is collaboration between 15 different partners from all over

the world [21-23]. Its aim is to provide affordable access to space and in-situ measurements of Earth's lower thermosphere/ionosphere region.

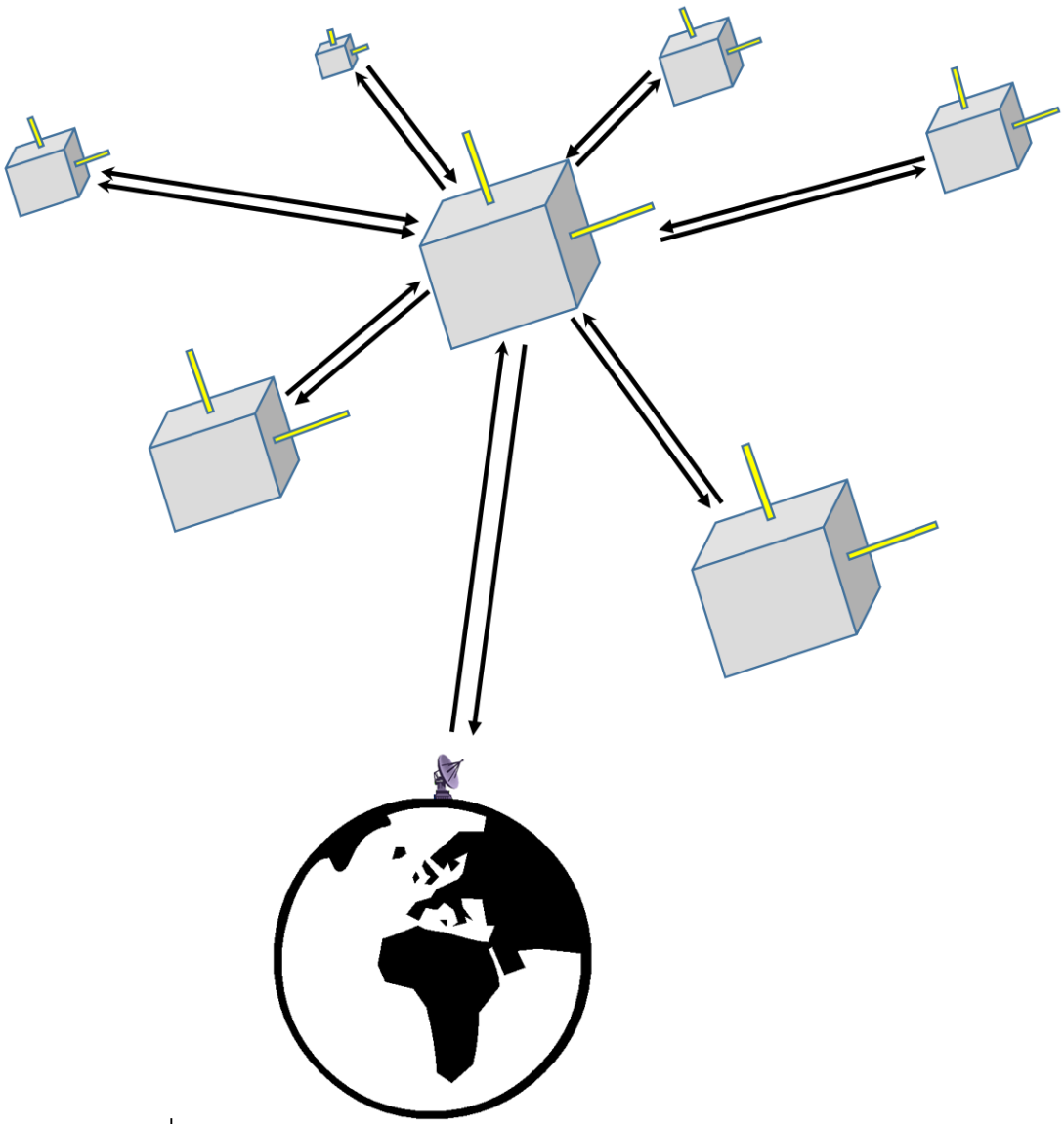

Figure 1.4. A swarm with seven small-sized 1U CubeSats.

There are many criteria and challenges when designing a CubeSat. The primary ones are listed in Table 1.2. Their limited size means only a small area is available for solar cells, which in turn limits the generated power that feeds all components. The other challenge is the small power budget of usually no more than 2W, which limits

or entirely eliminates backup units. Consequently, CubeSats have low reliability, and hence, they have a short lifetime ranging from a few weeks to a few months [24]. As a result, CubeSats need to operate autonomously and must be able to handle any anomalies that occur. They also need to be equipped with lightweight and small antennas that provide high gain and wide bandwidth. These antennas make it possible to track and control CubeSats from a ground station. In addition, antennas are important in space missions that require CubeSats to communicate with each other in a swarm and to transmit payload data; e.g., images to a ground station.

Table 1.2. Pico- satellites system challenges and their importance

Challenges	**Implications**	**Operating Ranges**
Small size	• Limited surface area, primarily used for solar cells, meaning the energy harvesting rate is small, which in turn affects operational lifetime. • Constrains available resources such as batteries, and hence, affects mission durability. • Bounds on antenna size.	$\leq 10\times10\times10$ cm^3
Small mass	• Limits the size and capacity of battery, which in turn bounds the power budget of communication components. • Precludes the use of standard Attitude Determination and Control Systems (ADCS) for pico-satellites with mass less than 1.3 kg [25]. • Obviates the use of high gain, and usually heavy, directional horn antennas. Moreover, additional weight will be incurred if satellites are equipped with complicated reflectors and arrays to achieve high gains.	$\leq$ 1.3 kg
Limited power	• Mass and surface area restrictions affect the amount of generated power from solar cells, which in turn limits redundancy. • Limits the use of high performance, but power hungry, elements such as steering arrays and ADCS. • Low hardware redundancy, and hence, increases the probability of system failure.	$\leq$ 2 W
Limited bandwidth and communication opportunities	• Affect applications that require high data rates. For example, mapping, and downloading high resolution images to a ground station [26]. • Reduced transmission capacity due to the loss of contact with ground stations.	1.2 – 9.6 kbit/s

1.3 Antennas for CubeSat Communications

CubeSat communications require the development of small size, low profile, low cost and high gain antennas. To date, past works on antenna designs for small satellites have considered different antennas. They include:

- *Omni-directional*

  They are required by the Telemetry, Tracking and Command (TTC) sub-system to facilitate space to ground communications. They include monopole, patch-excited cup and helix antennas. While simple to deploy, these antennas tend to radiate in all directions. They also occupy a large area. As a result, pico-satellites typically use lightweight and small sized micro-strip patch and slot antennas for TTC [27, 28].

- *High gain*

  These antennas are mainly used for high speed down-links to ground stations. High data rates require an antenna with a gain of about 12 dB [27]. However, the very limited space and power on pico-satellites make it difficult to accommodate such a high gain antenna. The most common type of high gain antennas used by conventional satellites is a horn antenna with a pointing mechanism and S-band quadrifilar-helix antennas; see [27]. In addition, the authors of [29] proposed a high gain deployable hemispherical helical antenna for CubeSat to ground communications.

- *Medium-gain and low backward radiation*

  These antennas are mainly used by receivers in the Global Positioning System (GPS) to ascertain the position, velocity, and timing of pico-satellites in LEO. Many types have been developed; namely, patch-excited cup and shorted–annular patch antennas. They have a gain of about 12 dB, operate at 1.575 and 1.227 GHz and have a small size. Also, they produce low back radiation to minimize interference with satellite components. Recently, in [27], the authors presented a Geohelix ceramic loaded quadrifilar-helix antenna.

- *Directive self-steering*

  The main function of these antennas is to provide circular polarization (CP) in order to establish communication links between satellites. Furthermore, beam steering techniques can be employed to increase directivity and achieve higher

gains [27]. In this respect, pico-satellites use self-steering. In contrast, conventional satellites employ dynamic beam steering [30].

- *Planar antennas*

  They have a number of characteristics, including low profile, low cost, small size, are easily to fabricate and do not require a deployment mechanism. These characteristics make planar antennas suitable for CubeSat communications. The major limitations of many low-profile planar antennas are their narrow bandwidth and relatively low gains. However, many techniques and approaches, such as photonic band-gap (PBG) structures, cavity-backed model, folded-patch approach, and asymmetry structure, can be used to enhance their gain and bandwidth.

1.4 Frequency Bands Allocation for CubeSats

CubeSats use an array of frequency bands to provide communication links between CubeSats and ground stations. These frequency bands include VHF (30-300 MHz), UHF (300 MHz – 3 GHz), S-band (2-4 GHz), C-band (4-8 GHz), and X-band (8-12 GHz). The majority of CubeSats operate at the amateur band. They use frequency of about 437 MHz which is a UHF-band for downlink communications and 144 MHz in VHF-band for uplink communications. Antennas that use these frequency bands are wire antennas, i.e., dipole and monopole antennas. Other CubeSats use patch and slot antennas that operates in the S-band or C-Band frequencies for downloading images to ground stations and providing a communication link between CubeSats. Recently, some CubeSat programs are operating in the X-Band frequencies to further reduce the size of the antenna.

1.5 Motivation

Most antennas for CubeSat communications are designed to cover a specific area. On the other hand, the weight and size restrictions of CubeSats constraint the antenna design space. In particular, solar cells compete with the space used to place antennas. Apart from that, some antenna designs for CubeSats require a deployment mechanism; examples include linear wire antenna, Yagi-Uda antenna, and helical

antenna [31-35]. A key concern is that any problems with their deployment system may lead to entire system/mission failure.

An obvious solution to the deployment problem is to use planar antennas, i.e., slot and micro-strip patch antennas. They, however, have low gains and efficiency [36]. Current 2.45 GHz patch antennas that are suitable for use on CubeSats have a maximum gain of 5.9 dB with bandwidth of 1500 MHz while for slot antennas the maximum gain is 4 dB with small resulting bandwidth of 110 MHz [37]. The resulting low gain is due to their bidirectional patterns.

1.6 Thesis Aims and Contributions

To date, no works have examined the suitability of existing planar antenna designs for use on CubeSats. This thesis, therefore, aims to study the suitability of existing small size micro-strip patch and slot antennas that have the ability to achieve high gain, beam steering, and wide bandwidth. In particular, this thesis aims to: (1) present a quantitative evaluation of the most suitable antenna designs for CubeSats, (2) design a low profile S-band patch antenna for CubeSats that improves upon current state-of-the-art in terms of bandwidth and gain, (3) design a unidirectional CPW-fed slot antenna with a superior gain using MSS, and (4) design a miniaturized cavity backed CPW-fed slot antenna with high gain that operates at 2.45 GHz.

Henceforth, this thesis contains the following contributions:

1. This thesis first provides a comprehensive and qualitative comparison of micro-strip patch and slot antennas in terms of their mass, size, gain, beam steerability, type of polarization, operating frequency band, and return loss.

2. This thesis then presents a quantitative evaluation of three planar antenna designs that best address CubeSats challenges on a common platform. Critically, it studies how their performance is affected by a 2U CubeSat body. It compares and evaluates these designs with and without a 2U CubeSat and recorded their performance in terms of volume, gain at 2.45 GHz, bandwidth, return loss, robustness, beam steerability and cost. In addition, the Quasi Newton method is used to shift the operating frequencies of shorted patch and

CPW-fed slot antennas to 2.45 GHz (S-band). This thus allows it to operate in the unlicensed Industrial, Scientific and Medical (ISM) band without critically affecting its radiation performance.

3. This thesis proposes a wide band F-shaped patch antenna for S-band CubeSat communications. To broaden bandwidth, it uses two arms of the upper patch with different lengths to generate a second resonant frequency. It then studies the effect of the arm length and width on the return loss, resonant frequency and impedance bandwidth on a 3U CubeSat. The antenna has a small size and achieves a wideband, high gain of 8.51 dB and small return loss of -32.85 dB at 2.45 GHz.

4. This thesis proposes the design of a high gain CPW-fed slot antenna for 2.45 GHz CubeSat communications. The antenna has the highest gain amongst antennas that are suitable for use on a CubeSat. A key novelty is the use of MSS to significantly increase the gain from 2.52 to 5.67 dB. This gain further improves to 9.71 dB when the CPW-feed slot antenna is placed on the surface of a cube satellite constructed using Aluminium. The antenna has been evaluated comprehensively using HFSS as well as on a 3U CubeSat platform.

5. This thesis proposes a low profile high gain cavity backed CPW-fed slot antenna that operates at 2.45 GHz. The main idea is to use a part of the CubeSat's body as a low profile cavity reflector to redirect the back lobe pattern forward. This design is more robust and occupies less surface area on CubeSats; i.e., 12.96% for 1U and 6.48% for 2U as compared to using a MSS. The proposed antenna has a small size of 36mm×36mm and a total gain of 8.6 dB; in contrast, amongst all previous S-band planar antennas that are suitable for CubeSats, the best gain is only 5.96 dB and the smallest size is $38\times38\times3.2$ mm^3 at 2.45 GHz.

1.7 Publications

This thesis has resulted in the following papers:

1. **F. EM. Tubbal**, R. Raad, K-W. Chin, and B. Butter, “S-band Shorted Patch Antenna for Inter Pico Satellite Communications,” *IEEE 8th International Conference on Telecommunication System, Services and Application (TSSA 2014)*, Bali, Indonesia, pp. 1-4, October, 2014.

2. **F. EM. Tubbal**, R. Raad, K-W. Chin, and M. A. Madni, “Low-profile Planar Antennas for Inter Cube Satellite Communications,” *4th International CubeSat workshop, London, United Kingdom, May 2015.*

3. **F. EM. Tubbal**, R. Raad, and K-W. Chin, “A Survey and Study of Planar Antennas for Pico-Satellites,” *IEEE Access*, vol. 3, pp. 2590-2612, December 2015.

4. **F. EM. Tubbal**, R. Raad, K-W. Chin, and B. Butters, "S-band Planar Antennas for a CubeSat," *International Journal on Electrical Engineering and Informatics*, vol. 7, no. 4, December 2015.

5. **F. Em. Tubbal**, R. Raad, K-W. Chin, B. Butters, L. Matekovits and G. Dassano "A High Gain S-band CPW-fed Slot Antenna for CubeSat Communications,". *Submitted to IEEE Access.*

6. **F. EM. Tubbal**, R. Raad, and K-W. Chin, "A Wideband F-shaped Patch Antenna for S-band CubeSat Communications," 10th International Conference on Signal Processing and Communication Systems (ICSPCS), Surfers Paradise, Gold Coast, Australia, pp. 1-4, 19-21 Dec. 2016.

7. **F. Em. Tubbal**, R. Raad, and K-W. Chin, "A Low Profile High Gain CPW-fed Slot Antenna with a Cavity Backed Reflector for CubeSats", unpublished.

1.8 Thesis Structure

The remainder of the thesis is organized as follows:

1. *Chapter 2.* This chapter presents the first comprehensive survey and study of planar antennas for pico-satellites. Specifically, this chapter provides a qualitative comparison of planar antenna designs and their suitability for use on CubeSats.
2. *Chapter 3.* This chapter presents a quantitative evaluation of the most suitable planar antenna designs on a common platform.
3. *Chapter 4.* This chapter studies and compares repurposed shorted patch and CPW-feed square slot antennas for CubeSat communications. Specifically, it studies the impact of a 2U CubeSat’s surface on the performance of these antennas. It also proposes the design of a wideband F-shaped patch antenna for S-band CubeSats communications. The key idea is to feed the resonance arms

of the upper F-shaped patch by a folded ramp-shaped patch. This generates two resonant frequencies and hence achieves a wide bandwidth.

4. *Chapter 5.* This chapter outlines a high gain S-band CPW-fed slot antenna for CubeSat communications. A key feature that results in high gain is the use of a MSS as a resonant cavity model. This has the effect of redirecting the back-radiation pattern forward.
5. *Chapter 6.* This chapter proposes a low profile high gain CPW-fed slot antenna. The main idea is to use a part of the CubeSat's body as a low profile cavity reflector to redirect the back lobe pattern forward.
6. *Chapter 7.* This chapter concludes the thesis, and provides a summary of research outcomes and future research directions.

Chapter 2

LITERATURE REVIEW: MICRO-STRIP PATCH AND SLOT ANTENNAS

This chapter presents a unique collection of techniques and approaches that apply to micro-strip patch and slot antennas in order to achieve miniaturization, high gain and wide bandwidth. It then provides an extensive qualitative comparison of these antennas in terms of gain, volume, mass, beam steerability, polarization, operating frequency and return loss.

2.1 Micro-strip Patch and Slot Antennas

There is growing interest in planar antennas that can be integrated easily with Radio Frequency (RF) and microwave circuits. However, using planar antennas for pico-satellite communications must overcome a number of constraints that affect their performance; see Table 2.1. They must have low profile, high gain, wide bandwidth, and achieve beam steerability. The following sections present planar antenna designs, problems addressed by a given antenna designs, their advantages and limitations.

2.1.1 Micro-strip patch antennas

Patch antennas have applications in the medical field such as skin cancer detection [38, 39], on CubeSats used for Earth observation [40], and radar scanning, i.e., detecting moving targets [38]. Figure 2.1 shows a typical micro-strip patch antenna that consists of a metal (‘Patch’) on the top of a grounded dielectric substrate. This patch can be made of different shapes; rectangular being the most common shape. Moreover, the patch antenna is fed by a micro-strip transmission line. The patch and feed line are usually made from copper.

Table 2.1. Antenna design challenges for pico-satellites

Design Properties	Performance	Relevant Works
Small size and low mass	• Low power consumption, easy to construct, cheap, occupy a small area, and provides sufficient real estate to mount solar cells. • Do not dominate the satellite profile or weight budget.	[40-56]
Circular polarization	• Eliminates polarization mismatch losses. • Only 3 dB loss regardless of antenna orientation.	[41-47], [52-54] and [6, 57-67]
Impedance matching	• Maximize power transfer or equivalently, minimize power loss. • Minimize signal reflection.	[6, 40-55, 57-70]
High gain and wide bandwidth	• Long distance communication, increased contact period with ground stations. • Enable inter-satellite communications.	[41, 42], [45-47], [52-54], [6, 56-66] and [69]
Frequency re-configurability	• The ability to radiate more patterns at different frequencies and polarizations to enhance system performance.	[64] and [69].
Beam steerabilty	• Saves power by directing an antenna's beam to a desired direction.	[54], [57], [61, 62], [6] and [65]

Table 2.2 shows designs aimed at micro-strip patch antennas with the goal of achieving beam steerability, increasing gain, reducing their size, and enhancing supported bandwidth. These designs achieve gains ranging from 1.53 to 18 dB, with an antenna size ranging from 3.14×0.64×0.078 cm^3 to 12×16.8×2.5 cm^3. Moreover, they work in the L, S, C and X frequency bands (1 – 14.15 GHz). In terms of gain and size, most of these designs are suitable for CubeSat communications.

The next section further discusses these proposals in more details in terms of their gain and steerability. After that Section 2.1.1.2 presents antennas that have wide bandwidth followed by Section 2.1.1.3, which presents those that are size sensitive.

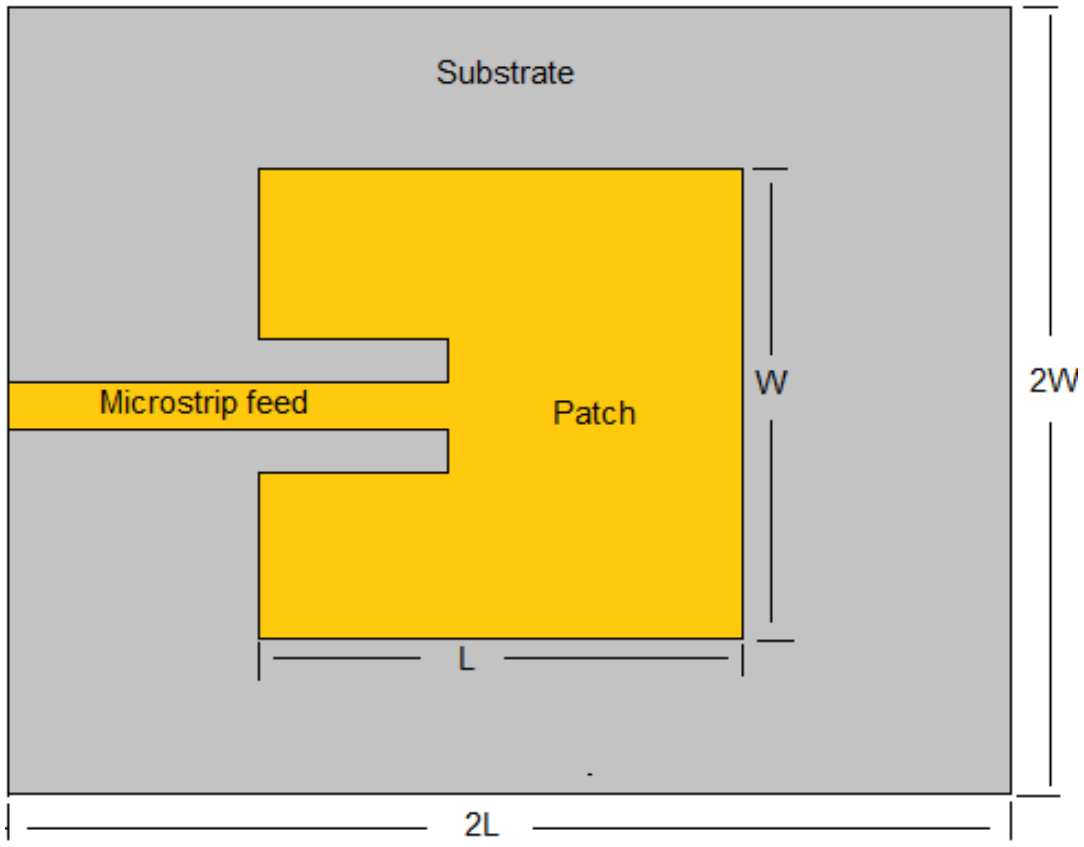

Figure 2.1. A micro-strip patch antenna.

Table 2.2. Different micro-strip patch antenna designs and their performance

Reference	**Gain (dB)**	**Volume (cm^3)**	**Band (GHz)**
Osorio et al. [6]	6.9	9×9×0.5	C-Band (5.8)
Ma et al. [61]	7.5	15×15×0.96	S- Band (2.37)
Hu et al. [65]	18	16×16×0.35	C-Band (6.175)
Nascetti et al. [40]	5.9	3.97×1.2×0.21	S-Band (2.45)
Mizuno et al. [62]	6.25	10×10×0.16	C-Band (10.5)
Budianu et al. [57]	4.8	10×10×0.16	S-Band (2.45)
Qian et al. [66]	5.02	12×16.8×2.5	Ku-band (14.15)
Montaño et al. [67]	n/a	8.01×8.01×2.25	S-Band (2.40)
Iwasaki [59]	6	7×7×0.16	L-Band (1.525)
Ferrero et al. [42]	6.2	2.7×2.7×0.0892	S-Band (3.5)
Massa et al. [58]	5.9	8.8×8.8×2.5	C-Band (4.32)
Chiu et al. [41]	2.58 or 2.4	5.4×5.4×0.7 and 4×4×0.7	C-band (3.5-6.5)
Malekpoor et al. [46]	4.9 or 3.9	2.8 ×1×0.7 and 1.8×1.5×0.7	UWB (3.57-11.98)
Holub et al. [44]	n/a	2.21×2.21×1.5	L-band (1.575) UHF-band (0.869)
Ouedraogo et al. [51]	5.96, 4.8, and 4.23	3.14 ×0.64× 0.078	S- band (2.45)
Addaci et al. [48]	n/a	$3.14 \times 2.7^2 \times 1.37$	S- Band (2.4-2.5)
Rahmadani et al. [43]	1.53	3.8 ×3.8	S- Band (2.45)
Malekpoor et al. [56]	8	3.4 ×1.3×0.7	C-Band (6.73)

2.1.1.1 Steerability and gain improvement

Recently, beam-steerable and high gain antennas have received considerable attention due to their enhanced radiation performance and suitability for long distance communications. The main techniques used to achieve beam steering include sequential phase-rotation, retrodirective array [62], beam forming algorithm [57], and for increasing gain, photonic band-gap (PBG) structures [66], and single proximity coupled feed [59]. The conventional pointing mechanisms, such as [6], for steering antenna beams are not suitable for use by pico-satellites because of their size and mass constraints. The following approaches are used to achieve steerabilty and to enhance antenna gains:

- *Sequential phase-rotation*

  Sequential phase-rotation is a popular approach. The main idea is to feed each sub-array element sequentially by making adjacent patches orthogonally oriented (90°) to achieve CP at the following phases: 0°, 90°, 180°, and 270°. In [6], Osorio et al. propose a square antenna array with nine identical elements (3×3).

Each element is formed by a 2×2 sub-array of rectangular patches. Adjacent patches are orthogonally oriented to provide CP. Beam steerability is achieved by feeding the sub-arrays at 0^0, 90^0, 180^0, and 270^0 using a phase shifter. They reported beam steerability and a high gain of 6.9 dB. The use of rectangular patches leads to a reduction in mutual coupling between adjacent patches. This improves performance due to the isolation between antenna arrays. This also leads to a reduction in interference between array elements. Its main limitation, however, is the low coupling between the feed line and the radiating patch. This significantly affects impedance matching and radiating efficiency. To solve this problem, Osorio et al. propose moving the feed line slot back to the centre of the patch where the coupling through the electrical dipole is maximized. Another limitation is its inability to switch between two different polarizations, which is an important feature as it helps enhance the reception of weak signals.

Micro-strip arrays can provide various radiation characteristics with their feed networks, which are often designed using power dividers (or a combiner) to deliver a RF signal with specific amplitude and phase to each radiating element. In [61], Ma et al. propose a technique to achieve polarization diversity and an electrically steerable radiation pattern. The main approach is to use a three quasi-lumped coupler and a 90^0 phase delay line. The operation of these couplers can be switched between the T-junction divider mode and 3-dB hybrid mode by controlling the capacitance value of the lumped capacitors. By connecting this feed network to four rectangular radiating elements of the micro-strip array, the T-junction divider provides linear polarization (LP) while a 3-dB hybrid [71] provides CP. This is important as it achieves the best signal strength and mitigates multipath fading. Moreover, the beam steering capability of circular polarisation allows a link to be established when re-orienting two satellites. It is interesting to note that steerability and high gains of 7.1dB and 7.5 dB are obtained for CP and LP respectively. One major drawback is the antenna size, i.e., $15\times15\times0.96$ cm^3, which exceeds the size of pico-satellites.

Power dividers, which distribute power to different radiating elements, facilitate beam steering control. In [65], Hu et al. use a two-way Wilkinson power divider [72] to feed a network array that has sequential rotated elements. This power divider provides high isolation and 90^0 phase shift between adjacent radiating elements and sub-arrays. This is important as it achieves broadband CP at high gains. They reported beam steerability, wide bandwidth and a superior gain of 18 dB. This design achieves wider bandwidth and much higher gain than the designs presented in [6] and [61]. Compared to [61], which uses a three-port power divider, the two-way divider in [65] occupies a smaller area because it reduces the total size of the feeding network layout. Its main limitation is the large antenna size (16cm×16cm×0.35cm). This has a non-negligible impact on the actual surface area used for solar cells, and hence energy harvesting rate, which in turn affects operational lifetime. Another limitation is the use of a 90^0 phase shifter, which has a significant impact on cost, dimension and is complex to control.

One of the most popular power divider designs is the Wilkinson power divider [73]. It splits the input power signal into *n* signals of equal amplitude and phase, and is commonly applied in antenna array systems that require parallel feed systems. In [40], Nascetti et al. used a Wilkinson structure to design a power divider that feeds a network array of four identical patches placed on a 1U CubeSat face. This power divider design provides high isolation between output ports at good impedance matching. The main idea is to feed every two adjacent patches that are orthogonally oriented (90^0) using a power divider to achieve CP at high gain. This is important as it increases the reception and signal strength; it thus helps establish communication links with a ground station and other CubeSats. The design achieves a maximum gain of 5.9 dB and a return loss of -15.05 dB at an operating frequency of 2.45 GHz for a single patch. Moreover, the authors used all four patches to achieve a high gain of 7.3 dB and a small return loss of -25 dB at 2.45 GHz. Compared to the designs in [61], [6], and [65], the one reported in [40] has a much smaller antenna size, i.e., $3.97\times1.2\times0.21 cm^3$, and less complex. However, it is used only on one face of a CubeSat. This means no cross-links communications when CubeSats are oriented toward a ground station.

- *Retrodirective (self-steering)*

  Approaches that use retrodirective arrays [74-76] are becoming popular due to their simplicity as compared to those that use phased-array and smart antennas. Specifically, retrodirective antennas are able to reflect an incident signal towards the source direction without any prior location information. In [62], Mizuno et al. use a retrodirective (self-steering) array. This technique is an alternative to dynamic beam steering and also helps increase gain. Note that that conventional phased-array antennas use phase shifters to achieve beam steerability. In contrast, retrodirective arrays steer their beams by sensing the incoming signal without the need for phase shifters. Consequently, they are cheaper, less complex, lighter, and smaller in size. Compared to smart antennas that rely on digital signal processing for beam control, e.g., [61], and [6, 65], retrodirective array systems are much simpler and potentially faster because it does not require computation. However, their main limitation is the use of a high local frequency that is set to twice the incoming radio frequency. Hence, they incur higher power, which is a key concern when they are used on energy-constrained pico-satellites.

- *Beam forming algorithm approach*

  Different antenna array systems use beam forming algorithms to control radiation patterns. Budianu et al. [57] propose to install a micro-strip patch antenna on each face of CubeSats. Each antenna provides CP. A beam forming algorithm is then used to identify the spatial signal signature of a receiver and thus maximizes directivity to said receiver. Also, the six antennas, one on each face of a CubeSat, ensure a communication link remains available at all times regardless of the CubeSat's orientation. Compared to the designs in [61] and [6, 65] that use complex digital signal processing and a phase shifter to steer beams, beam forming algorithms are simpler as they are based on simply adding the electrical fields of adjacent antennas, and hence, have higher gains. However, this approach occupies precious space that otherwise could be used for solar cells.

- *Photonic band-gap (PBG) structures*

  Surface-wave losses in patch antennas lead to a decrease in radiation efficiency and gain. Therefore, surface-wave suppression techniques are needed to enhance

radiation pattern efficiency. Most of these techniques are related to periodic structures [77-81]. The most popular ones are PBG structures [82]. In [66], Qian et al. propose to surround a patch antenna with a square-lattice of small metal pads. This leads to a substantial suppression of surface waves excited in the dielectric substrate. They reported a radiation efficiency of 85% and a gain of 5.02 dB. In general, this technique achieves wider bandwidth, higher gain, lower backside radiation, beam shape control and surface wave suppression. Unfortunately, the resulting antenna is not steerable.

- *Single proximity coupled feed*

  A proximity coupled feed technique is used to transfer power between the micro-strip line and the radiating patch based on electromagnetic field coupling [83]. In [59], Iwasaki presents a design for a circularly polarized patch antenna with a single proximity couple feed line. This antenna has a cross slot with unequal lengths on its patch. A single proximity coupled feed is an electromagnetically coupled method. This electromagnetic field coupling is carried out to transfer power between the micro-strip line and the radiating patch. This leads to higher isolation between the DC supply and RF signal. It achieves a CP without the need for an external circular polarizer. This is important as it is less complex and incurs less weight and size. Iwasaki reported a high gain of 6 dB at CP which is important for cross-link communications in pico-satellites. Another advantage is the ability to control gain, resonant frequency and antenna size.

2.1.1.2 Antenna bandwidth enhancement

The main techniques used to enhance bandwidth include agile polarization [42], cavity [58], U-slot and L-slit geometries [41], folded-patch approach [46], and transparent mesh line geometry [67]. All these techniques achieve significant enhancement in bandwidth ranging from 3.8% in the 3.8 GHz frequency band to 98.22% in bands ranging from 4 to 11 GHz. Moreover, these approaches have no significant effect on antenna size. All these approaches and techniques are presented in more details as follows:

- *Agile polarization*

  Antennas of this type are able to dynamically change their polarization state, i.e., they can have either linear (vertical or horizontal) or CP (left or right hand) [84]. In [42], Ferrero et al. designed a novel quad-polarization agile patch antenna to achieve simple polarization reconfigurability and to enhance bandwidth. The main approach is to feed a radiating patch with two orthogonal slots that are excited by a tuneable quasi-lumped coupler (QLC). These couples can be switched between two different operating modes: 3-dB hybrid coupler and directional coupler via a DC bias voltage to achieve agile polarization capabilities. This is important as it addresses multipath fading. The resulting antenna has a wide 3 dB axial ratio CP bandwidth of 3.8% with respect to the centre frequency of 3.5 GHz.

- *Cavity model*

  This technique is used to analyze micro-strip patch geometry and to provide a better way to model radiation patterns [85]. In [58], Massa et al. developed a cavity model for a printed annular patch antenna to achieve higher bandwidth and simplified match feeding system. The key idea is to connect (shorting) the inner edge of the annular patch antenna by a cylindrical conducting wall. This in turn reduces the antenna's stored energy. As bandwidth (BW) depends on the ratio between the radiated power (P_r) and stored energy (W_t) of the antenna ($BW = P_r/W_t$), reducing the amount of stored energy leads to an increase in bandwidth. This is important for systems requiring wider coverage; e.g., in [57] the authors use six antennas on the surface of pico-satellites to achieve a wide bandwidth in order to establish crosslinks between satellites. Advantageously, the impedance around their edge is low, which allows the use of a coplanar micro-strip without the need for an external matching network. This is important as it simplifies the whole design and enhances matching capability. In addition, the annular antenna design in [58] works as a circular patch antenna to provide circular or double polarization. Moreover, annular design provides wider bandwidth and better coverage.

- *U-slot and L-slit geometries*

  U-slot and L-slit are two common geometries employed by antennas with dual-band operation as they help enhance bandwidth [86]. In [41], Chiu et al. propose two approaches based on U-slot and L-slot geometries to enhance the bandwidth of a conventional quarter-wave patch antenna. The key idea is to include a folded inner small patch within the larger patch. Also, shorting walls are used to reduce the overall size of the antenna to nearly a quarter wavelength of the centre operating frequency (3.5 to 6.5 GHz). This is important because it increases bandwidth and reduces antenna size. Chiu et al reported a significant enhancement in bandwidth with a voltage standing wave ratio (VSWR) of less than two. The bandwidth of a U-slot antenna is 53.54% (3.57 to 6.18 GHz) while for L-slit it is 45.12% (4.265 to 6.75 GHz). Compared to the micro-strip patch antenna designs in [42, 58], the one reported in [41] has a much wider bandwidth than the design in [58] and smaller than that of [42].

- *Folded-patch feed*

  Folded-patch feed is used by ultra-wideband (UWB) patch antennas [87, 88], [89]. In [46], Malekpoor et al. use two different approaches to design shorted patch antennas with significant enhancement in impedance bandwidth. The first approach is to feed unequal resonance arms of the upper patch by a folded ramp-shaped patch. This helps enhance bandwidth without incurring any increase in patch size. In the second approach, they use a folded ramp-shaped feed and one pin in the centre of the upper patch to increase bandwidth. They also use shorting pins between the patches and the ground plane to miniaturize their size. They reported a significant enhancement in impedance bandwidth; specifically, 94.17% at 4.13 to 11.48 GHz, and 98.22% at 3.57 to 10.46 GHz, for first and second techniques respectively. This is very important as they enable high data rates. Compared to the designs in [42, 58] and [41], the proposed antenna in [46] has a much wider bandwidth, i.e., 3.57 to 10.46 GHz and is smaller in size, i.e., $2.8 \times 1 \times 0.7$ cm^3 and $1.8 \times 1.5 \times 0.7$ cm^3.

- *Transparent mesh line geometry*

  A meshed structure is an alternative to those that are made of transparent materials. They have high transparency; i.e., 80% and good efficiency; i.e., 50% [90]. Montaño et al. [67] propose a transparent mesh printed patch antenna design to be placed on the face of a 3U CubeSat for downlink or ground communications. The designed antenna consists of a 4.34 cm^2 square meshed lines on 8.01 cm^2 squared ground plane. The main idea is to implement copper grid lines on a high transparent substrate; i.e., quartz material. The resulting meshed antenna is then placed underneath solar cells. This is very important as it maximizes the efficacy of the solar panels. Moreover, the gain, operating frequency, efficiency, and bandwidth are enhanced by varying the mesh lines width. Montaño et al. reported a bandwidth of 80 MHz and return loss of -22 dB at a resonance frequency of 2.4 GHz. Compared to the designs in [41, 42], [46] and [58], the proposed antenna design in [67] provides more space for solar cells; i.e., its affords a CubeSat more power.

2.1.1.3 Patch antenna miniaturization

The main techniques used to reduce antenna size include meandering [44], metamaterial [51], cylindrical skirts with shorting pins [48], artificial magnetic conductor [43] and shorting pins [56]. These techniques are capable of reducing the antenna size by $3.14\times0.6^2\times0.078$ to $3.14\times2.7^2\times1.37$ cm^3. Techniques and approaches that are used to miniaturize the patch antenna size are as follows:

- *Meandering*

  This technique reduces the size of micro-strip patch antennas without affecting their resonant frequency. This is important as there is a constant demand for small antennas that operate at high frequencies; e.g., distributed pico-satellites systems [91]. Holub et al. [44] use a multilayer meanderly folded shorted patch structure to miniaturize micro-strip patch antennas. This means repeatedly folding the cavity of conventional patch antenna and hence, the electrical length of the whole N-times folded cavity and the resonant frequency remain constant. This decreases the original shorted (quarter-wavelength) patch by 1/N, where N is a number of

vertically placed patch plates. Holub et al. tested two antenna prototypes; the first design has two cavity meanders and resonant frequency of 1.575 GHz. The second design has three cavity meanders and resonant frequency of 0.869 GHz. They reported two structures with physical lengths of 2.21cm and 1.63 cm. This is significant as the resulting physical lengths are much smaller than those of conventional rectangular patch antennas (9.52cm).

- *Metamaterial*

  This is an important technique as it provides higher levels of miniaturization such as negative permeability metamaterial, μ-negative (MNG) metamaterial, a volumetric metamaterial and magneto-dielectric embedded-circuit metasubstrate [92-95]. Ouedraogo et al. [51] introduced a new design methodology that produces highly miniaturized patch antennas with a low profile, low cost, and are easy to fabricate. The key idea is to place complementary split-ring resonators horizontally between the patch and the ground plane. Optimizing the split rings geometry leads to high levels of miniaturization. Ouedraogo et al. simulated three miniaturized patch antennas at 2.45 GHz and with different radii of 1.2, 0.8, and 0.6 cm to achieve 1/4, 1/9, and 1/16 of the traditional patch area respectively. Compared to traditional patch antennas, they achieve a size reduction of 75% with good impedance matching. This thus makes them suitable for use on pico-satellites. They, however, have smaller bandwidth; i.e., 1.2% (29.4 MHz), 0.8% (19.6 MHz) and 0.4% (9.8 MHz) and have a low gain because of their back loop pattern.

- *Cylindrical skirts with shorting pins*

  The main advantage of wire patch antennas is their low profile, large bandwidth and monopolar type radiation pattern. However, their ground planes are generally too cumbersome as compared with the size of the radiating element [96]. In [48], Addaci et al. demonstrated a new design with a smaller, low profile circular wire patch antenna that operates in the 2.4-2.5 GHz; i.e., the ZigBee application frequency band [97]. The key idea is to bend the metallic plates of the upper and lower patches to form cylindrical skirts. The upper patch is a radiating element while the lower patch is a ground plane. These two patches are then connected

using shorting pins. Moreover, the main advantage of upper and lower skirts is their ability to provide a better control of antenna performance in terms of resonant frequency and its overall dimension. Also, the distance between shorting wires and feeding pins allow the control of the antenna's operating frequency without changing its dimensions. They reported a miniaturization ratio of 42% and bandwidth of 4.7%. Compared to the patch antenna design in [51], the one in [48] has a wider bandwidth and higher front to back ratio.

- *Artificial magnetic conductor*

  An Artificial Magnetic Conductor (AMC) is a structure with a distinct reflection phase property. Specifically, it introduces a zero-degree reflection phase shift to incident waves [98]. To this end, Rahmadani et al. [43] investigated the use of AMC in miniaturizing micro-strip patch antennas. Specifically, they replaced the antenna ground plane with an AMC structure, and thereby, allowing it to act as a virtual ground plane. This is important as it has good radiation patterns without unwanted ripples or side lobes and it reduces the antenna size by 31%. The main limitation is its low gain; i.e., 1.53 dB.

- *Shorting pins*

  Shorting pins help enhance patch antenna performance characteristics; i.e., bandwidth, as well as reduce their size [99]. Malekpoor et al. [56] designed a small size E-shaped micro-strip patch antenna. The main technique is to use two shorting pins between the edge of the upper patch (asymmetric E-shaped patch) and the ground plane. This increases the effective electrical length of the patch and reduces its physical size. Moreover, the use of shorting pins leads to a lower resonant frequency and wider bandwidth. The other approach is the use of an asymmetric E-shaped patch with unequal resonance arms to generate three resonant frequencies and hence achieve a wide bandwidth. Malekpour et al. reported a wide -10 dB bandwidth; i.e., 4110 MHz (3.34-7.45GHz), high peak gains; i.e., 5, 6.3 and 8 dB, and low return losses; i.e., -25, -28, and -22 dB at resonant frequencies of 4.74, 6.13 and 6.73 GHz respectively. Compared to the antenna designs in [43, 44], [48], and [51], the one in [56] has much wider bandwidth, provides higher gains, and is small; i.e., $3.4 \times 1.3 \times 0.7$ cm^3.

Amongst all micro-strip patch antenna designs, i.e., those in [41, 42], [44], [46], [40, 48], [51], [56-59], [61, 62], [6], [65-67], [84-89], the one in [65] has the highest gain at 18 dB and operates in the 6.175 GHz. However, its size, i.e., 16×16×0.35 cm^3, rules it out for use by CubeSats. On the other hand, the design in [42] has the smallest dimension at 2.7×2.7×0.0892 cm^3 and a high gain of about 6 dB. In terms of operating frequency, all the designs in [41, 42], [43, 44], [46], [40, 48], [51], [56-59], [61, 62], [6], [65-67], and [84-89] are suitable for satellite links and wireless communication applications as they operate in the Super High Frequency (SHF) band (2-30 GHz). However, the most suitable frequency band for pico-satellites is the S-band (2-4 GHz). Moreover, one limitation of the antenna designs in [41], [43, 44], [46], [40, 48], [51],[56], [58] and [67] is the lack of steerability. This is very important for cross links, and secure communications.

2.1.2 Slot antennas

Figure 2.2 shows a typical slot antenna that is normally made of an infinite conducting sheet (ground plane) that has a rectangular slot cut. The micro-strip line is used to feed the slot antenna by applying a voltage across the slot. This generates an electrical field and currents within and around the slot. Slot antennas are cheap, as they are constructed from low cost materials, easy to fabricate, robust, have good radiation performance and have very small profile. These advantages make slot antennas suitable for pico-satellite communications.

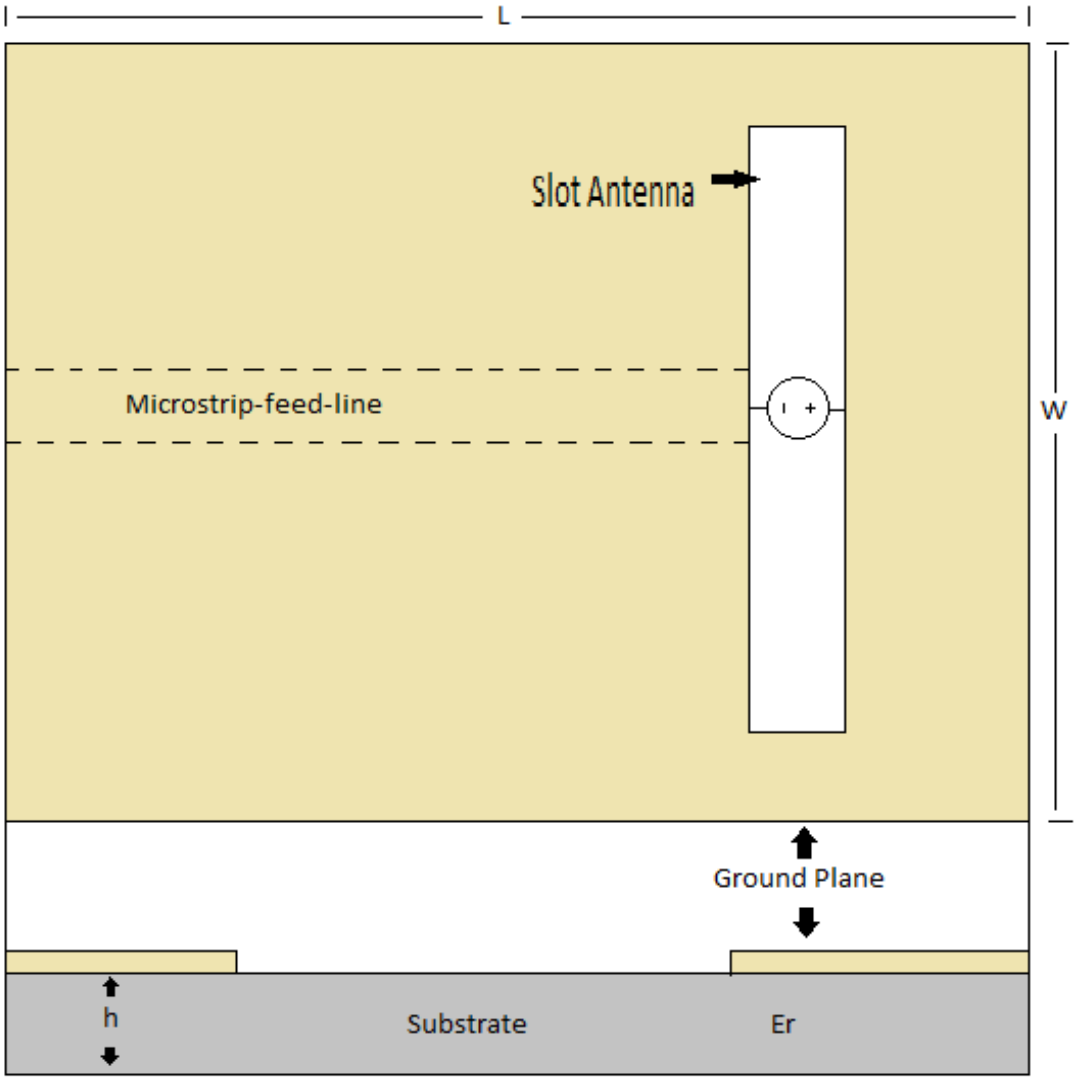

Figure 2.2. A rectangular slot antenna.

Different techniques and approaches are used in [45, 47, 49, 50, 52-55, 60, 63, 64, 68-70] to enhance the radiation pattern of slot antennas, whilst reducing their size. The superior gain of 12.45 dB of miniaturized slot antennas reported in [70] leads to better and long distance communication between pico-satellites, and with a ground station. However, their main limitation is the narrow bandwidth and large antenna size; i.e., 16×17×0.68 cm^3. On the other hand, the design of [50] has a small antenna size; i.e., 5.327×5.327×0.05 cm^3, and a low gain of 2.7 dB. In terms of bandwidth, Liao et al. [45] reported a significant enhancement in the CP bandwidth of 51.7% at the 2.45 and 3.15 GHz frequency bands, high gain of 5 dB and small antenna size;

i.e., 6×6×0.08 cm^3. To date, the only design with steerability is the one reported in [64] where reconfigurable polarization is achieved using a quasi-lumped quadrature coupler. Further details can be found in section 2.1.2.1. In order to make the designs in [45, 46, 49, 50, 52-55, 60, 63, 68-70] steerable, researchers have employed different techniques and approaches. For example, using arrays and external circuits. These works are further discussed in the following sections.

2.1.2.1 Steerability and gain improvement

Beam-steering and high gain antennas are key components in applications that require tracking and frequent satellites repositioning. The main techniques used include the cavity-backed model [54], half mode substrate integrated waveguide (HMSIW) [52], quasi-lumped quadrature coupler (QLQC) [64], and parasitic patch and windowed metallic superstrate [70]. These techniques are discussed below:

- *Cavity-backed model*

  This is an important technique as it suppresses the back-lobe radiation of the antenna, and hence increases its directivity and gain [100]. In [54], Sievenpiper et al. describe the use of a cavity-backed model for a low-profile slot antenna that operates in the 2.34 GHz to achieve higher gain and better radiation performance. The key idea is to use a thin cavity-backed crossed-slot antenna with a single probe feeding network. The use of two orthogonal crossed-slots with slightly different lengths provides circular vertical polarization. This is important as it enhances the signal strength and reception; hence, it helps establish cross-links between satellites. Furthermore, this technique prevents back radiation. This in turn increases the antenna gain and facilitates long distance communications. They reported a gain of 4 dB for LP and CP. The main limitation is the use of a quarter wave depth cavity that results in a non-negligible increase to the total antenna weight as the added cavity is of size 6.3 × 6.3 × 0.3 cm^3.

- *Half mode substrate integrated waveguide*

  The main advantage of this technique is the reduction in micro-strip patch antenna size whilst maintaining the same resonant frequency. In [52], Razavi et al. applied

this technique to create a novel low-profile circularly polarized cavity-backed antenna for right and left-hand polarization based on half mode substrate integrated waveguide technique [101]. The key idea is to use triangular quarter-wave length patches as a cavity. The resulting antenna has two electrical fields with equal magnitude and 90-degree phase shift. This is important as it achieves high gain and CP. Moreover, applying HMSIW to the cavity backed antenna design of [52] leads to a further reduction of the substrate integrated waveguide (SIW) that is used in conventional metallic cavity-backed antennas. They reported high gains of 4.87 and 4.2 dB for right and left hand CP. Compared to the design in [59], the one reported in [52] has a much smaller structure waveguide and hence smaller antenna size; i.e., $3.7\times1.61\times0.078$ cm^3, wider bandwidth; i.e., 1.74% (153 MHz) and similar gains of about 4.20 to 4.80 dB.

- *Quasi-lumped quadrature coupler (QLQC)*

  This tuneable coupler has the ability to generate polarization diversity with frequency agility [102]. To this end, Row et al. [64] propose a novel design for a frequency agile slot antenna with reconfigurable polarization. This is an important capability as switching between circular and linear polarization at high gains leads to better signal strength. The main approach is to implement the ring slot antenna with a metallic reflector and then to excite it with a QLQC. The use of a reflector ensures the back radiation is reduced and hence, increases gain. Moreover, QLQC works in two different modes; quadrature hybrid mode and T-junction power divider mode to provide circular and linear polarizations respectively. They reported a high gain of 4.5 dB and a bandwidth of about 2.9% (1.77 GHz).

- *Parasitic patch and windowed metallic superstrate*

  This technique has the ability to increase antenna gain significantly. This is important for many applications that require high gains; e.g., point-to-point communications. In [70], Tu et al. present a novel low-profile, high gain slot antenna that operates in the 2.35 to 2.55 GHz band. The main approach is to print parasitic patches symmetrically to the feeding line. This changes the bi-directional radiation pattern to unidirectional and hence, increases slot antenna gain. In addition, placing a windowed metallic superstrate above the slot antenna leads to

further gain enhancement. The main advantage is the superior gain of about 12.45 dB for long distance communications. Its main limitation is its large size; i.e., 16×17×0.6 cm^3. Compared to the designs in [52] and [54, 64], the design in [70] has a much higher gain and provides longer communication distance.

2.1.2.2 Antenna bandwidth enhancement

The main techniques used to enhance bandwidth include using a coplanar waveguide (CPW) [45], inductive elements [47], series feed configuration [53], folded and self-complementary structures [63], asymmetry structure [60], and distributed and lump elements [69]. All these techniques achieve significant enhancement in bandwidth ranging from 2.1% (0.027 GHz) to 51% (1.5 GHz) and operate in the 0.336 to 3.15 GHz range. Moreover, these approaches have no significant effect on antenna size. The following sections provide the main approaches used for bandwidth enhancement:

- *Coplanar waveguide (CPW) feed*

  This feed mechanism is an alternative to using a micro-strip-line because it has many advantages such as low dispersion, low radiation leakage, and the ability to effectively control the characteristic impedance of an antenna [103-105]. In [45], Liao et al. present a square slot antenna that has excellent broadband CP bandwidth. This is important for modern wireless communication as the signal level remains constant with varying antenna angles. This is required for a cross link communication between a transmitter and a receiver. The main approach is to feed the slot antenna with a lightening-shaped feed-line from the centre signal strip of the feeding CPW, and then to embed a tuning stub in the feeding. Moreover, Liao et al. [45] embed two symmetrical F-shaped slits in the opposite corners of the ground plane to introduce more resonant branches. They reported a superior bandwidth of 51.7% at the 2.45 and 3.15 GHz frequency bands. It, however, suffers from back-lobe radiation which in turn reduces gain.

- *Series inductive elements*

  Behdad et al. [47] presented a small antenna with a wide bandwidth. This is important as it leads to better communication performance and coverage, less fabrication cost, and thus is more suitable for pico-satellites. The key idea is to examine the use of multi-resonance (double resonant) antenna structures at 850 MHz and inductively loaded miniaturized slot antenna at 1 GHz. The use of series inductive elements along the antenna slot leads to a reduction in the guided wavelength of the resonant slot line. This in turn decreases the overall antenna length. In addition, using a double resonant antenna leads to significant bandwidth enhancement. As a result of using a single slot antenna (SEA), the antenna has a bandwidth of 0.9% (8 MHz) while 2.54% (21.6 MHz) for a double slot antenna (DEA). This is an improvement of about 1.64%. Behdad et al. [47] remarked that the only limitation is the need for an external network for impedance matching.

- *Series feed configuration*

  This configuration is mainly used to improve CP bandwidth. In [53], Row presents a CP squarer-ring slot antenna design that operates in the 2.695 GHz and has a small size and wide bandwidth. The main approach is to feed the narrow square-ring slot antenna with a series micro-strip-line-feed configuration. They use a coupling strip to feed the two orthogonal sides of a square ring slot antenna with the same amplitude at 90 degrees out of phase by optimizing slot side lengths. This is important as it achieves CP without the need to use an external coupler, which in turn enhances bandwidth and reduces antenna size. Moreover, Row uses a micro-strip impedance transformer to achieve good impedance matching at 50 ohms. He reports a CP bandwidth of 6.1% (2.695 GHz) at a return loss of about -30 dB. Compared to the designs in [45, 47], the antenna in [53] has wider bandwidth. Its main limitation is its back-lobe radiation, which decreases gain.

- *Folded and self-complementary structures*

  Folded and self-complementary structures approaches are mainly used to increase the bandwidth of miniaturized antennas. Azadegan et al. [63] employ such structures to increase bandwidth. Their first approach is to use a complementary

pair of miniaturized slot antennas; i.e., a miniaturized folded printed wire. The main idea is to increase the radiating aperture of the antenna without increasing the total antenna size or reducing its efficiency. Additionally, replacing slot lines by metallic strips to work as a ground plane leads to wider bandwidth of about 0.60% (0.336 GHz). The second approach is to implement a self-complementary folded antenna structure. This approach is a combination of the first approach and a normal folded slot antenna. Furthermore, its final structure is a self-complementary H-shaped antenna with a wide bandwidth of 2.1% (1.3 GHz). Azadegan et al. [63] pointed out that this design can be matched easily without the need for external matching networks. This is important as it leads to less complex and low cost designs.

- *Asymmetry structure*

  This technique is simple and is mainly used for CP bandwidth enhancement. In [60], Wong et al. propose a square and annular printed ring antenna that achieves 3 dB axial ratio CP bandwidth and operates in the 1.5 and 1.720 GHz band. This is significant as CP is important for establishing cross-link communications. Moreover, achieving wider bandwidth and higher gain means better and longer communication distance between any two satellites. The key idea is to introduce some asymmetry into the structure of the ring slot antenna in order to enhance its bandwidth and to obtain good CP. The resulting design achieves a higher bandwidth of 4.3% (0.0645 GHz) while for an annular ring slot antenna it is 3.5% (0.0602 GHz). The main limitation is the slight asymmetry in radiation patterns. The authors posit that this is due to the asymmetry inherent in the antenna structure.

- *Distributed and lump elements*

  This technique enhances bandwidth by varying the CP antenna frequency. Lee et al. [69] propose a lightweight annular-ring slot antenna that operates in the 1.58 and 2.59 GHz bands. The main approach to obtain CP is to excite the square ring slot antenna using a L-shaped coupling strip. This provides good CP bandwidth and has a stable radiation pattern across all supported bandwidth. Moreover, distributed and lump elements are used to vary the CP operating frequency to

enhance its bandwidth. The reconfigurability of the operating frequency is important as it leads to better CP performance. Compared to the designs in [53, 60] and [47, 63], the antenna design in [69] has wider bandwidth; i.e., 730 MHz. However, the main limitation of the design in [69] is its large size; i.e., $10\times10\times0.16$ cm^3.

2.1.2.3 Slot antenna miniaturization

Recall that pico-satellites are limited in size and they must be light. Consequently, miniaturization of employed antennas is critical. In this respect, the following techniques have been used to yield a reduction ranging from $3.7\times1.61\times0.078$ (smallest) to$16\times17\times0.68$ cm^3 (largest):

- *Inductive load*

  The approach involves loading the antenna with series inductive elements (coiled wire) along the aperture of the slot antenna. In [49], Azadegan et al. present a novel small slot antenna that works in the 0.3 GHz frequency band. The main approach is to short the slot line with an inductor; the line has an electrical length is less than a quarter wavelength. Moreover, they use a substrate with rectangular spiral geometry. This is important as it leads to higher antenna efficiency. The main limitation, as pointed out by the authors, is the resulting narrow bandwidth; i.e., 1.6% (4.8 MHz). This is because a higher inductive load leads to a reduction in bandwidth. Another limitation is the dramatic increase in dielectric and ohmic losses [106] that are attributed to the concentration of fields over a very small area of substrate. An open problem is how to increase gain and bandwidth without increasing physical size and loss.

- *Physical aperture expansion*

  This is an effective technique that expands the physical size of an antenna's slot to enhance bandwidth and to achieve high efficiency without increasing antenna size. Azadegan et al. [50] propose a new miniaturized antenna structure with a large radiation conductance (physical aperture), bandwidth, and efficiency as compared to the miniaturized slot antenna presented in [49]. Advantageously, the resulting

antenna has the same size. This is important as it leads to high communication performance, and less fabrication cost. The key idea is to increase only the physical aperture of the folded slot to as large as that of the miniaturized slot in the design of [49]. This increases the bandwidth and the efficiency of the folded slot antenna without increasing its overall size. Moreover, they use a coplanar waveguide. This significantly reduces matching impedance but the resulting antenna has a low gain.

- *Loading wires*

  Its main advantage is its ability to reduce the operating frequency without increasing antenna length. In [68], Ghosh et al. present a new miniaturization technique for planar slot antennas using loading wires. These wires are used on either sides of the antenna aperture and they penetrate the substrate or a cavity backing to compensate for the reactive environment. This is important as it leads to a reduction in resonant frequencies without increasing antenna size. The authors propose two slot antenna prototypes; namely, one on a dialectic substrate that operates in the 2.32 GHz band, and another on a ground plane with backing cavity that operates in the 3.26 GHz band. A reduction of 28.83% in resonant frequency is achieved for the slot antenna on a dielectric substrate, and 45.52% for the slot antenna on the ground plane. Moreover, the use of backing cavity suppresses back radiation, and improves gain.

- *Series of parallel strip lines*

  This technique is mainly used as an alternative to the traditional cavity-backed model. Hong et al. [55] outline a new technique to reduce the size of cavity-backed slot antennas (CBSA) by substituting the traditional cavity structure with a series of miniaturized transmission line type resonators. The main idea is to design the slot antenna using a finite width metallic strip connected to a number of parallel short-circuited micro-strip lines that have the same physical and electrical length as the width of the ground plane. This reduces the physical length of micro-strip lines while retaining their electrical length. They achieve a size reduction of approximately 65%. Furthermore, despite its reduced physical dimensions, the

antenna has a gain of 3.7 dB with excellent impedance matching, and high radiation efficiency.

The foregone twelve slot antenna designs aim to achieve beam steerability, high gains, small size, and wide bandwidth. As Table 2.3 shows, all these designs achieve gains ranging from 1.7 to 12.45 dB, with an antenna size ranging from $3.7\times1.61\times0.078$ cm^3 to $16\times17\times0.68$ cm^3. Moreover, they work in the UHF, L, S, C and X frequency bands (0.3 – 8.8 GHz). In terms of gain, bandwidth and size, all these designs are suitable for pico-satellites communications.

Table 2.3. Different slot antenna designs and their performance

Reference	Gain (dB)	Size (cm)	Band (GHz)
Sievenpiper et al. [54]	4	6.3×6.3×0.03	S-band (2.34)
Razavi et al. [52]	4.8	3.7×1.61×0.078	X-band (8.8)
Row et al. [64]	4.5	11×10×0.22	L-Band A (1.67), B (1.77) and C (1.9)
Tu et al. [70]	12.45	16×17×0.68	S-band (2.45)
Liao et al. [45]	5	6×6×0.08	S-band (2.45 and 3.15)
Behdad et al. [47]	1.7	5.73×5.94×0.05	UHF-band (0.848, 0.85 & 0.86)
Row [53]	3.3	5.4×5.4×0.16	S-band (2.695)
Azadegan et al. [63]	4.5	10×8×0.0787	UHF-band (0.336) and L-band (1.3)
Wong et al. [60]	3.5	8×8×0.16	L-Ban (1.5) and (1.720)
Lee et al. [69]	3	10×10×0.16	L-band (1.58) and S-band (2.59)
Azadegan et al.[49]	3	5.5×5.5×0.0787	UHF-band (0.3)
Azadegan et al. [50]	2.7	5.327×5.327×0.05	UHF-band (0.337)
Ghosh et al. [68]	2.3	12×12×0.254	S-band (2.3 and 3.26)
Hong et al. [55]	3.7	5.3×4.6×0.685	S-band (2.25)

2.2 Qualitative Evaluation

This section provides a qualitative comparison of planar antenna designs and their suitability for use on pico-satellites. Table 2.4 summarizes their features and performance in terms of mass, size, gain, beam steerability, type of polarization, operating frequency band, and return loss. Most designs are relatively small, light, have small return loss and provide CP. Amongst all antenna designs listed in Table 2.4, only the designs in [6, 57, 61, 62, 65] and [54] have steering capability. On the other hand, non-steerable designs require external circuits and arrays in order to become steerable; this, however, adds extra cost and complexity to the design. Moreover, the design in [65] achieves the highest gain of 18 dB at a wide bandwidth of 47.8% (2.95 GHz); however, its size is very large, i.e., exceeds 10 cm, and is not suitable for pico-satellites. In terms of bandwidth, the designs of [46] and [56]

demonstrate a significant bandwidth enhancement of 98% (3.57-10.46 GHz) and 76.18% (3.43-7.45 GHz) respectively. As set out in Table 2.4, the following criteria is used to determine the most suitable antenna designs for use on pico-satellites: small physical size at the lower end of operating frequencies, wide bandwidth, small return loss (< -10 dB), steerability and relatively high gain. The most important factor is antenna size. The best designs that address most of the pico-satellite's challenges are to be found in [45, 46] and [56]. They achieve wide bandwidth, are small and have high gains at lower end of operating frequencies. Their main limitation is their lack of steering capability. In chapter 3, the designs in [45, 46] and [56] will be evaluated on a common platform.

Table 2.4. Comparison between all types of planar antennas

Ref	Method	Gain (dB)	Volume (cm^3)	Mass	Beam Steerability and type	Polarization & Bandwidth (BW)	Freq. (GHz)	Return Loss (dB)	Suitability for CubeSats
[6]	Sequential phase-rotation	6.9	9 × 9 × 0.5	162g	Electronic using digital phase shifter	CP	5.8	-25	✓
[61]	Sequential phase-rotation	CP=7.1 LP = 7.5	15×15 × 0.96	Light	Electrically steerable	CP or LP with BW= 3.4%	2.37	-35	×
[65]	Sequential phase-rotation	18	16 × 16 × 0. 35	Light	Electrically steerable	CP & 47.8% with AR<1 dB	6.175	-27	×
[62]	Retrodirective	6.25	10×10×0.16	Light	Self-steering	CP	10.5	n/a	✓
[57]	Beam forming algorithm	4.8	10×10×0.16	heavy	Electrically steerable	CP	2.45	n/a	✓
[66]	PBG structures	5.02	12×16.8×2.5	Light	Not steerable	CP = 5.4 %	14.15	-12	×
[67]	Transparent mesh line geometry	n/a	8.01×8.01×2.25	Light	Not steerable	CP & 80 MHz	2.40	-20	✓
[59]	Single proximity coupled feed	6	7 ×7 × 0.16	Light	Not steerable	CP	1.525	-40	✓
[42]	Agile polarization	CP = 4 and LP = 6.2	2.77×2.77×0.0892	Light	Not steerable	CP or LP & 3.8%	3.5	-34	✓
[58]	Cavity model	5.9	8.8 × 8.8 × 2.5	Light	Not steerable	CP	4.32	-12	✓
[41]	U-slot and L-slit geometries	U-slot = 2.58 L-slit = 2.4	U-slot = 5.4×5.4×0.7 L-slit = 4×4×0.7	Light	Not steerable	U-slot – CP & 53.54% L-slit – CP & 45.12%	U-slot = 4.5 L-slit = 5.5	U-slot = -15 L-slit = -24.3	✓
[46]	Folded-patch feed	1^{st} 4.9 2^{nd} 3.9	1^{st} = 2.8×1×0.7 2^{nd} =1.8×1.5×0.7	Light	Not steerable	1^{st} = CP with 94.17% 2^{nd} = CP with 98.22%	1^{st} = 5 2^{nd} = 4.2	1^{st} = -23.69 2^{nd} = -34.15	✓
[44]	Meandering	n/a	2.21 × 2.21 × 1.5	Light	Not steerable	1^{st} with 2.98% 2^{nd} with 1.15%	1^{st} = 1.575 2^{nd} = 0.869	1^{st} = -28 2^{nd} = - 30.5	✓
[51]	Meta-material	5.96, 4.86, & 4.23	$3.14 \times r^2 \times 0.078$ r =1.2, 0.8, and 0.6	Light	Not steerable	Cross polarization	2.45	-26	✓

[48]	Cylindrical skirts with shorting pins	n/a	$3.14 \times 2.7^2 \times 1.37$	Light	Not steerable	Cross polarization with 4.7% (116.34 MHz)	2.45	-30.5	✓
[40]	Sequential phase-rotation	5.9	3.97×1.2×0.20	Light	Not steerable	CP with 1500MHz	2.45	-25	✓
[43]	Artificial magnetic conductor	1.53	3.8×3.8×0.32	Light	Not steerable	CP with 4.08% (100 MHz)	2.45	-13	✓
[54]	Cavity-backed model	4	6.3 × 6.3 × 0.03	Light	Steerable	CP	2.34	-12	✓
[52]	Half mode substrate integrated waveguide.	RHCP= 4.8 LHCP= 4.2	3.7 × 1.61 × 0.078	Light	Not steerable	RHCP with 1.7% LHCP with0.66%	8.67	RHCP=-33 LHCP= -20	✓
[64]	Quasi-lumped quadrature coupler	CP = 4.5 LP = 4	11 × 10 × 0.22	Light	Not steerable	CP or LP	CP = 1.67 LP = 1.9	CP = -23 LP = -16.5	✓
[70]	Parasitic patch and windowed metallic superstrate	12.45	16×17×0.68	Light	Not steerable	CP BW= 80 MHz	(2.45)	-15	×
[45]	Coplanar waveguide (CPW) feed	5	6 × 6 × 0.08	Light	Not steerable	CP BW= 1500 MHz	3.45	-17	✓
[47]	Series inductive elements	1.7	5.73 × 5.94 × 0.05	Light	Not steerable	CP with 21 MHz	0.848	-35	✓
[53]	Series feed configuration	3.3	5.4× 5.4 × 0.16	Light	Not steerable	CP, BW=6.1%	2.695	-34	✓
[63]	Folded and self-complementary structures	1^{st} = 4.5 2^{nd} = 1.3	1^{st} = 10 × 8× 0.0787 2^{nd} = 4×4×0.0787	Light	Not steerable	Cross polarization with 1.1-2.1 %	1^{st} = 0.336 2^{nd} = 1.3	1^{st} = -26.5 2^{nd} = - 28	✓
[60]	Asymmetry structure	3.8	8 × 8 × 0.16	Light	Not steerable	CP	1.72	n/a	✓
[69]	Distributed and lump elements	3	10 × 10 × 0.16	Light	Not steerable	CP	1.58	-10	✓
[49]	Inductive Load	3	5.5 × 5.5 × 0.0787	Light	Not steerable	Cross polarization	0.3	-25	✓
[50]	Physical aperture expansion	2.7	5.327×5.327× 0.05	Light	Not steerable	Cross polarization	0.337	-30	✓
[68]	Loading wires	2.3	12×12×0.254	Light	Not steerable	Cross polarization	3.26	-18	×
[55]	Series parallel strip lines	3.7	5.3×4.6×0.685	Light	Not steerable	CP	2.25	-30	✓

[56]	Shorting Pins	5, 6.3 and 8	3.4×1.4×0.7	Light	Not steerable	n/a	4.74, 6.13 and 6.73	-24, -28.5, and -22	✓

2.3 Summary

This chapter has presented a comprehensive survey of small micro-strip patch and slot antennas. These antennas are light, small in size and achieve circular and cross polarization. Thus, they are most suited for use on pico-satellites. This chapter also presented an extensive qualitative comparison of antenna designs in terms of their features, design challenges, limitations, advantages and performance. Amongst all previous S-band planar antennas, the most suitable designs that address most of the CubeSat challenges are shorted patch, CPW-feed square slot and asymmetric E-shaped antennas.

A number of open problems are identified. First, most current designs are non-steerable. Second, current micro-strip patch antennas that are suitable for CubeSats have a maximum gain of only 5.9 dB at 2.45 GHz. Third, current slot antennas have low gains and narrow bandwidth due to their bidirectional radiation pattern. One solution is to use quarter wave depth cavities to redirect the back-radiation pattern forward and hence increase the total gain. However, this cavity incurs additional weight, is expensive to construct and is difficult to integrate with planar circuits. Another technique is to use a metallic reflector [108]. However, the distance between the reflector and the slot antenna is high, i.e., 30.5 mm for 2.45 GHz. This makes it unsuitable for CubeSats. Fourth, existing micro-strip patch and slot antennas that are suitable for CubeSats have not been evaluated on a common platform. In particular, their performance at 2.45 GHz in the presence of a CubeSat's body is unknown.

To address the aforementioned limitations, Chapter 3 provides a quantitative evaluation of shorted patch, CPW-feed square slot and asymmetric E-shaped antennas. In particular, Chapter 3 evaluates the effect of a 2U CubeSat body on the performance of the said antennas. Then Chapter 4 outlines a repurposed shorted patch and CPW-feed square slot antenna for use on the 2.45 GHz frequency band. Apart from that, from Table 2.4, it can be seen that most of the reviewed designs are non-steerable. To this end, Chapter 5 and 6 propose to use a CPW-fed slot antenna configuration by placing a single antenna on each face of a CubeSat to achieve beam steering. Furthermore, Table 2.4 shows that the maximum gain of current patch antennas that are suitable for use on a CubeSat is only 5.9 dB. Thus, Chapter 4

presents a wideband F-shaped patch antenna for S-band CubeSats communications. The results show that it has a high gain of 8.5 dB with a wide bandwidth of 1121 MHz. Table 2.4 also shows that slot antennas have low gain due to their back-lobe radiation. To address this problem, Chapter 5 and 6 present a unidirectional high gain CPW-fed slot antenna. The main idea is to use metasurface substrate and a CubeSat's body to redirect the back-lobe radiation forward and hence achieve a superior gain. The next chapter provides a quantitative evaluation and comparison of the most suitable existing patch and slot antennas for CubeSats.

Chapter 3

MICRO-STRIP AND SLOT ANTENNAS FOR CUBESATS

To date, no works have compared existing micro-strip patch and slot antennas and evaluated their suitability for CubeSat communications. Therefore, this chapter addresses this gap. It compares and evaluates the most suitable micro-strip patch and slot antennas on a common platform. Critically, it studies how their performance is affected by a 2U CubeSat body, and present their performance in terms of volume, gain at 2.45 GHz, bandwidth, return loss, robustness, beam steerability and cost.

3.1 Quantitative Evaluation

As mentioned in Chapter 2, the designs of [45, 46] and [56] address most of the pico-satellite challenges listed in Table 1.2 and they provide good radiation performance as compared to all other reviewed planar antenna designs. However, their performance in the presence of a satellite body is unknown.

This section first presents the CPW-feed square, shorted patch, and asymmetric E-shaped micro-strip patch antenna designs. Then it presents results from experiments, conducted using HFSS version 16 [107], concerning each antenna design with and without the effect of a 2U (10cm×10cm×20cm) CubeSat body. The section concludes with comments on the suitability of the aforementioned antennas for CubeSat communications.

3.1.1 CPW-feed square slot antenna [45]

Figure 3.1 (b) shows the square slot antenna model under study. The antenna has a total size of 60×60 mm^2; it is fabricated on a FR4 substrate that is 0.8 mm thick. The coplanar wave guide feed line technique is used with a fixed width of a single strip; i.e., 4.2 mm and the gap between the line and ground plane is 0.3 mm in length in order to achieve 50 Ω matching. To enlarge the CP bandwidth, the ground plane has

two symmetrical F-shaped slits. This CP bandwidth can be further enhanced by varying the dimensions of the lightening-shaped feedline. The evaluated antenna operates at resonant frequencies of 2.45 and 3.2 GHz; see Figure 3.4. It shows that the obtained resonant frequency 3.2 GHz is slightly lower than the resonant frequency obtained by the authors of [27], i.e., 3.45 GHz. This margin of error is acceptable as both frequencies are located within the operating -10 dB bandwidth 2.3 to 3.8 GHz. To observe the effect of the satellite body on the antenna's performance, the CPW-feed square slot antenna is mounted on the 2U CubeSat face; see Figure 3.1 (a).

3.1.2 Shorted patch antenna using folded-patch techniques [46]

Figure 3.2 (b) shows the tested shorted patch antenna model. The upper and lower patches have dimensions 18×15 and 7.5×6.5 mm^2 respectively. These patches are connected together via a folded ramp-shaped part. Also, they are connected to a 30×30 mm^2 ground plane through shorting pins and probe feed. Moreover, in order to obtain wider bandwidth, air substrate and folded ramp-shaped part are used to decrease the quality factor (Q) and inductive reactance of the probe feed. The main purpose of using shorting pins at the edges of the upper patch is to achieve miniaturization at wide impedance bandwidth. In addition, the centre pin on the upper patch is used to broaden the impedance bandwidth by generating resonances at 4.45 and 7 GHz. Figure 3.2 (a). shows the shorted patch antenna on a 2U CubeSat.

3.1.3 Miniaturized asymmetric E-shaped micro-strip patch antenna with folded-patch feed [56]

Figure 3.3(b) shows a 3D model of a miniaturized asymmetric E-shaped micro-strip patch antenna. The upper patch resembles an asymmetric 'E' with a total size of 34×13 mm^2. The folded-patch feed or lower patch has a rectangular shape with size 23×5 mm^2. The upper and lower patches are connected to the ground plane through shorting pins. Air is assumed to be the supporting substrate. The shorting pins are used to decrease the physical antenna size by increasing its electrical length. Moreover, the unequal arms of the asymmetric E-shaped patch (upper patch) are

designed to produce three different resonant frequencies to enlarge the antenna's bandwidth. Figure 3.3 (a) shows the implementation on a 2U CubeSat body.

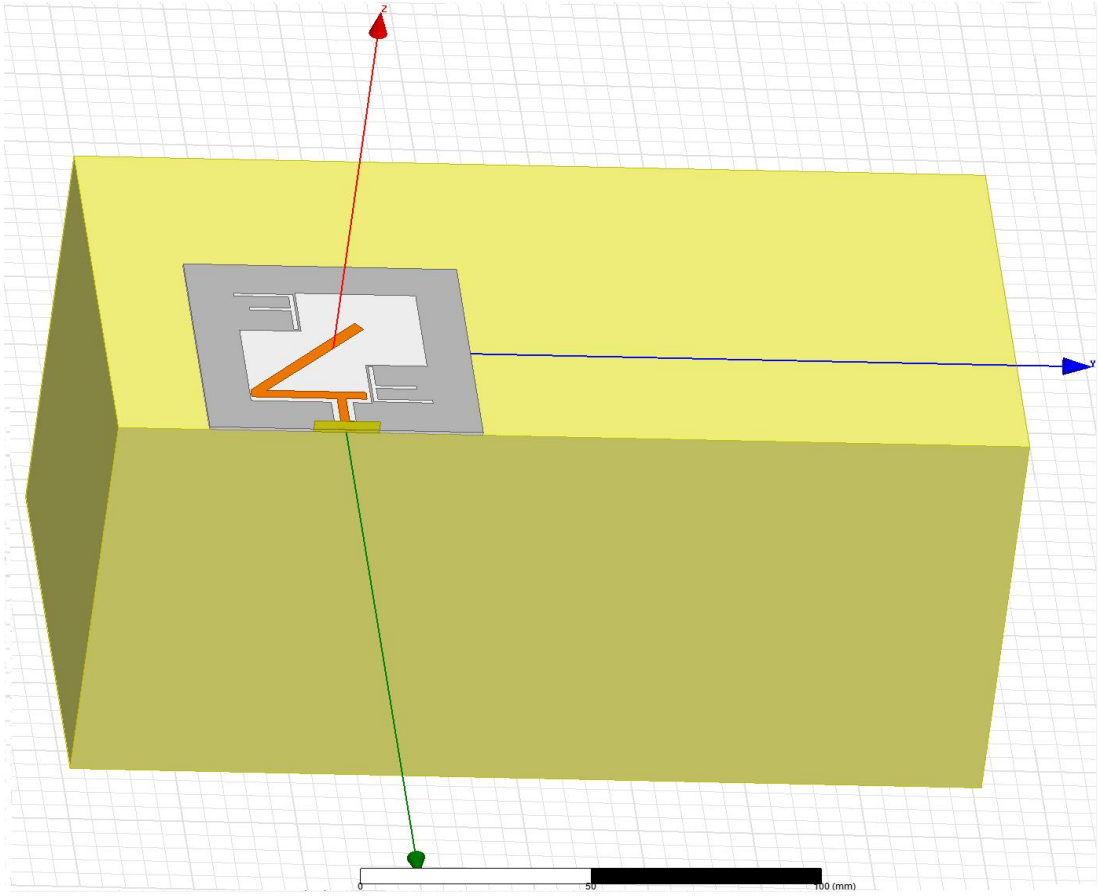

(a)

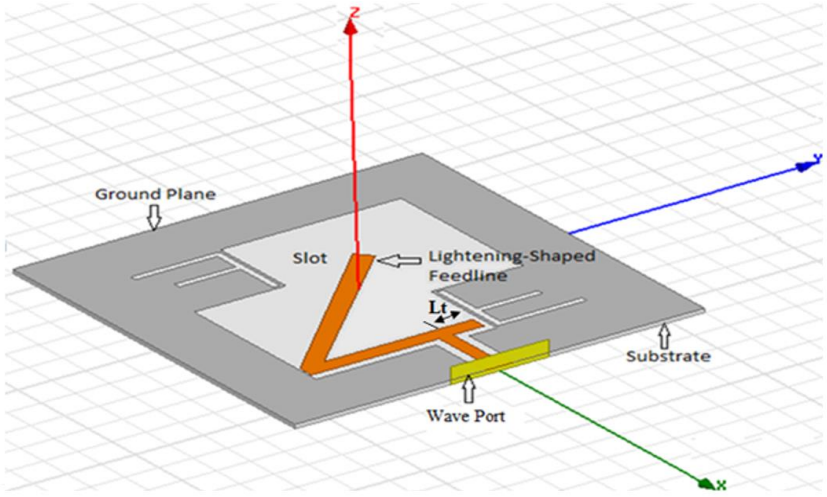

(b)

Figure 3.1. A CPW-feed square slot antenna: (a) installation on a 2U CubeSat face, and (b) geometry

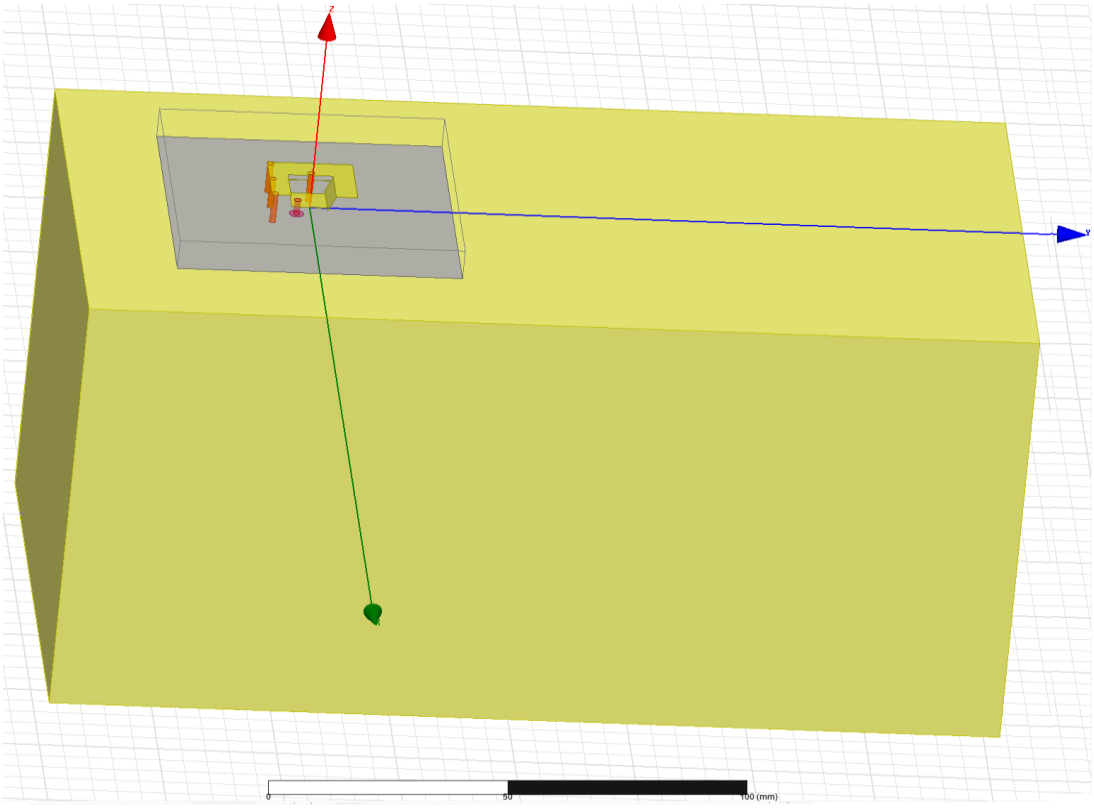

(a)

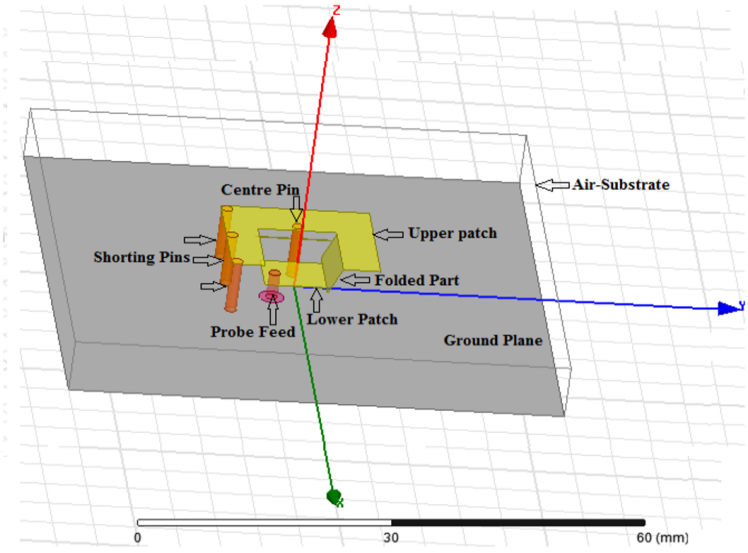

(b)

Figure 3.2. Geometry of a shorted patch antenna (a) with a CubeSat, and (b) without a CubeSat.

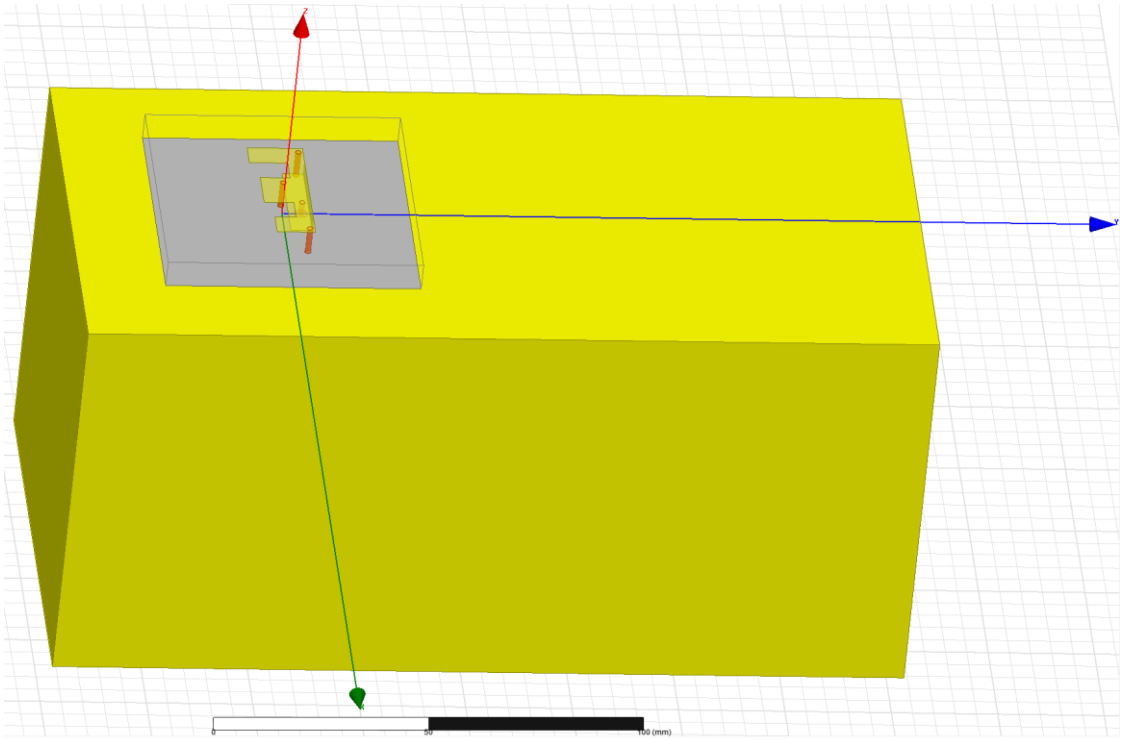

(a)

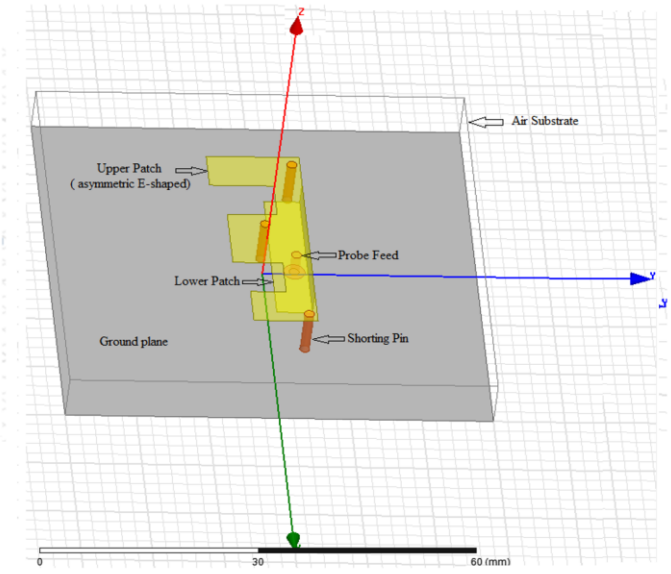

(b)

Figure 3.3. Geometry of an asymmetric E-shaped patch antenna (a) with a 2U CubeSat, and (b) without a 2U CubeSat.

3.2 Simulation Results

- *CPW-feed square slot antenna*

  Figure 3.4 shows the return loss over different frequencies for the CPW-feed square slot antenna with and without the effect of a CubeSat body. The CubeSat body has a significant effect on the return loss; it recorded increases from -27.5 to -10 dB. This means most of the power is reflected back to the antenna instead of being radiated into the space. Moreover, the operating frequency increases from 3.2 to 4.1 GHz. As shown in Figure 3.4, the -10 dB bandwidth without a CubeSat is 1600 MHz (2.3-3.9 GHz).

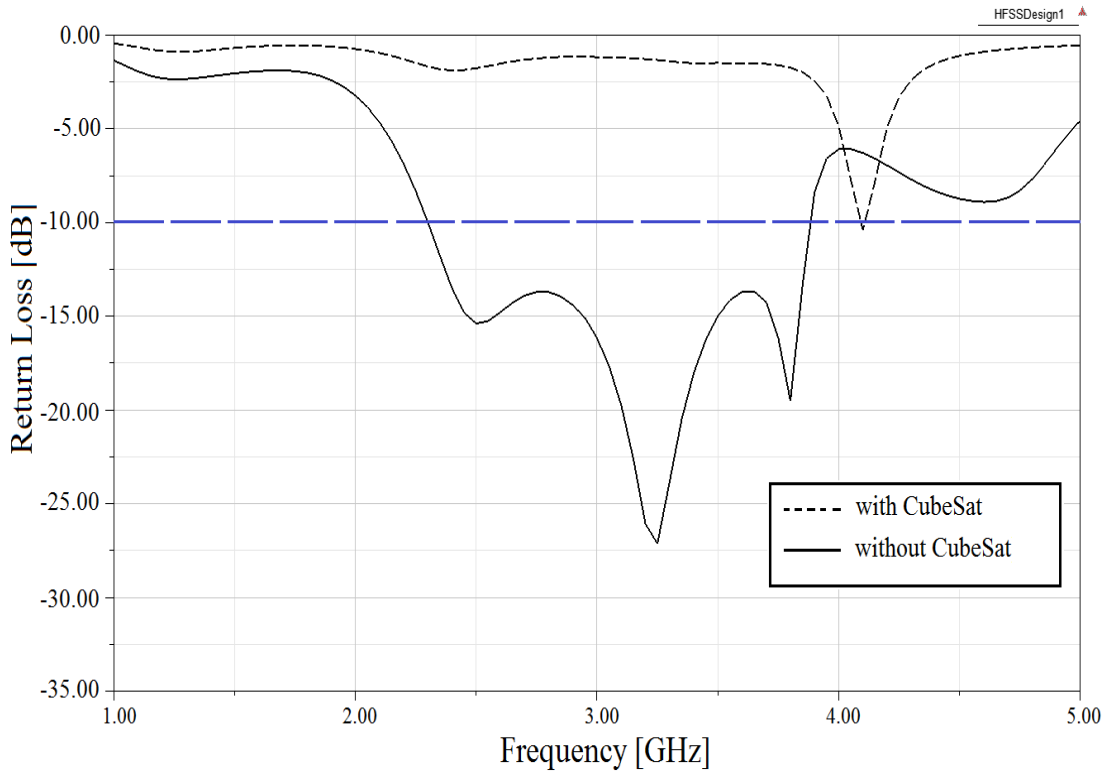

Figure 3.4. Return losses (S_{11}) of a CPW-feed square slot antenna.

Figure 3.5 shows the axial ratio of the CPW-feed square slot antenna with and without the effect of the 2U CubeSat body. Without the CubeSat, the antenna achieved a wide 3 dB axial ratio bandwidth of about 1120 MHz, ranging from 2.28 to 3.4 GHz. The CubeSat's surface has a significant effect on the axial ratio.

In particular, placing the CPW-feed square slot antenna on the 2U CubeSat body reduces the 3 dB axial ratio bandwidth from 1120 MHz (without CubeSat) to 174 MHz (with CubeSat).

Figure 3.6 presents the peak gain of the CPW-fed square slot antenna. In the presence of a CubeSat body, the antenna achieves a gain of about 1.4 dB at 3.2 GHz. The maximum gain with and without the effect of the CubeSat body is 2.7 and -5 dB respectively at frequencies of 3.6 and 3 GHz respectively; see Figure 3.6. The 3D gains at 3.2 GHz are shown in Figure 3.7 (a) and (b). It shows that for the CubeSat case, the antenna has a higher gain.

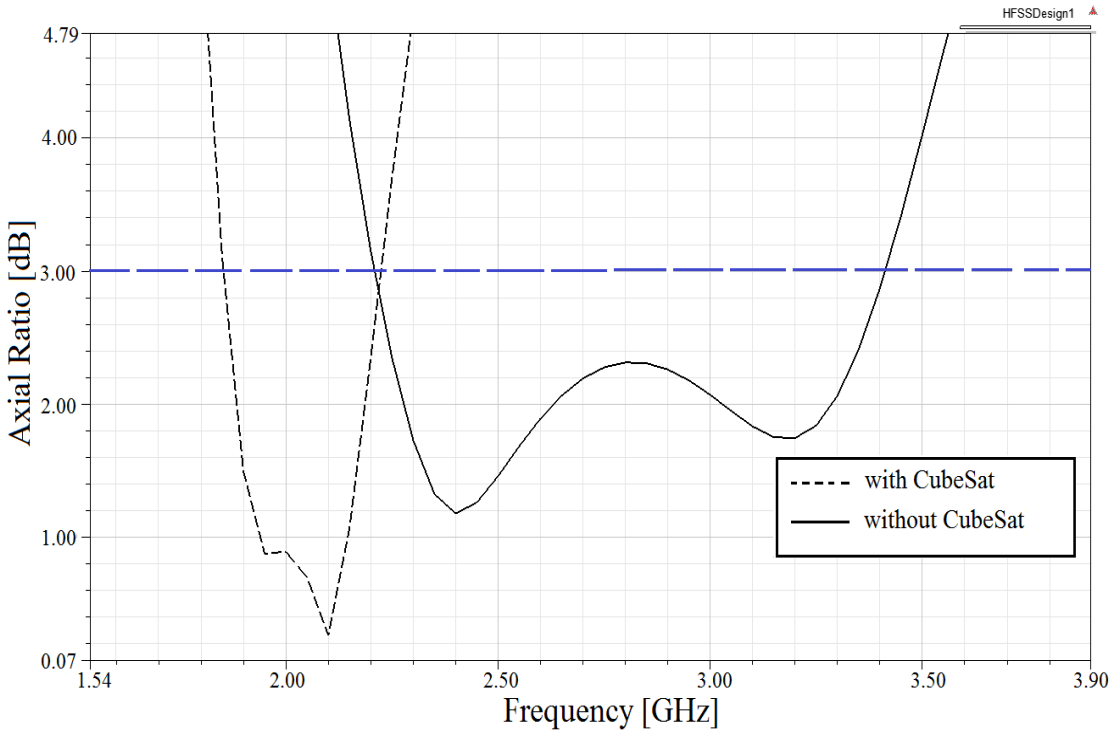

Figure 3.5. The axial ratio of the CPW-feed square slot antenna.

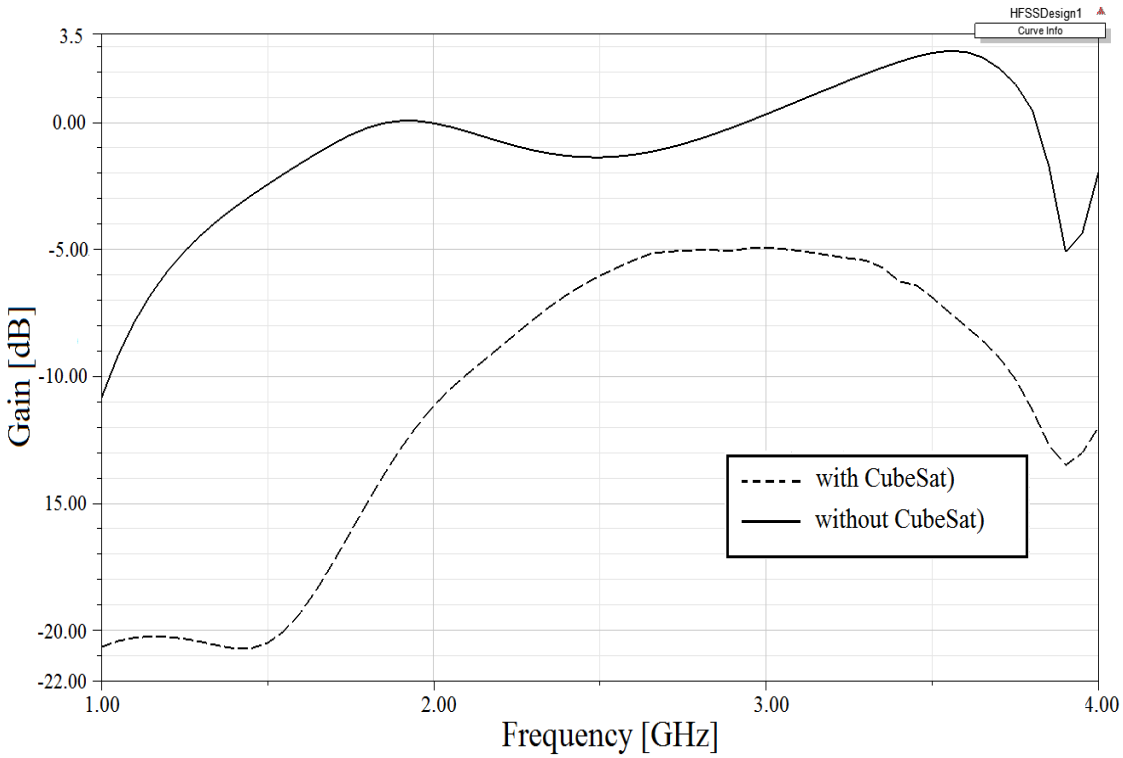

Figure 3.6. 2D gain of a CPW-feed square slot antenna.

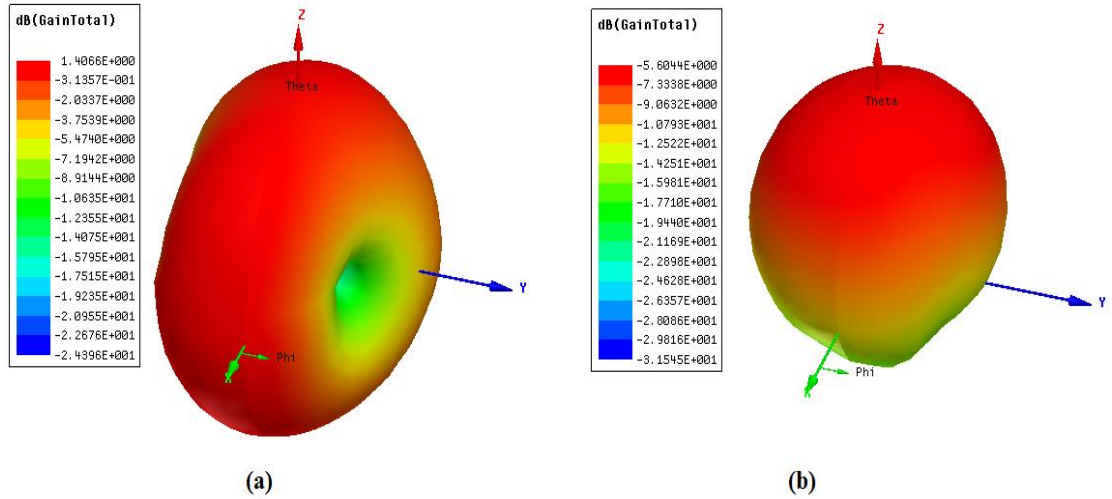

Figure 3.7. 3D gain of a CPW-feed square slot antenna at 3.2 GHz: (a) without, and (b) with a CubeSat.

- *Shorted patch antenna*

  Figure 3.8 depicts the return losses of the shorted patch antenna with and without the effect of a CubeSat body. The satellite body has a significant effect on the return loss; it decreases (or improves) from -26.5 to -43.3 dB. This means more power is radiated into space and less power is reflected. Moreover, there is a slight shift of 0.2 GHz in the first resonant frequency and 0.5 in the second resonant frequency. Compared to the shorted patch antenna without a CubeSat, the shorted patch antenna with a CubeSat has less bandwidth; i.e., 7150 MHz and much smaller return loss; i.e., -43.3 dB at 4.3 GHz; see Figure 3.8.

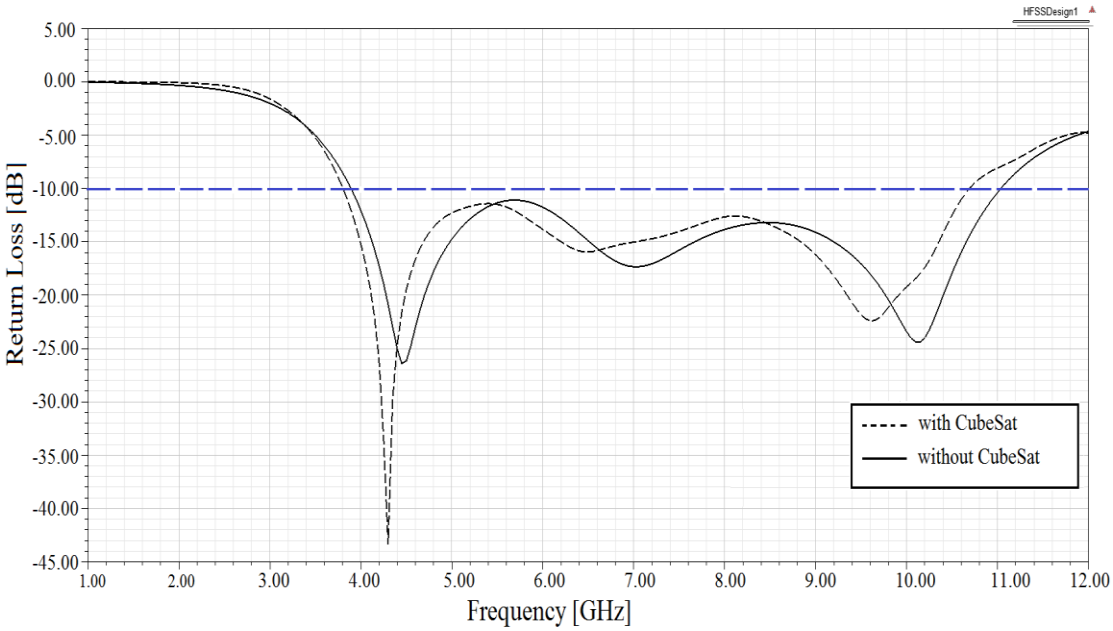

Figure 3.8. Return loss (S_{11}) of the tested shorted patch antenna.

This chapter now studies the effect of a 2U CubeSat body on the axial ratio and gain of the shorted patch antenna. Figure 3.9 shows the simulated axial ratio of the shorted patch antenna with and without a CubeSat as a function of frequency. It shows that the axial ratio for the CubeSat case has a smaller CP bandwidth; i.e., 650 MHz. The CubeSat body also has a significant effect on the shorted patch antenna gain. Without the CubeSat, the gain increased by 2.1 dB over the 2 to 4.5 GHz frequency range and decreased by 1 dB over the 5.2-9 GHz range when the

antenna is placed on the 2U CubeSat; see Figure 3.10. The peak gain of the shorted patch antenna with and without a CubeSat is 4 and 6.2 dB respectively at 4.3 GHz. This is because the aluminium surface of the CubeSat reflects some of the back lobe radiation forward. Hence, this yields further improvement in gain.

Figure 3.11 shows a 3-D plot of the shorted patch antenna far field radiation pattern. Without the CubeSat, the antenna has a maximum gain of 4.0 dB as compared to 6.22 dB when used on the CubeSat. The radiation pattern of the shorted patch antenna for the without CubeSat case is uniform. In contrast, it is non-uniform and the maximum gain is not at the broadside direction (Z direction) when the antenna is used on a CubeSat.

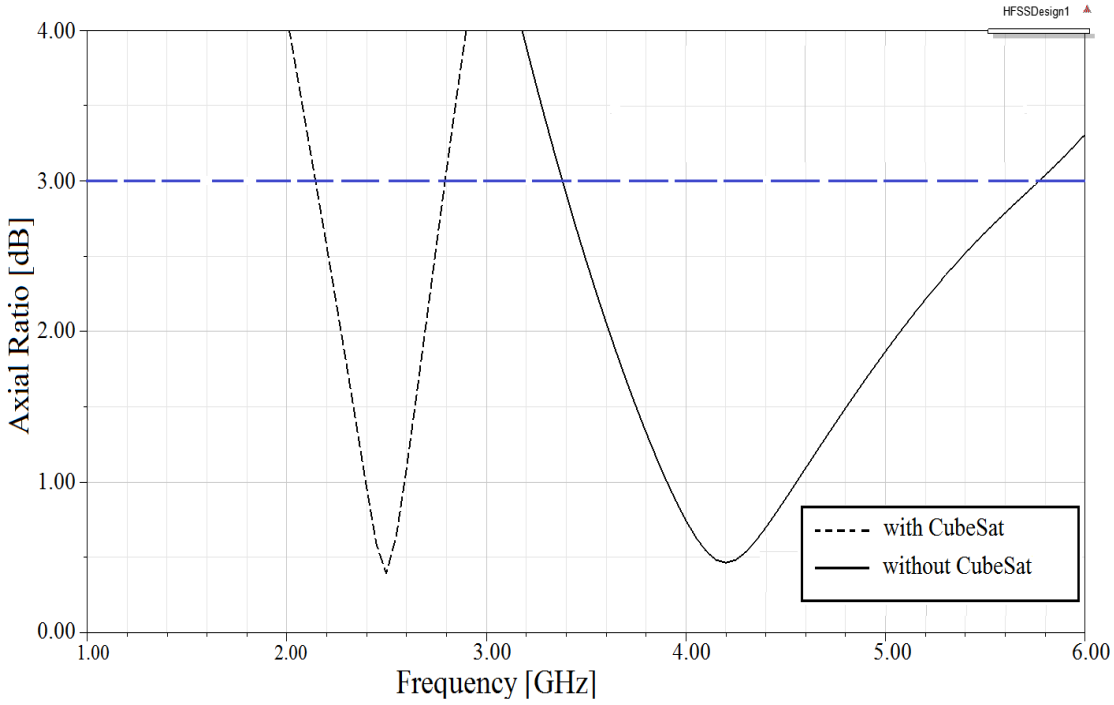

Figure 3.9. The axial ratio of the shorted patch antenna.

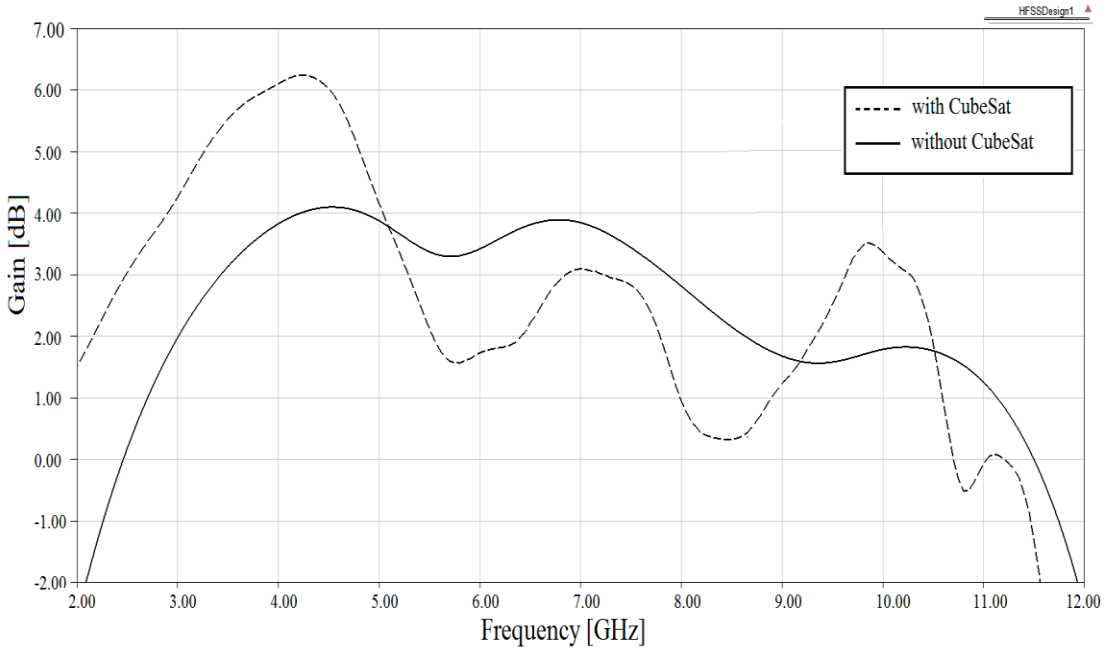

Figure 3.10. 2D gain of tested shorted patch antenna.

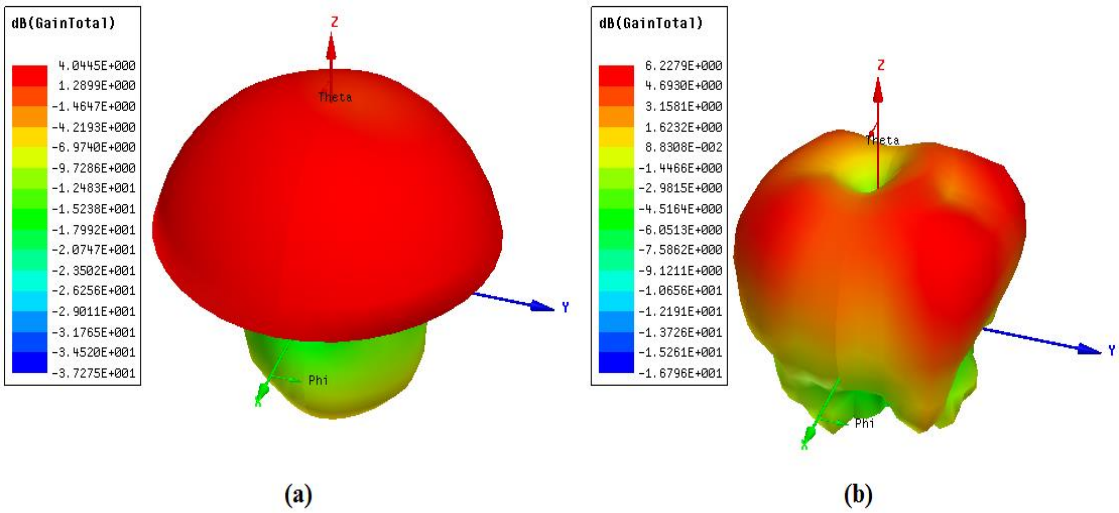

(a) (b)

Figure 3.11. 3D gain of the tested shorted patch antenna at 4.3 GHz: (a) without, and (b) with CubeSat.

- *Asymmetric E-shaped patch antenna*

  Figure 3.12 shows the simulated return losses of the asymmetric E-shaped patch antenna with and without the effect of the CubeSat body. It shows that for both tested cases, the antenna has a similar resonant frequency of 6.5 GHz. When the antenna operates on the CubeSat, it achieves a wide impedance bandwidth; i.e., 2300 MHz. On the CubeSat body, its bandwidth increased by about 100 MHz. Also, the return loss at the resonant frequency of 6.5 GHz decreases (or improves) slightly from -14 to -15.2 dB.

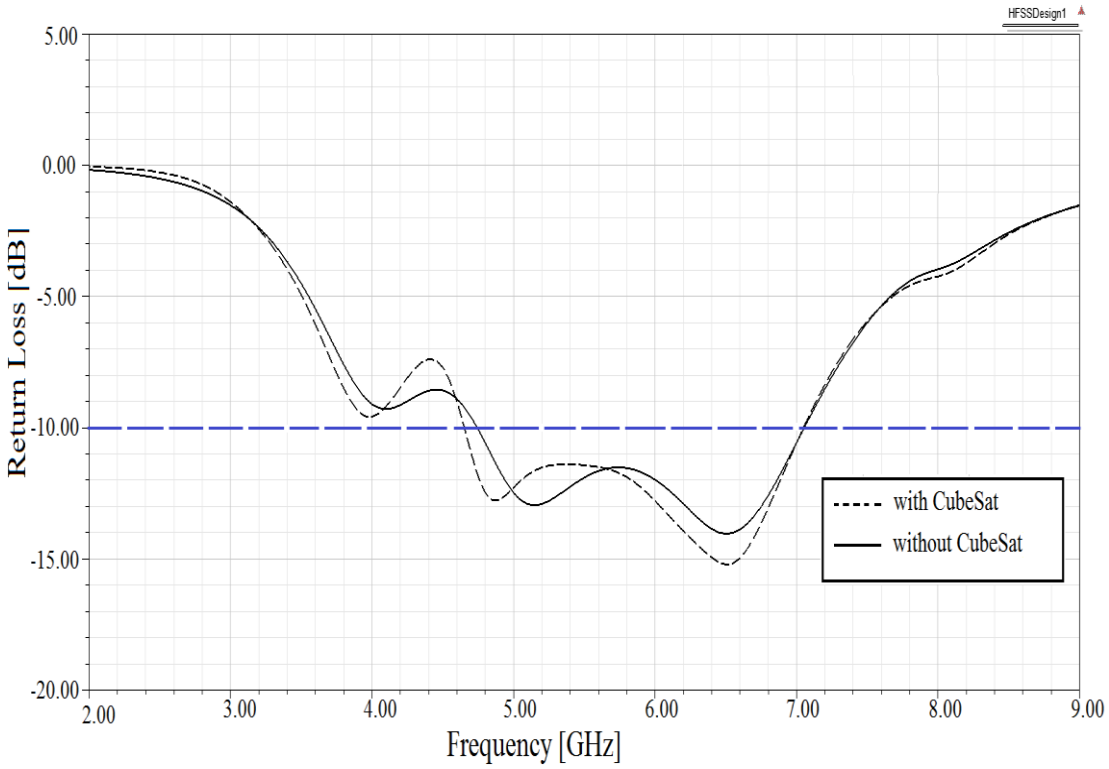

Figure 3.12. Return losses (S_{11}) of the asymmetric E-shaped patch antenna.

Figure 3.13 shows the simulated axial ratio of the asymmetric E-shaped patch antenna with and without the effect of the 2U CubeSat body. On the CubeSat, the antenna's axial ratios are 0.9, 0.15 and 1.85 dB at frequencies of 2.3, 5.35 and 6.3 GHz, respectively. The achieved 3-dB axial ratio bandwidths are 200 MHz (2.2-2.4 GHz) and 1400 MHz (5-6.4 GHz). Without the CubeSat case, the asymmetric E-shaped patch antenna has an axial ratio of 3.07 dB at 5.15 GHz. This means the

CubeSat body causes axial ratios of less than 3 dB and enlarges the 3-dB axial ratio bandwidth; i.e., 1400 MHz (5-6.4 GHz).

Figure 3.14 shows the gain of the asymmetric E-shaped patch antenna versus varying frequencies. It shows that the CubeSat body affects the E-shaped patch antenna by increasing its gain over the frequency range of 3 to 6.7 GHz and decreasing its gain for frequency ranging from 6.7 to 9 GHz. The gain of the antenna at resonant frequencies of 4.6 and 6.5 GHz is increased by 0.8 dB when used on the CubeSat; see Figure 3.14. The peak gain of the E-shaped patch antenna on the 2U CubeSat is 8.4 dB at a resonant frequency of 5.8 GHz.

Figure 3.15 illustrates the simulated 3D gains of the asymmetric E-shaped patch antenna with and without the 2U CubeSat body at 4.75 GHz. Compared to the without CubeSat case, the antenna with CubeSat has a higher 3D gain; i.e., 7.3 dB. However, the radiation pattern of the antenna with a CubeSat is non-uniform.

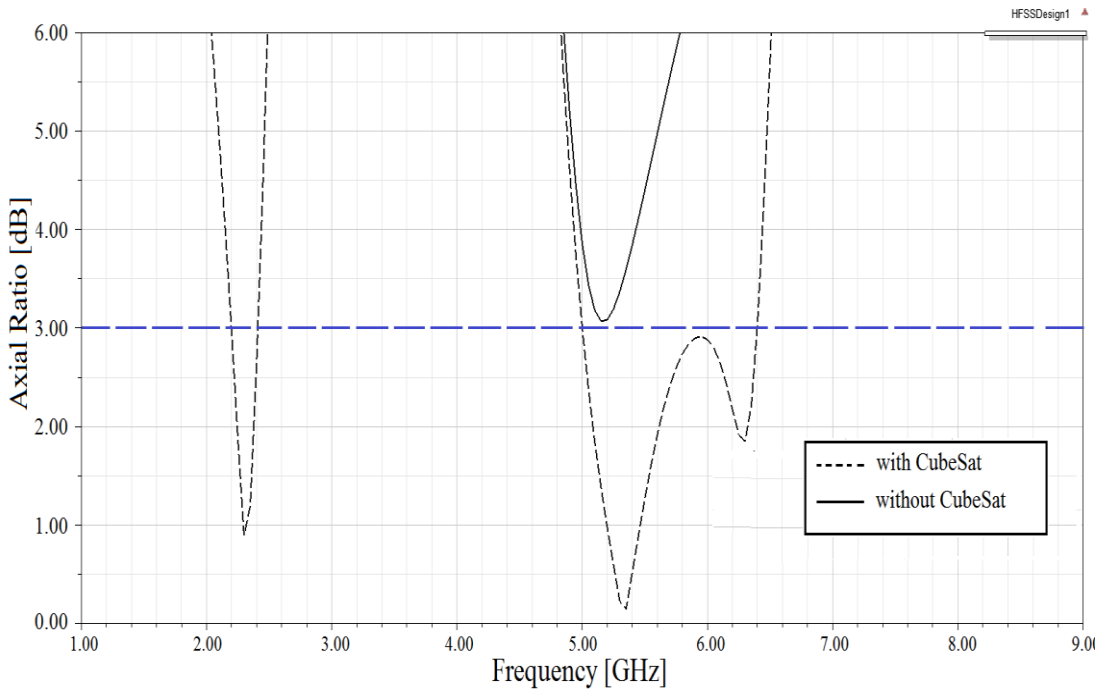

Figure 3.13. The axial ratio of the tested asymmetric E-shaped patch antenna.

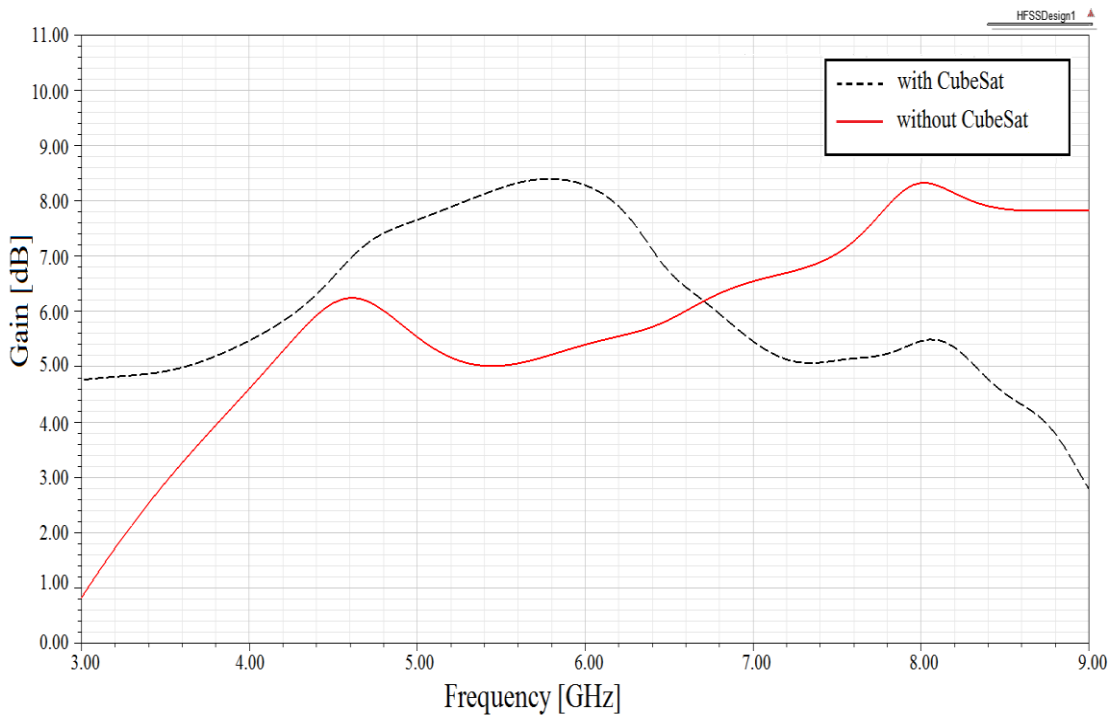

Figure 3.14. 2D gain of asymmetric E-shaped patch antenna.

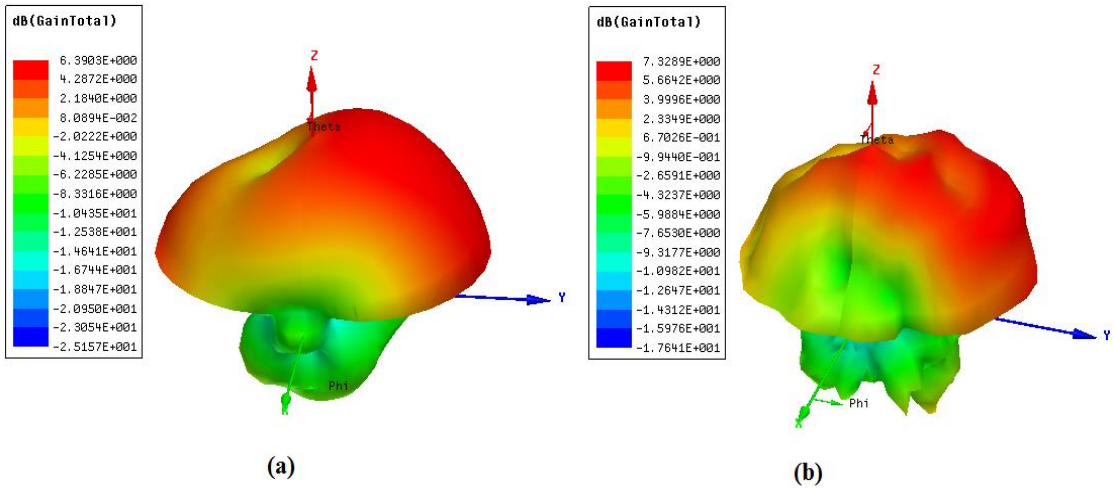

Figure 3.15. 3D gains of asymmetric E-shaped patch antenna at 4.75 GHz: (a) without, and (b) with a CubeSat.

3.3 Comparison of All Three Designs

This section now provides a comparison between the three antenna designs. In particular, it compares the effects of a 2U CubeSat body on their return losses, axial ratios (AR) and gains. Figure 3.16 plots the return losses of the shorted patch, asymmetric E-shaped micro-strip patch and CPW-feed square slot antennas. Compared to the asymmetric E-shaped patch antenna and CPW-feed square slot antenna, the shorted patch antenna has a smaller return loss; i.e., -43.3 dB at 4.3 GHz, and a much wider -10 dB bandwidth; i.e., 6900 MHz (3.8-10.7 GHz). In terms of resonant frequency, only the shorted patch antenna operates close to the S-band (2-4 GHz) with a resonant frequency of 4.3 GHz (with CubeSat); see Figure 3.16. However, this resonant frequency; i.e., 4.3 GHz, does not belong to the 2.4-2.5 GHz unlicensed Industrial, Scientific and Medical (ISM) band, which is preferred for CubeSat communications. Therefore, the operating frequency of the shorted patch antenna needs to be shifted to 2.45 GHz. Moreover, the CPW-feed square slot antenna has very high return loss when used on a CubeSat; i.e., -10 dB and a small non-uniform bi-directional radiation pattern. This is because the attached side of the antenna is not a ground plane and hence the satellite body acts as a ground plane and significantly affects the antenna's performance. One solution is to insert a PVC plastic sheet between the antenna and the CubeSat body [108]. Another solution is to keep some distance (air gap) between the antenna and the satellite body. This gap should be set such that there is no capacitance between the dielectric and the CubeSat body. Consequently, the satellite body will act as a reflector, and leads to higher gains.

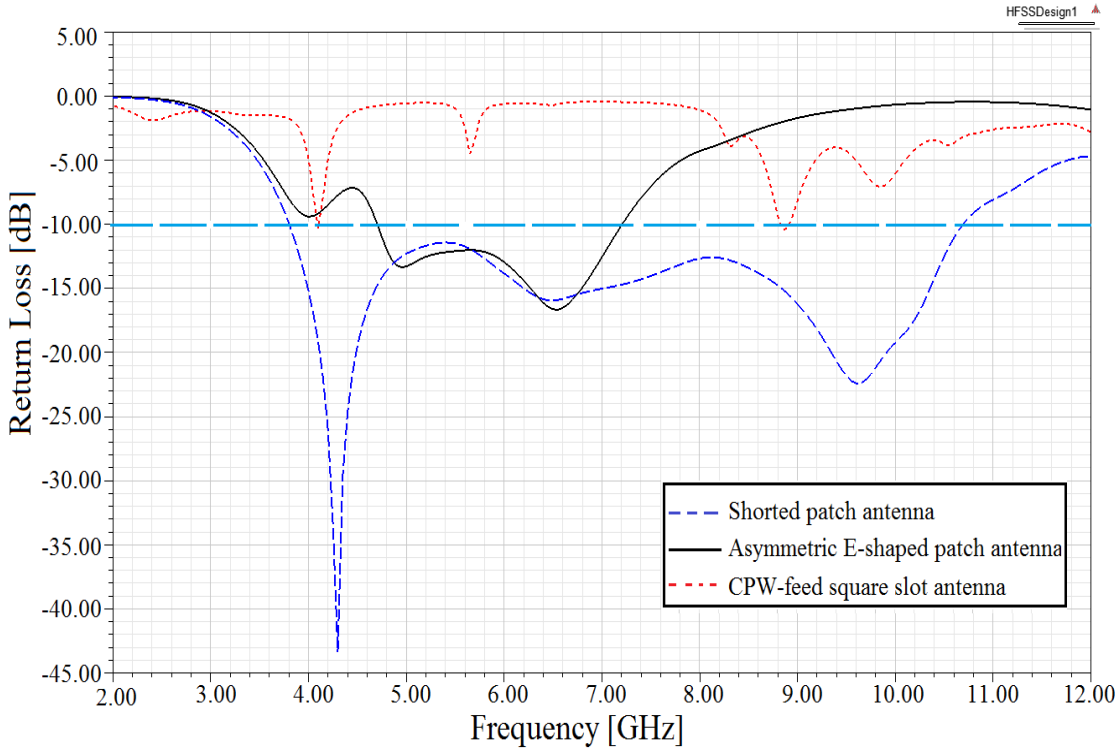

Figure 3.16. Return losses of the shorted patch, asymmetric E-shaped patch and CPW-feed square slot antennas on a 2U CubeSat body.

Figure 3.17 shows the axial ratios of the shorted patch, asymmetric E-shaped micro-strip patch and CPW-feed square slot antennas. All three antennas have an axial ratio less than 3 dB at different operating frequencies. Compared to the shorted patch and CPW-feed square slot antennas, the asymmetric E-shaped patch micro-strip patch antenna has a wider 3 dB axial ratio bandwidth; i.e., 1400 MHz, and a smaller axial ratio; i.e., 0.14 dB. In the S-band frequencies (2-4GHz), the shorted patch antenna has a wider 3 dB axial ratio bandwidth than that of asymmetric E-shaped patch and CPW-feed square slot antennas; see Figure 3.17. In terms of gain, the asymmetric E-shaped patch antenna has the highest peak gain of 8.39 dB at 5.8 GHz as compared to shorted patch and CPW-feed square slot antennas; see Figure 3.18. The peak gain of the shorted patch, asymmetric E-shaped micro-strip patch and CPW-feed square slot antennas in the 2.4-2.45 GHz band is 3, 4.4 and -6.3 dB, respectively. Further improvement in gain is needed for CPW-feed square slot antenna if it is to be used on pico-satellites.

The simulated radiation patterns of all three antennas on two planes ($xz: \varphi = 0°\ and\ yz: \varphi = 90°$) are illustrated in Figure 3.19. Their radiation patterns are rather symmetric in the xz and yz planes. The maximum radiation of the E-shaped patch and CPW-feed square slot antennas occur exactly at the boresight direction ($\theta = 0°$). Compared to CPW-feed square slot and shorted patch antennas, the E-shaped micro-strip patch antenna has the widest Half Power Beam Width (HPBW); e.g., 76^0 (xz-plane), and the highest peak gain at its boresight direction; e.g., 5.17 dB.

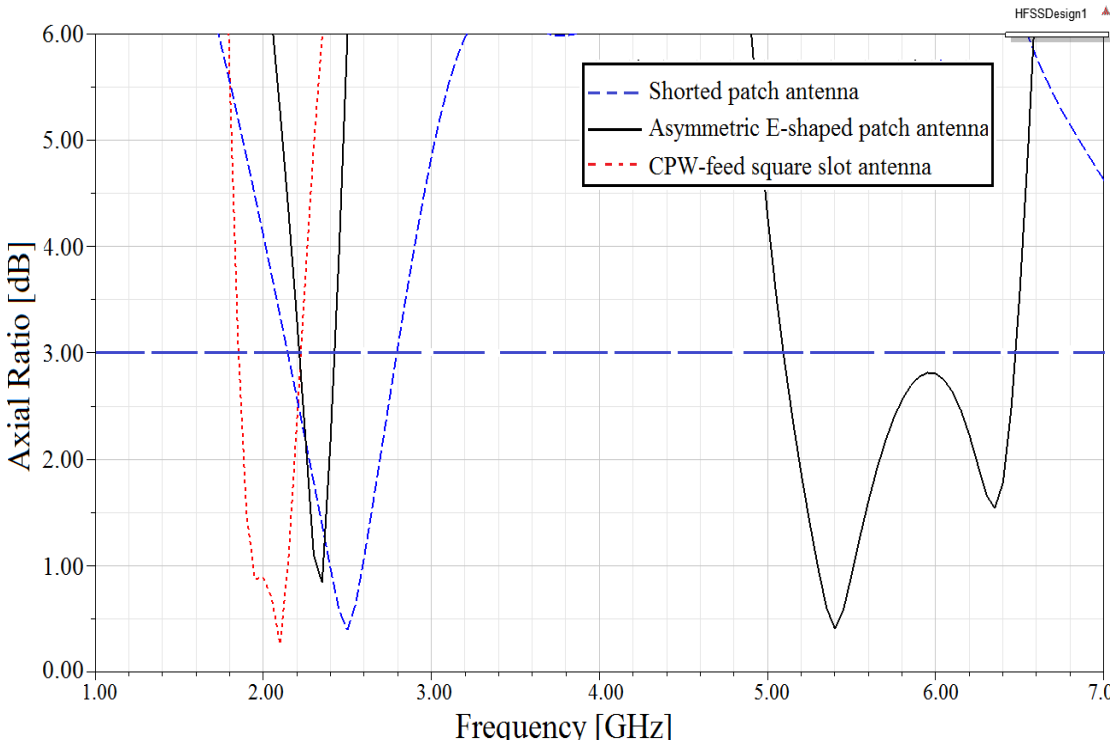

Figure 3.17. The axial ratio of the shorted patch, asymmetric E-shaped patch and CPW-feed square slot antennas on a 2U CubeSat body.

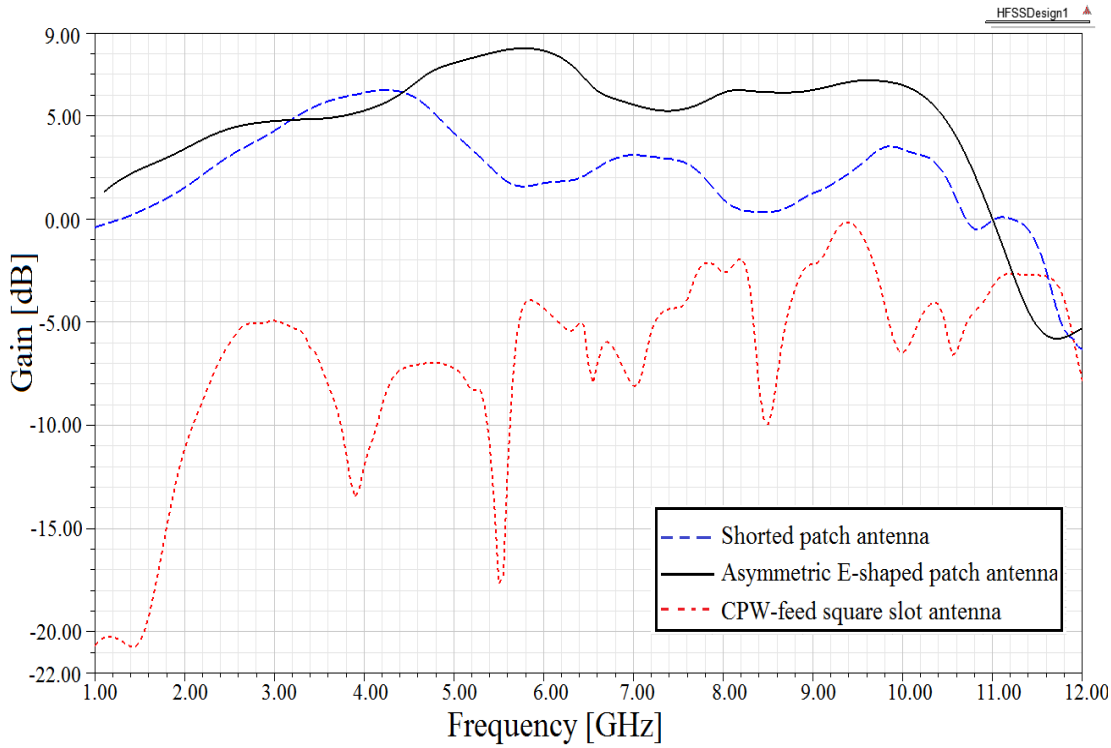

Figure 3.18. A comparison of gain of the tested shorted patch, asymmetric E-shaped patch and CPW-feed square slot antennas on a 2U CubeSat body

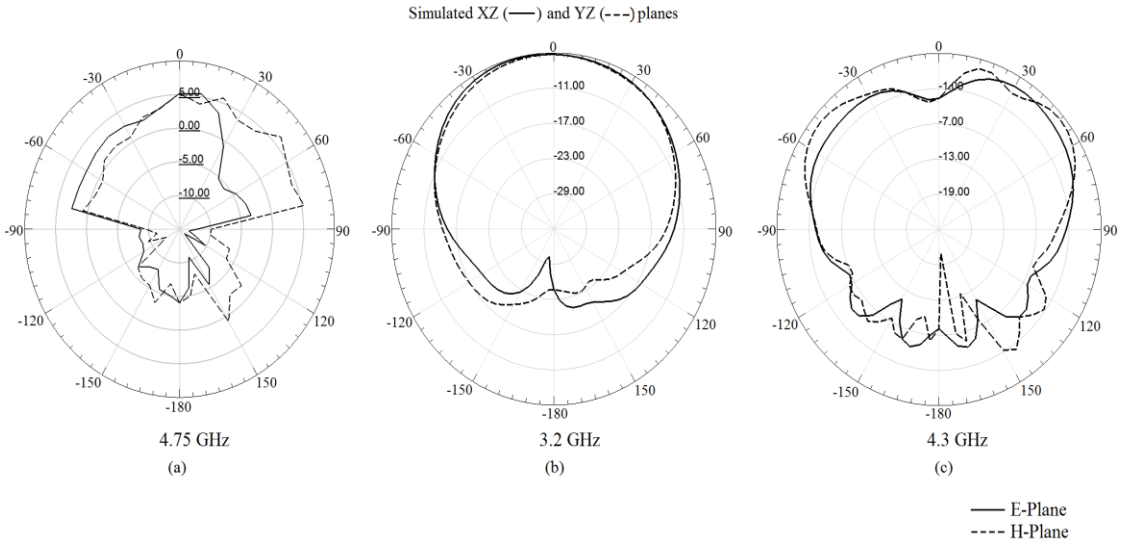

Figure 3.19. Simulated radiation patterns of an (a) E-shaped patch, (b) CPW-feed square slot, and (c) shorted patch antennas.

Table 3.1 compares all three candidate antennas in terms of volume, gain, bandwidth, return loss, robustness, beam steerability, and affordability. It shows that all three designs are relatively small, have wide bandwidth, and are cheap. These antennas, however, are non-steerable and are not designed to operate at 2.45 GHz. The asymmetric E-shaped patch antenna design has a superior gain over the shorted patch and CPW-feed square slot antennas. This is important as it enables long distance communications. This means fewer CubeSats will be required to participate in a swarm. Alternatively, they allow a swarm to operate over large areas. Another advantage of the asymmetric E-shaped patch antenna design is its very small return loss, meaning more power is radiated into space and less power is reflected.

Shorted patch, asymmetric E-shaped micro-strip patch and CPW-feed square slot antennas can have different placement configurations on a 2U CubeSat. For satellite to ground station communications, placing an antenna on only one CubeSat face is sufficient. One example is to use an array on one face of the CubeSat for ground station communications [40]. This antenna should always be pointed to the ground station. This can be achieved by orienting the CubeSat using magnetic torqueing. Another configuration enables satellite-to-satellite (cross-link) communications. This will require more than one antenna on multiple faces of a CubeSat. As an example, the authors of [57] propose to place an individual antenna on each face of a 3U CubeSat.

Table 3.1. Evaluation of the most suitable planar antenna designs for inter CubeSat communications

	Shorted patch antenna [46]	*Asymmetric E-shaped patch antenna [56]*	*CPW-feed square slot antenna [45]*
Volume	Small	Medium	Small
Gain	Low	High	low
BW	Wide	Wide	small
S_{11}	Small	Very small	Very high
Robustness	Weak	Weak	Strong
Beam steerability	Not steerable	Not steerable	Not steerable
Affordability (cost)	Cheap	Cheap	Cheap

3.4 Conclusion

This chapter has presented an evaluation of the following antennas on a common platform: shorted patch, CPW-feed square slot and asymmetric E-shaped antennas. In particular, it evaluates the effect of a 2U CubeSat body on their performance. The results show that the performance of the CPW-feed square slot antenna is affected significantly by the 2U CubeSat body if due care is not taken. It also finds that the asymmetric E-shaped patch antenna design achieved a high gain of 7.3 dB at 4.75 GHz with a bandwidth of 2300 MHz. Its main limitation, however, is its high operating frequency of 4.75 GHz. To lower its operating frequency, its overall size needs to be increased. Finally, the shorted patch and CPW-feed square slot antennas have a small size and operates at lower operating frequencies as compared to the E-shaped antenna.

Both shorted patch and CPW-feed square slot antennas do not operate at the desired CubeSat ISM operating frequency of 2.4-2.5 GHz band. Therefore, the next chapter presents shorted patch and CPW-feed square slot antennas that operate at 2.45 GHz. Then it compares these antennas and their performance when they operate on a 2U CubeSat. In addition, the next chapter also presents a newly designed wideband F-shaped patch antenna.

Chapter 4

S-BAND PLANAR ANTENNA DESIGNS FOR CUBESATS

As mentioned in Chapter 3, the designs in [46] and [45] do not operate in the 2.45 GHz (S-band). This band is important because most of the antennas for pico satellites are designed to work in the 2.4-2.5 GHz unlicensed ISM band. Thus, the resulting swarm of CubeSats do not need a government permit to operate. To this end, this chapter presents the required improvements to shift the operating frequencies of the antennas in [45, 46] to 2.45 GHz (S-band) without critically effecting their performance. Then it compares their performance in the presence of a CubeSat body. The main findings are that the new S-band shorted patch and CPW-fed square slot antennas have narrow bandwidths and low gains. Specifically, the -10 dB bandwidth of shorted patch antenna is reduced from 6900 to 870 MHz and the gain is reduced by about 1 dB when its frequency is shifted to 2.45 GHz. As for the new CPW-fed square slot antenna, its bandwidth reduced from 1600 to 530 MHz and its gain from 3.2 to 2 dB. Henceforth, to address the aforementioned limitations, this chapter also proposes a newly designed wideband F-shaped patch antenna that operates in the unlicensed ISM band (2.45 GHz), has a wide bandwidth and achieves a superior gain.

4.1 Evaluation and Improvements of Shorted Patch and CPW-fed Square Slot Antennas

4.1.1 New shorted patch antenna

Figure 4.1 shows a simulation model of the shorted patch antenna in [46]. It consists of upper and lower patches with dimensions of 1.8×1.5 and 0.75×0.65 cm^2 respectively. These patches are connected together via a folded ramp-shaped part. Also, they are connected to a 3×3 cm^2 ground plane through shorting pins and probe feed. Moreover, in order to use a short probe length, it uses the air substrate and the

folded ramp-shaped part. This leads to a decrease in both quality factor (Q) and the inductive reactance of the probe and hence enhancement of the bandwidth. The main purpose of using shorting pins at the edges of the upper patch is to achieve miniaturization at wide impedance bandwidth. In addition, the centre pin at the upper patch is used to broaden the impedance bandwidth by generating resonances at 4.4 and 6.95 GHz.

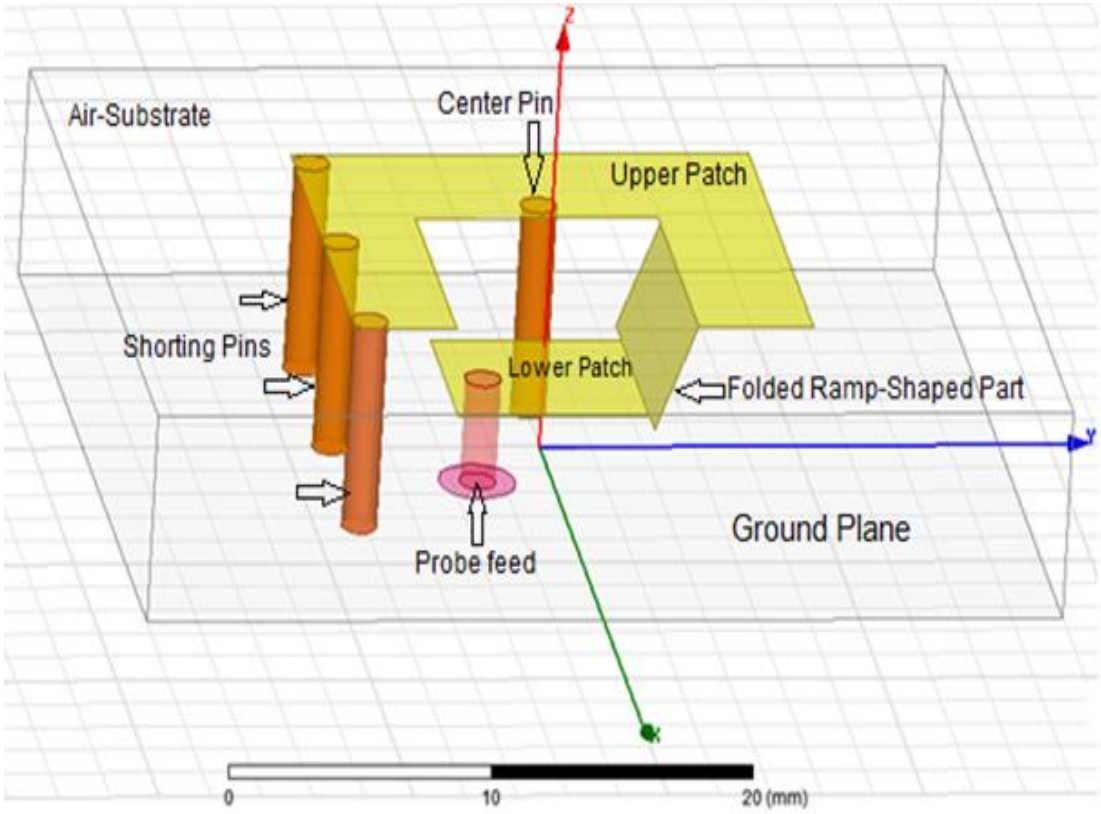

Figure 4.1. Geometry of the shorted patch antenna in [46].

The aforementioned shorted patch antenna design operates at 4.4 GHz. However, the target frequency is 2.45 GHz. Hence a frequency shift is required for the shorted patch antenna design in [46]. A frequency shift is possible by increasing the size of the antenna subject to the size and weight constraints of CubeSats. To this end, the Quasi-Newton method provided by the HFSS simulator [109] is used to re-dimension the antenna. The Quasi Newton method works on the basis of finding the minimum or maximum of a cost function by varying the variables to meet the operating frequency of 2.45 GHz (constraint). In this design's case, the decision variable is the

length of the antenna's dimensions with range 0.653 (minimum) to 1.959 mm (maximum). The aim is to achieve a minimum return loss (design parameter) at an operating frequency of 2.45 GHz (constraint). Therefore, the Quasi-Newton method minimizes the value of return loss (S_{11}) by varying the antenna lengths 100 times (iterations) from 0.653 to1.959 mm by the following minimum and maximum step size: 0.013 and 0.13 mm. The results show that the antenna size must be increased by a factor of 1.3 mm to achieve a minimum return loss of -27.6 dB at an operating frequency of 2.45 GHz.

4.1.2 New CPW-feed square slot antenna

Figure 4.2 depicts the structure of the square slot antenna model in [45]. This antenna has a total size of 60×60 mm^2; it is fabricated on a FR4 substrate with a thickness of 0.8mm. The CPW feed line technique is used with a fixed width of 4.2 mm over a single strip. To achieve a good impedance matching between the 50 Ω transmission line and the impedance at the antenna, the gap between the CPW-feed line and ground plane is found to be 0.3 mm using HFSS. In addition, the CPW-feed square slot antenna operates at 3.2 and 9.1 GHz; see Figure 4.5. Its initial operating frequency of 3.2 GHz is shifted to 2.45 GHz (S-band) by re-dimensioning the entire antenna parameters. In particular, the Quasi Newton optimization method is used to re-dimension the antenna to achieve an operating frequency of 2.45 GHz. The resulting antenna size is 1.25 mm and has a return loss S_{11} of -25 dB at an operating frequency of 2.45 GHz.

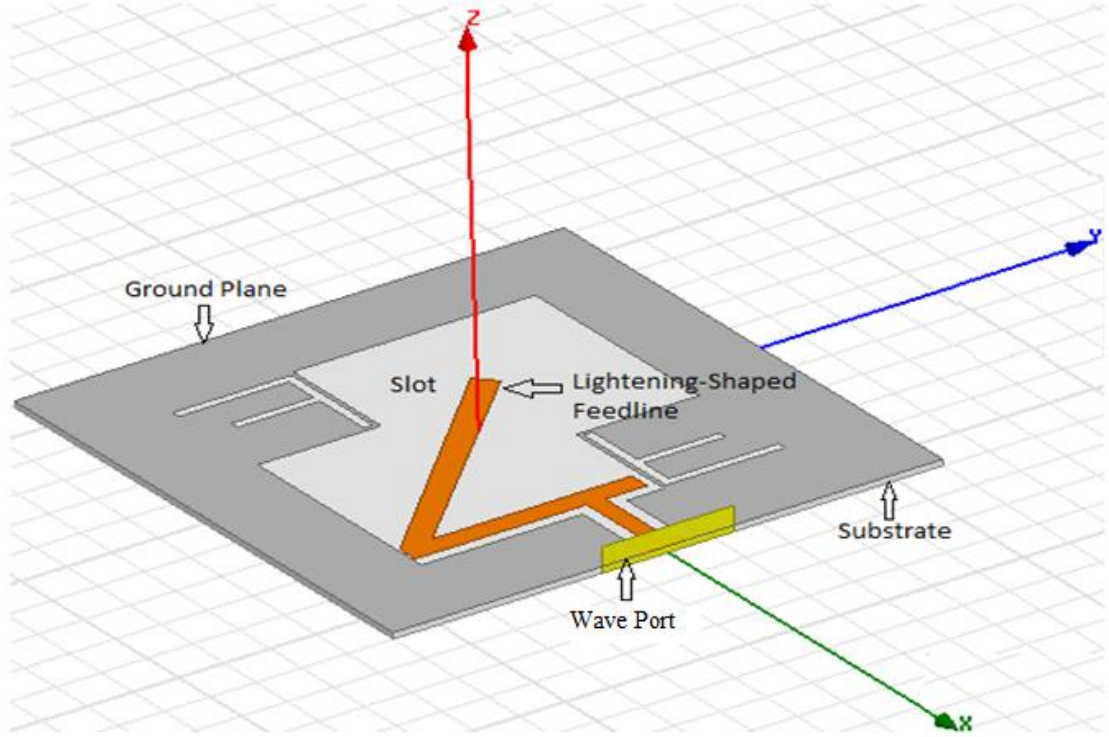

Figure 4.2. Geometry of CPW-feed square slot antenna in [45].

4.1.3 Evaluation

This section first compares the original design of [45] and [46] in terms of return loss, bandwidth, gain and antenna size. It also studies the effect of a 2U CubeSat Aluminium body on the performance of the antenna designs; see Figure 4.3 and 4.4. Figure 4.5 plots the return losses of the shorted patch and CPW-feed square slot antennas with and without a CubeSat body. It shows that the CubeSat body has a significant effect on the shorted patch antenna performance and very small effect on the CPW-feed square slot antenna's performance; see Figure 4.5 and 4.6. The return loss of shorted patch antenna is dramatically improved (decreased) from -26.3 to -43.3 dB when it is placed on a CubeSat surface. This is important as more power is radiated into space and less power is reflected.

As shown in Figure 4.6, the peak gain of the shorted patch antenna at 4.3 GHz is 4 dB without a CubeSat and 6.2 dB with a CubeSat. Moreover, the peak gain of the CPW-feed slot antenna has slightly improved; i.e., 1.93 dB, when the antenna is place on a CubeSat's surface. The peak gain of the CPW-feed square slot antenna is

2.8 dB without a CubeSat and 3.1 dB with a CubeSat. Compared to the CPW-feed square slot antenna, the shorted patch antenna has wider bandwidth; i.e., 1600 MHz, and higher gains; i.e., 4 dB (without CubeSat) and 6.2 dB (with CubeSat). This is important for CubeSats as it provides longer communication distance and therefore decreases the number of CubeSats to be used in a swarm.

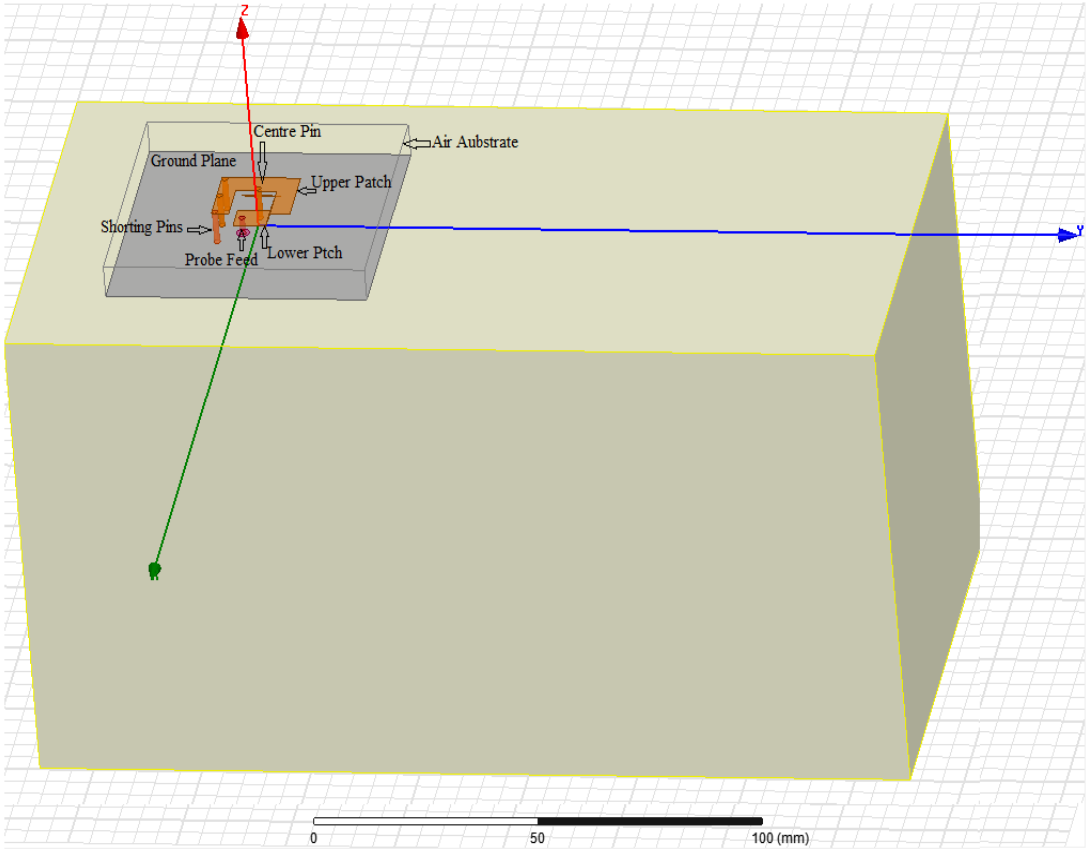

Figure 4.3. Geometry of shorted patch antenna on a 2U CubeSat body.

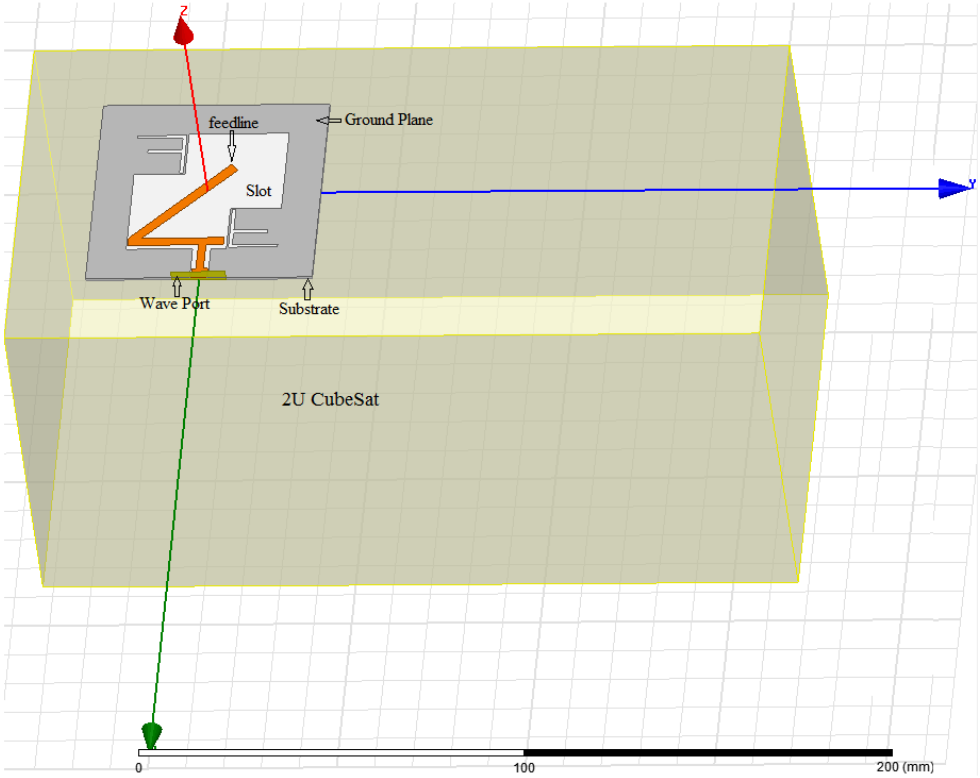

Figure 4.4. Geometry of CPW-feed square slot antenna on a 2U CubeSat body.

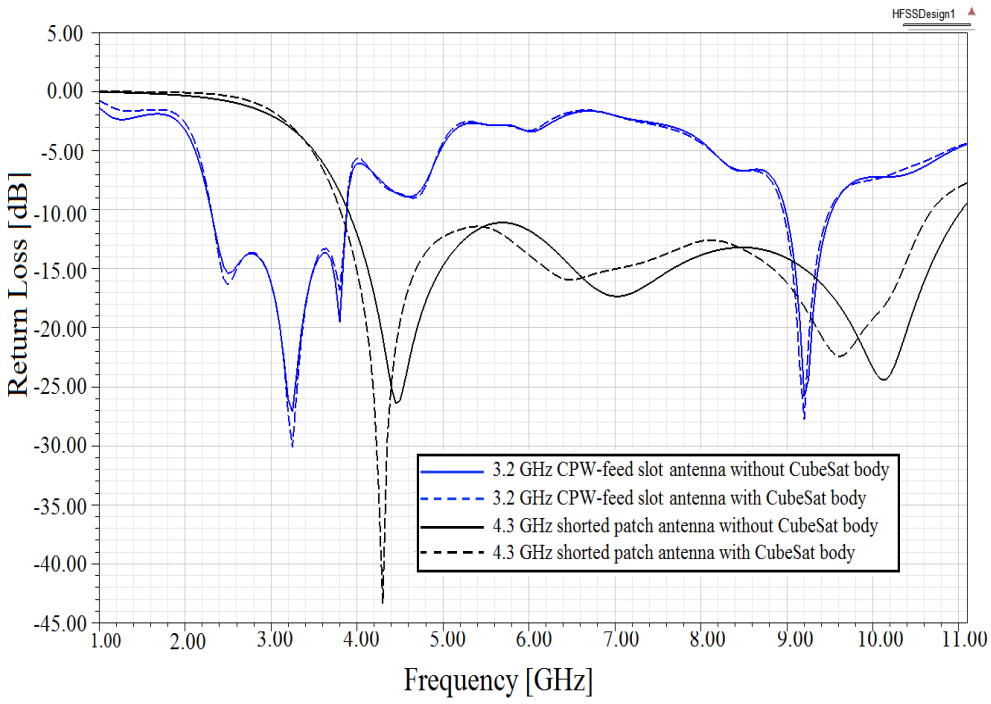

Figure 4.5. The simulated return loss of shorted patch and CPW-feed square slot antennas with and without a CubeSat.

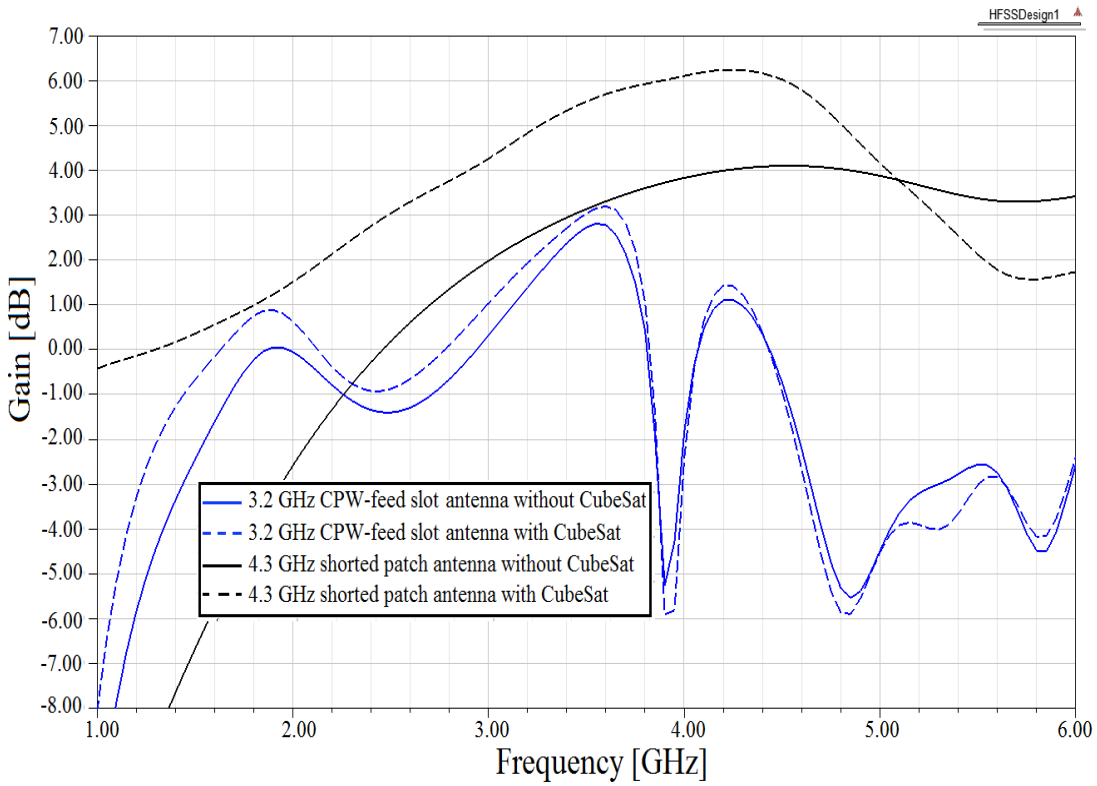

Figure 4.6. The simulated 2D gain of shorted patch and CPW-feed slot antenna with and without a CubeSat body.

- *New shorted patch and CPW-feed square slot antennas*

  This section now presents and compares the results of the re-dimensioned shorted patch and CPW-feed square slot antennas. Figure 4.7 depicts the simulated return losses of the 2.45 GHz shorted patch and CPW-feed square slot antennas with and without a CubeSat. Both modified antennas operate at 2.45 GHz as their resonance frequency has been shifted to 2.45 GHz. The simulated fractional impedance bandwidth of the modified shorted patch antenna is 870 MHz. It is 530 MHz for the modified CPW-feed square slot antenna.

  Figure 4.7 plots the return loss over different frequencies for the new shorted patch and CPW-feed square slot antennas. Compared to the new S-band CPW-feed square slot antenna, the new S-band shorted patch antenna has smaller return loss of about -27.5 dB at 2.45 GHz and wider -10 dB bandwidth; i.e., 870 MHz (2.13-3 GHz). In terms of total gain, the new shorted patch antenna achieves

higher gain of 5.3 dB at an operating frequency of 2.45 GHz; see Figure 4.8. However, the modified shorted patch antenna has larger physical size; i.e., 83×83 mm^2, as compared to the modified CPW-feed square slot antenna. The main limitation of the modified CPW-feed square slot antenna is its low gain at 2.45 GHz. Hence, further improvements are proposed and applied in order to enhance its total gain in the following section.

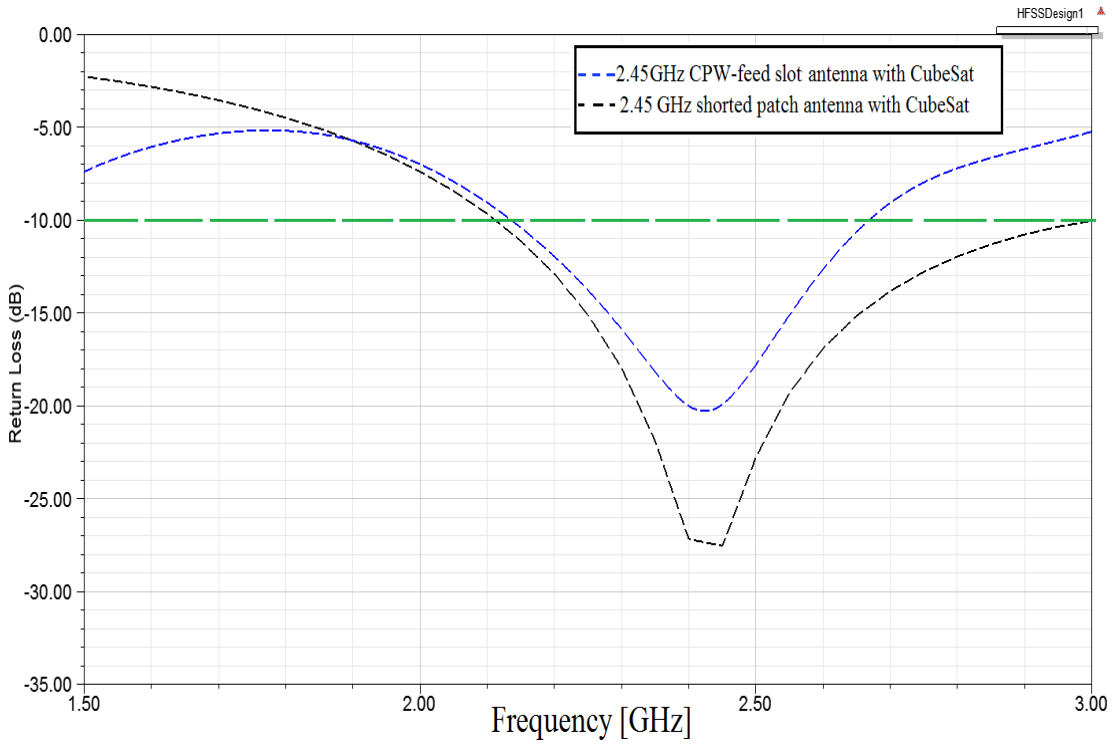

Figure 4.7. Simulated return losses of re-dimensioned shorted patch and CPW-fed slot antennas on 2U CubeSat.

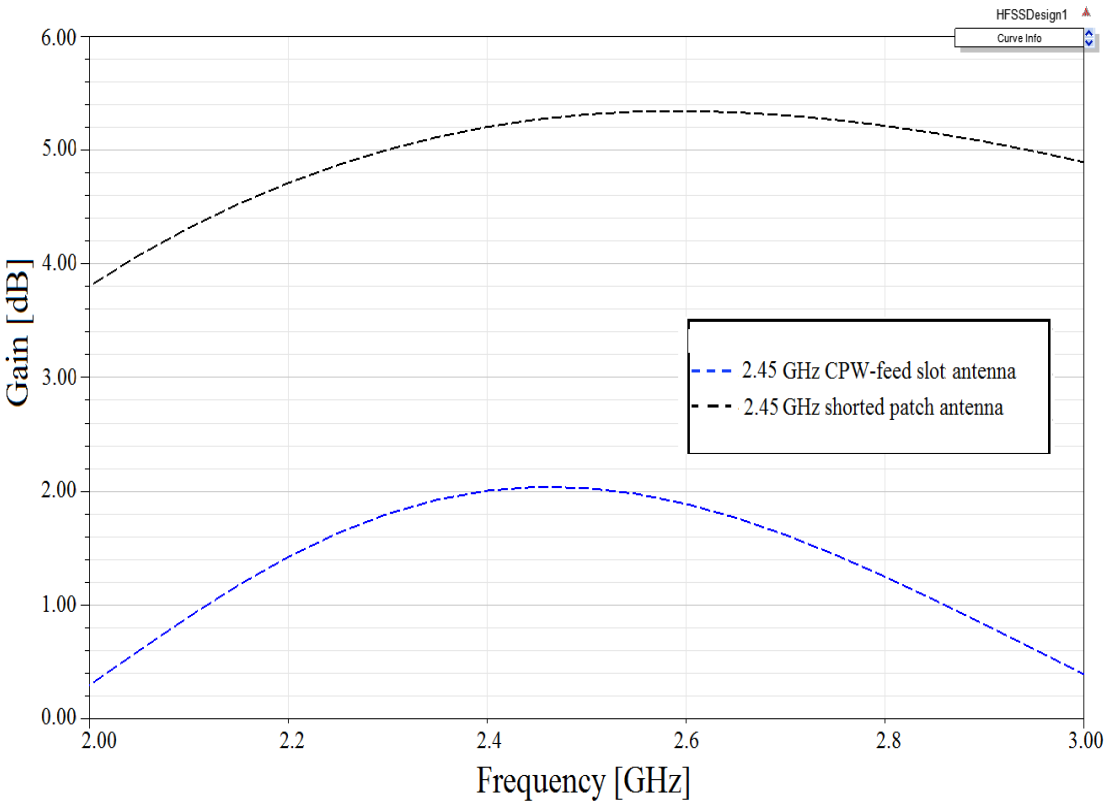

Figure 4.8. The simulated 2D gain of the modified shorted patch and CPW-feed slot antenna.

Table 4.1. Return loss, BW, gain and size of modified antennas

Antenna	Frequencies (GHz)	BW (MHz)	Gain (dB)	Size (mm^2)
Modified Shorted Patch Antenna	2.45	870	5.3	83×83
Modified CPW-feed Square Slot Antenna	2.45	530	2.00	75×75

- *Gain enhancement of the new CPW-feed square slot antenna*

  Figure 4.9 shows the new structure of the re-dimensioned CPW-feed square slot antenna after removing the F-shaped slits and creating a square slot. F-shaped slits were embedded in the design of [45] to enlarge its bandwidth, i.e., 1600MHz. However, removing F-shaped slits from the antenna structure leads to a significant decrease in bandwidth, i.e., 530 MHz, and hence increases the total antenna gain from 2.00 to 2.52 dB; see Figure 4.10. Moreover, the resulting

bandwidth reduced from 1600 to 530 MHz but remains sufficiently wide for CubeSat communications.

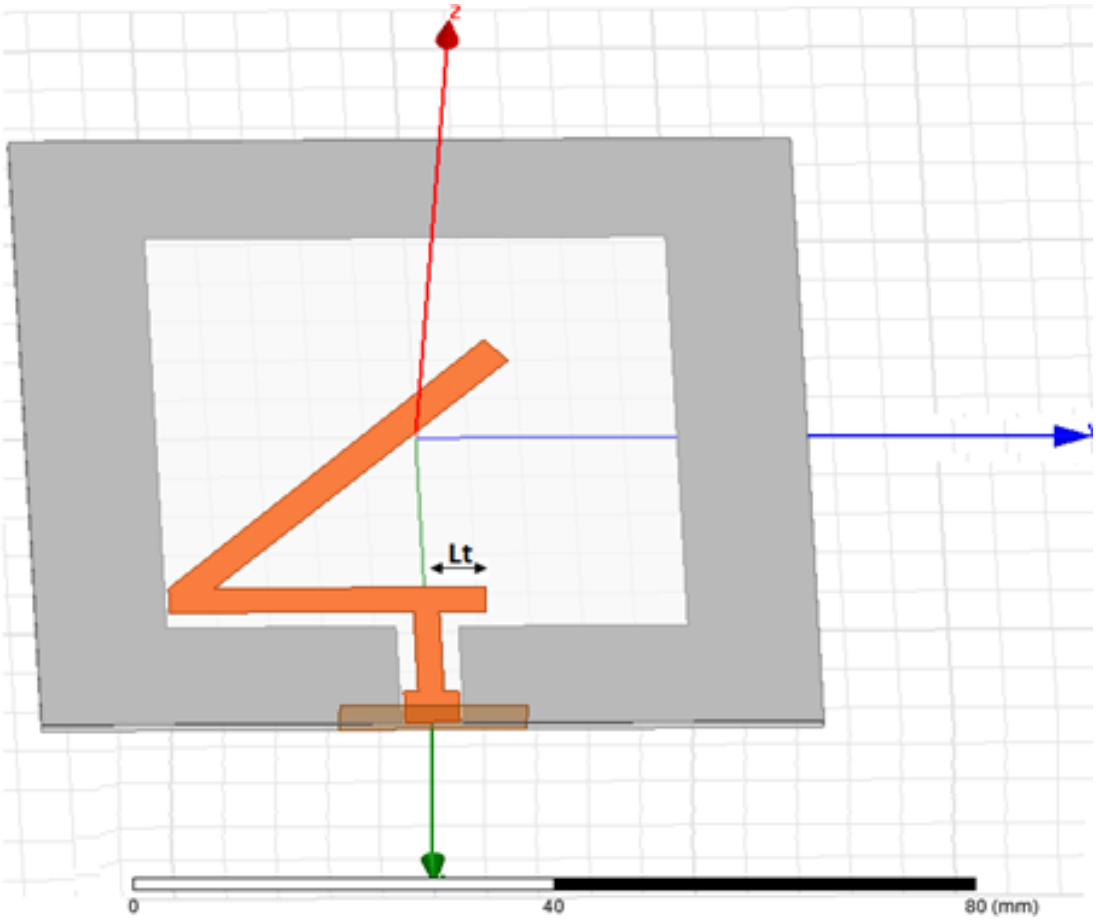

Figure 4.9. Geometry of the re-dimensioned CPW-feed square slot antenna without F-shaped slits.

As shown in Figure 4.11, the length of the horizontal tuning stub L_t has a great effect on the impedance bandwidth and the total gain. Figure 4.11 shows that with decreasing L_t the operating frequency increases and return loss (S_{11}) decreases. Hence, the resulting antenna has better impedance matching. The best L_t value is 7.5 mm. This value shifts the operating frequency to 2.45 GHz with a small return loss, i.e., -27.5 dB, wide -10 dB bandwidth, i.e., 730 MHz (1.9-2.63 GHz), and achieved total gain of 2.52 dB. An immediate future work is to apply further gain enhancement and size miniaturization techniques such as the

Metasurface Superstare (MSS) [110-112] to increase gain and using series of parallel strip lines [55] or loading wires [68] to achieve further miniaturization.

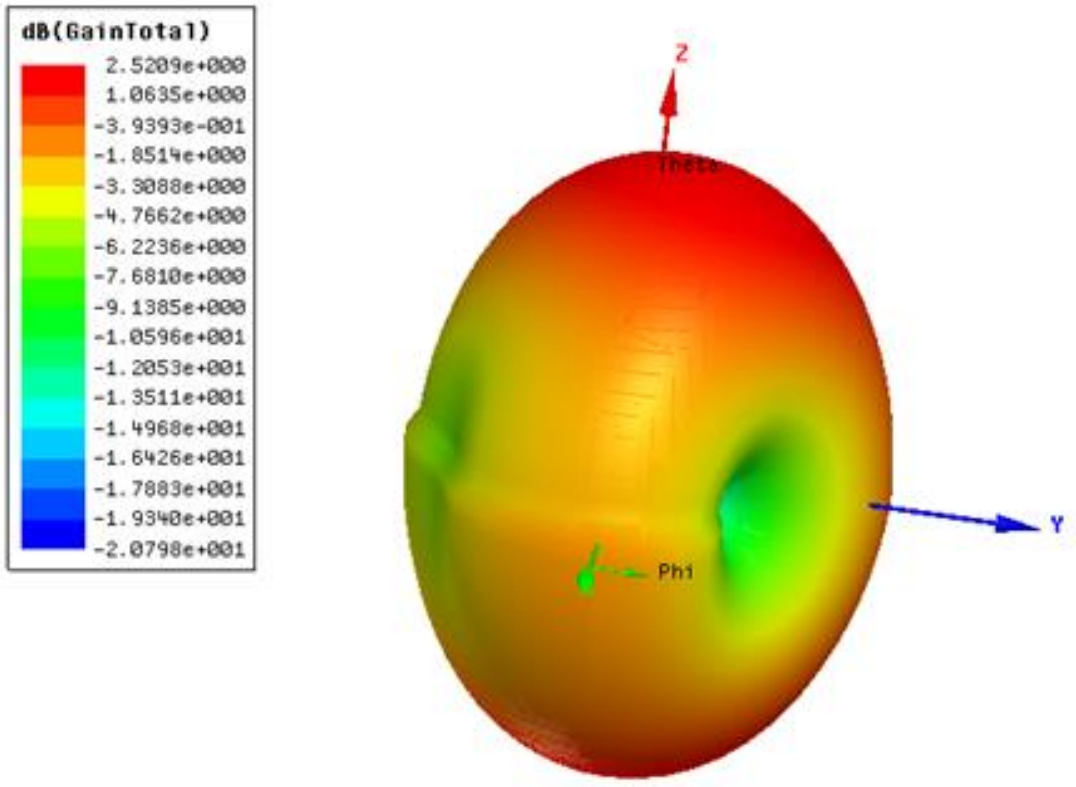

Figure 4.10. Total 3D gain of the re-dimensioned CPW-feed square slot antenna without F-shaped slits.

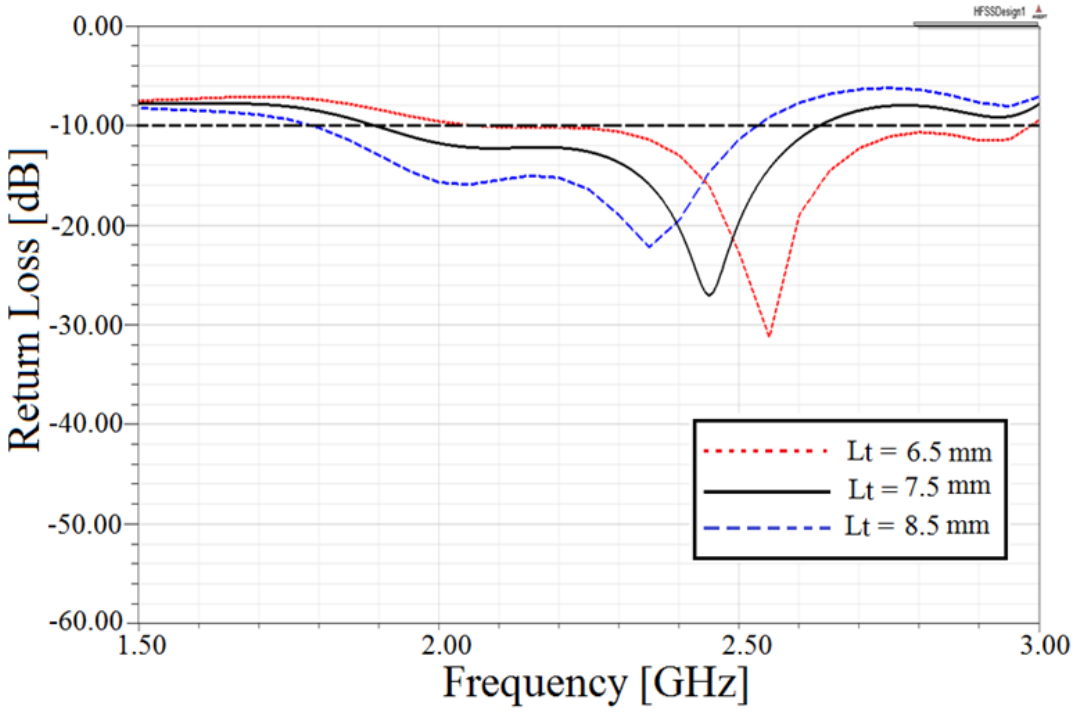

Figure 4.11. Simulated return loss against frequency for the various L_t values.

4.2 Newly Designed Wideband High Gain F-shaped Patch Antenna

There are many approaches that can be employed to widen the bandwidth of patch antennas. One common technique is to use U-slot and L-slit patch antenna geometries. The main idea is to incorporate a folded inner small patch within a larger patch. The authors of [41] reported a bandwidth enhancement of 53.54% (3.57-6.18 GHz) at the resonant frequency of 4.5 GHz and 45.12% (4.26-6.75 GHz) at 5.5 GHz. However, the resulting antenna has a low gain of about 2.5 dB. Another approach is by interleaving two patch antennas [113]. The main idea is to use a folded ramp-shaped feed and one pin in the centre of the upper patch to increase bandwidth. The authors also used shorting pins between the patches and the ground plane to miniaturize the antenna's size. Although the modified S-band shorted patch antenna presented in [113] has a wideband of 320 MHz (2.200-2.520 GHz), its size is reasonably large at 83×83 mm^2, making it unsuitable for used on CubeSats.

This section proposes a wideband 2.45 GHz F-shaped patch antenna for CubeSats communications. The main idea is to feed the resonance arms of the upper F-shaped

patch by a folded ramp-shaped patch. This generates two resonant frequencies and hence achieves a wide bandwidth. Moreover, three shorting pins between the edges of the upper patch (F-shaped patch) and the ground plane are used to increase the effective electrical length of the patch and hence reduces its physical size. In addition, shorting pins are also used to lower the resonant frequency and widen bandwidth. Compared to all previous S-band planar antennas, see the survey in [37] and listed in Table 4.2 for convenience, the wide band F-shaped patch antenna design achieves a higher gain, i.e., 8.51 dB, has a wider bandwidth of 1121 MHz (1.606-2.727 GHz) and has small size of 33.8×88.4 mm^2, which means less surface area on a CubeSat; i.e., 29.8% for 1U and 14.9% for 2U.

Table 4.2. A comparison between S-band patch antennas for CubeSats and the proposed antenna

Ref.	***Antenna Type***	***Gain [dB]***	***Bandwidth [MHz]***	***Size [mm^2]***
[61]	Four-element microstrip patch array	7.1	320	15×15
[113]	Shorted patch antenna	3.51	320	83×83
[67]	Patch antenna	n/a	80	80×80
[51]	Circular patch antennas	5.96	50	3.14×1.2^2
[48]	Wire patch antenna	n/a	116.34	3.14×2.7^2
Proposed antenna	**F-shaped patch**	**8.51**	**1121**	**33.8×88.4**

4.2.1 Antenna design and structure

Figure 4.12 shows the structure of the proposed antenna. It consists of an upper F-shaped patch, a folded patch feed and three shorting pins. The antenna uses the CubeSat's surface as a ground plane with air substrate; see Figure 4.12 (a). It is fed by a 50 Ω coaxial probe at (x_0, y_0) and supported by the three shorting pins that are connected between the upper F-shaped patch and ground plane. These shorting pins generate low resonant frequencies and hence increases bandwidth and help reduce the size of the antenna. The diameter of the shorting pins that provides the optimal antenna bandwidth is 3.64 mm. Moreover, to reduce the coaxial probe length and inductance at the feed section, the folded patch technique from [88] is used and fed at a height of h_1= 18.4 mm. The length of the arm L_1 and the width of the slot W_2 is studied using HFSS to obtain their optimal value. These parameters play a significant role in enhancing the antenna's performance; i.e., bandwidth, resonant frequency and

return loss. They also produce two resonant frequencies and hence improve bandwidth. The Quasi Newton method which is available in HFSS software is used to obtain the optimal dimensions that provide the best performance of the proposed antenna. The optimal parameter values of the proposed antenna are as follows: h_1= 18.4 mm, h_2= 9.5 mm, L=33.8 mm, W= 88.4 mm, W_1= 20.8, W_2= 15.6, W_3= 36.4 mm, L_1= 20.8 mm, L_2= 23.4 mm, L_3= 10.4 mm, L_4= 13 mm, x_0= 0 mm and y_0= 10.4 mm.

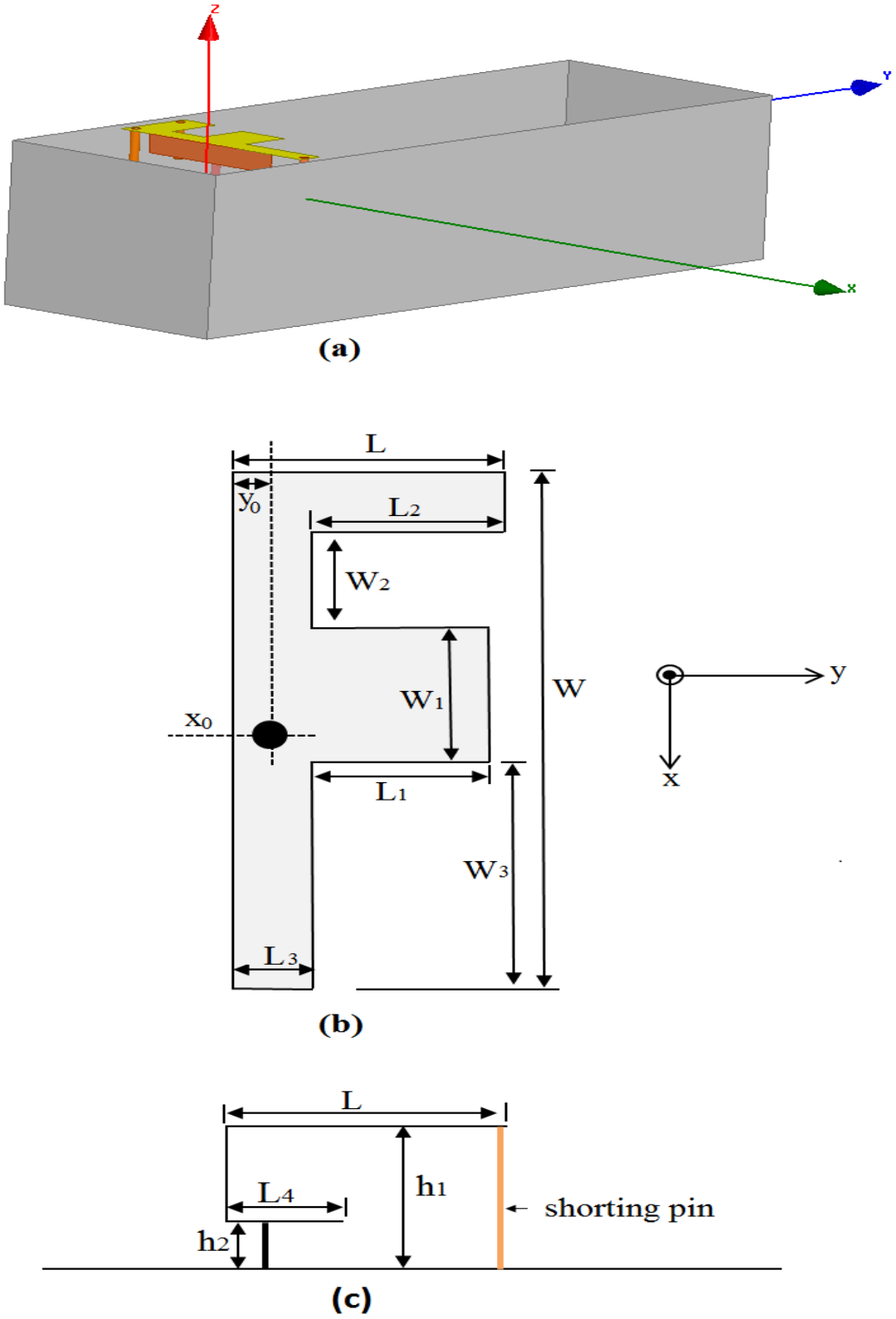

Figure 4.12. Configuration of the wideband F-shaped patch antenna. (a) a 3D view of the proposed antenna in HFSS on a 3U CubeSat, (b) top view, and (c) side view.

4.2.2 Results and discussion

The simulation results are obtained using the HFSS simulator. Figure 4.13 shows the simulated return losses of the F-shaped patch antenna with the following L_1 lengths: 18.8, 20.8 and 22.8 mm. Other parameters are fixed. It shows that the second (fundamental) resonant frequency increases when L_1 increases while the first resonant frequency is barely affected. The required resonant frequency of 2.45 GHz is obtained at L_1=20.8. Moreover, when L_1 is set to 18.8 mm, the F-shaped patch antenna becomes a dual-band antenna rather than wideband. The most suitable length is L_1= 20.8 mm as it provides wide bandwidth; i.e., 1121 MHz, and small return loss of -32.85 dB at resonant frequency 2.45 GHz. This means good impedance matching.

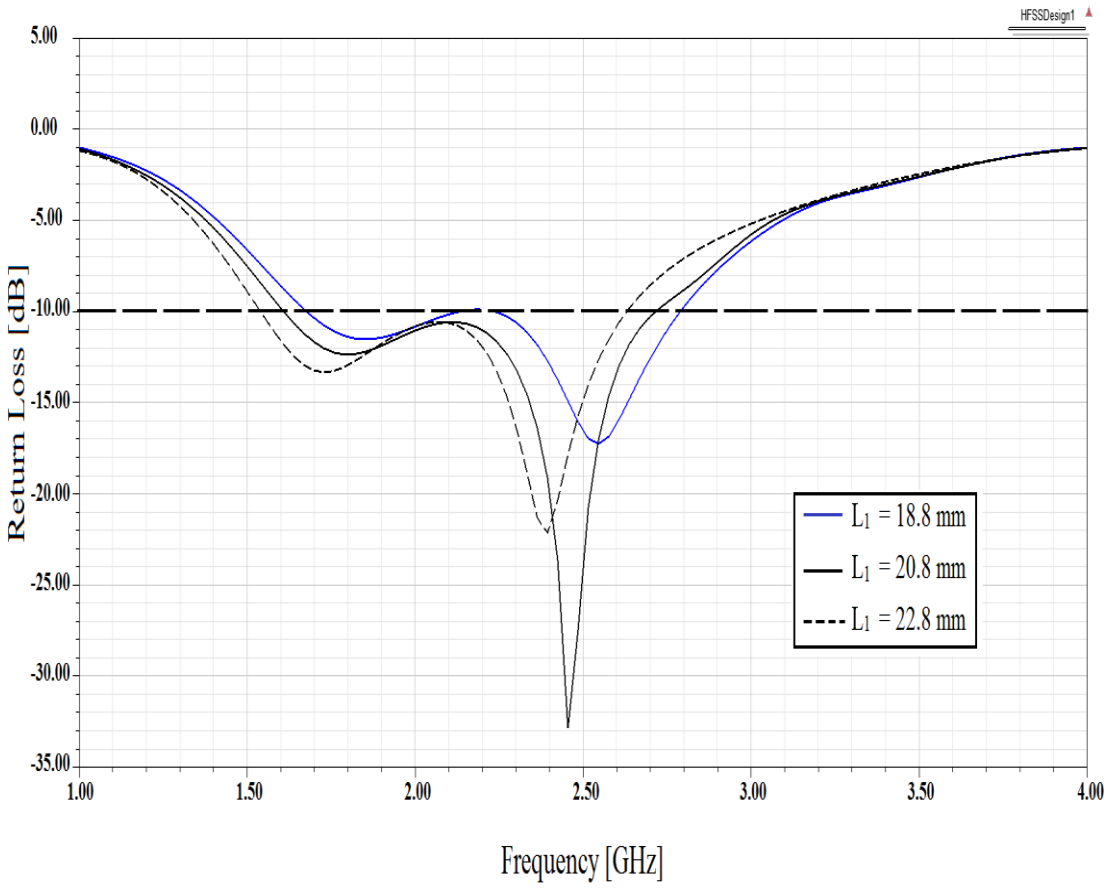

Figure 4.13. Simulated return loss against frequency for various L_1 values.

Figure 4.14 shows the simulated return loss of the proposed antenna with different slot width values and L_1 =20.8 mm. The width W_2 is varied from 8.6 to 22.6 mm.

The slot width W_2 has no effect on the resonant frequency and the bandwidth of the F-shaped patch antenna. However, the return loss S_{11} increases when the width W_2 decreases. In addition, when W_2 is set to 22.6 mm, a dual band resonant mode is obtained. Hence, small -10 dB impedance bandwidth, i.e., 600 MHz (2.12 – 2.72 GHz) is achieved. The most suitable width is W_2 = 15.6 mm as it provides an impedance bandwidth of 1121 MHz (1.606-2.727 GHz) and a small return loss of -32.85 dB at resonant frequency 2.45 GHz. This means large bandwidth, high bitrate, low reflected power and good impedance matching; see Figure 4.14 and 4.17.

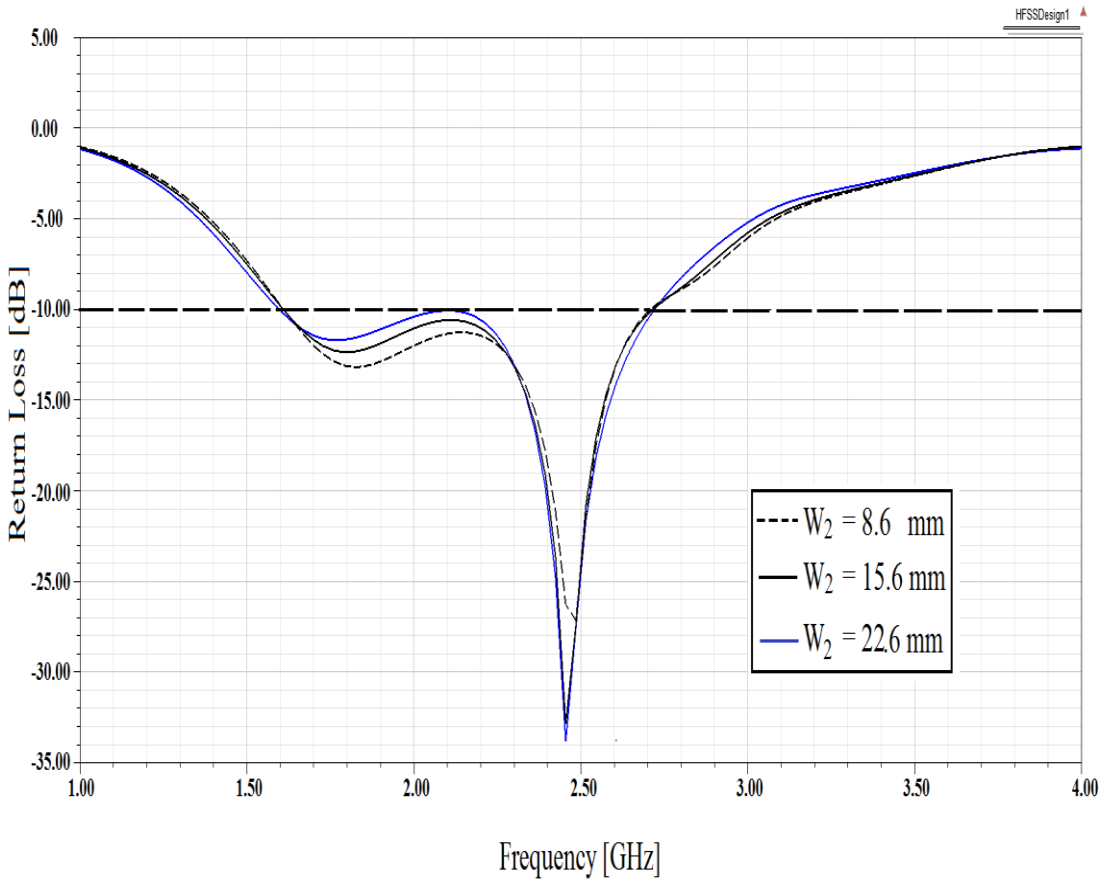

Figure 4.14. Simulated return loss against frequency for various W_2 values.

Figure 4.15 and 4.16 show the 3D and 2D simulated radiation pattern at the resonant frequency of 2.45 GHz. The back lobe is significantly reduced because of the large ground plane, namely the CubeSat's surface, and hence a unidirectional pattern is achieved. This is important as it increases the total gain and decreases the

interference with the electronics inside the CubeSat. The maximum achieved gain is about 8.51 dB with a 20^0 elevation tilt and HPBW of 98.34^0 at a resonant frequency of 2.45 GHz.

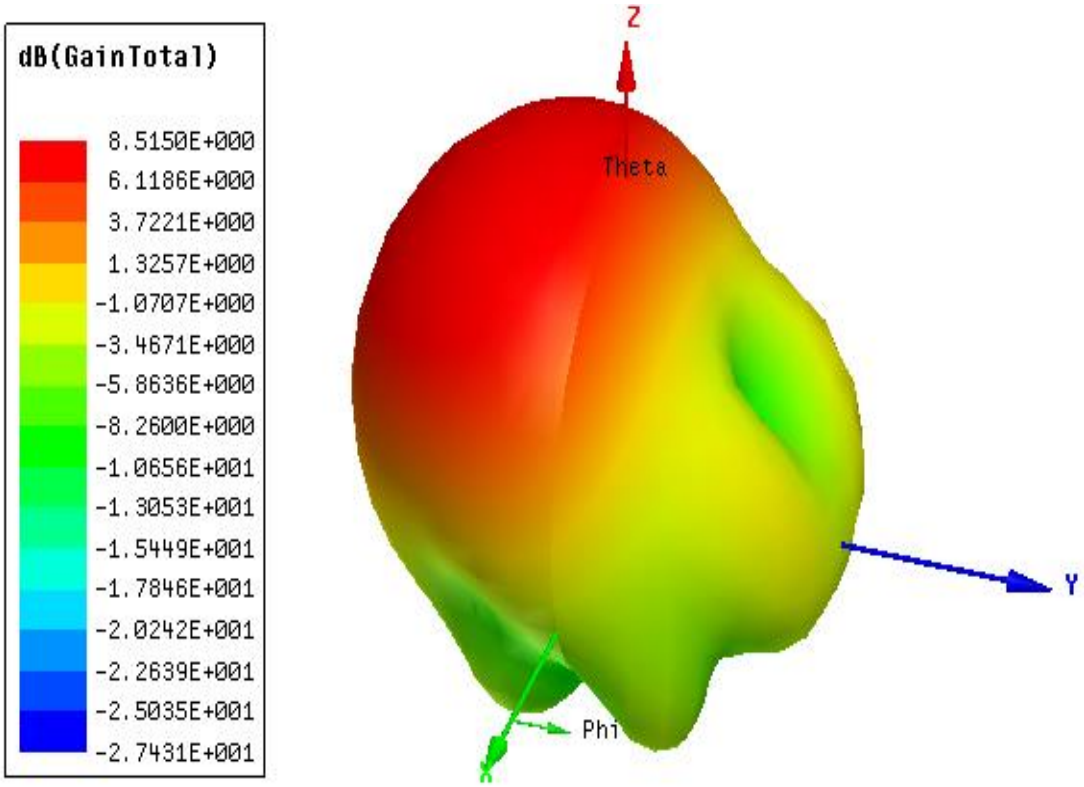

Figure 4.15. 3D gain at 2.45 GHz.

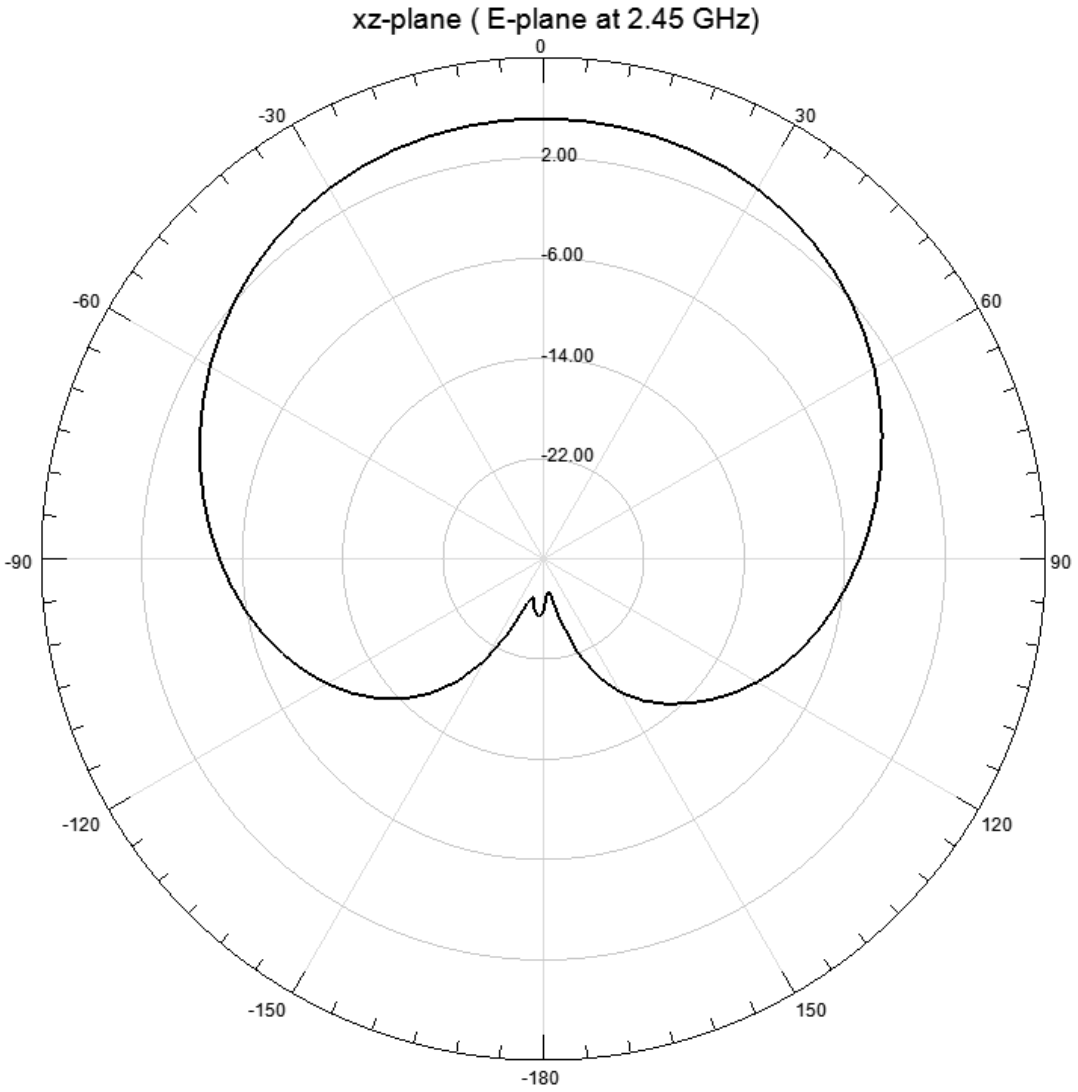

Figure 4.16. Simulated radiation pattern of the proposed F-shaped patch antenna at 2.45 GHz.

Figure 4.17 depicts the simulated input impedance (real and imaginary parts) of the F-shaped patch antenna in the 1 – 3.5 GHz frequency bands. Good impedance matching is obtained at 2.45 GHz with almost 50 Ω real part and zero imaginary parts (inductance). The input impedance (real and imaginary parts) is 50+j0 Ω at the resonant frequency of 2.45 GHz. This means very small reflection with most power radiated into space.

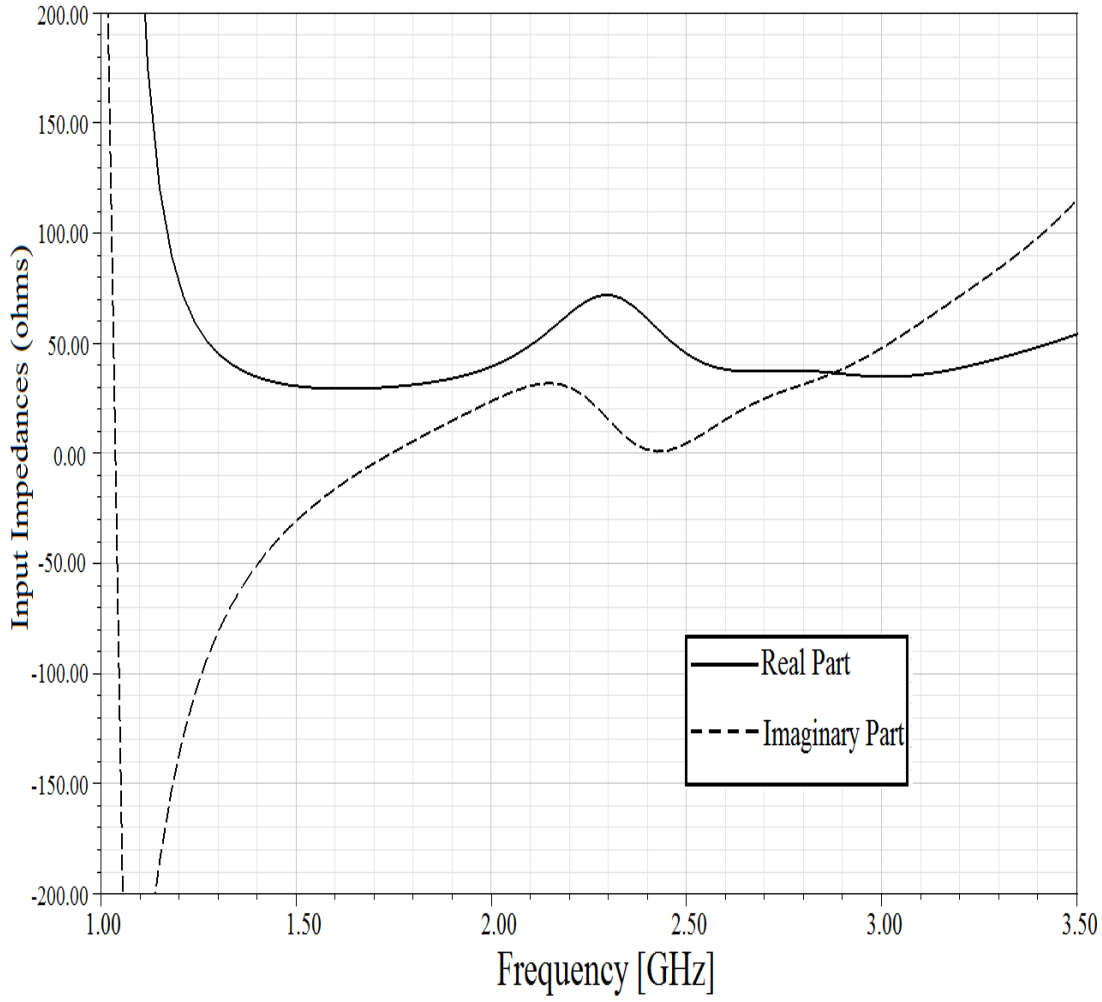

Figure 4.17. Input impedance of the proposed F-shaped patch antenna.

4.3 Conclusion

This chapter has studied and compared repurposed shorted patch and CPW-feed square slot antennas that are suitable for CubeSat communications; i.e., they operate on the 2.45 GHz band and can be mounted on a 2U CubeSat body. Simulation results show that the modified shorted patch and CPW-feed square slot antennas have return losses that are well below -10 dB and achieve impedance bandwidth of 870 and 530 MHz respectively. This chapter also presented a gain enhancement of the modified CPW-feed square slot antenna by changing its geometry. In particular, the F-shaped slits are replaced with a square slot. This improved CPW-feed square slot antenna

has a resonance frequency of 2.45 GHz and provides a total gain of 2.52 dB at 2.45 GHz.

To address the problems of narrow bandwidth and low gain of the new shorted patch and CPW-fed slot antennas, this chapter also proposed a wideband F-shaped patch antenna for S-band CubeSats communications. Its simulated return loss is below -10 dB from 1.606-2.727 GHz (a bandwidth of 1121 MHz). The antenna size is small; i.e., 33.8×88.4 mm^2. Simulated results show it has a resonant frequency of 2.45 GHz, a small return loss of -32.85 dB, a high gain of 8.51 dB and good impedance matching of 50 Ω.

As mentioned, the main limitation of the new CPW-fed slot and shorted patch antennas is their low gain. This is because of their bidirectional radiation pattern. Therefore, the next chapter presents a unidirectional high gain S-band CPW-fed slot antenna using a MSS technique.

Chapter 5

HIGH GAIN S-BAND CPW-FED SLOT ANTENNA FOR CUBESATS

As mentioned in Chapter 4, the new shorted patch and CPW-fed slot antennas have narrow bandwidth and low gains. Ideally, CubeSats should employ an antenna with wide coverage while at the same time has a high gain. However, the limited size and low mass of CubeSats pose real challenges to any antenna design. Another challenge is that CubeSats cannot be repositioned after deployment, and thus may be oriented poorly for communications.

To address the aforementioned challenges, this chapter proposes a high gain coplanar waveguide (CPW)-fed slot antenna that operates at 2.45 GHz (S-band). A key feature is the use of a MSS [114] as a resonant cavity model. This allows the proposed antenna to have high gains because the MSS redirects the back radiation pattern forward [115]. Advantageously, its use allows the proposed antenna to occupy less space than using a reflector as in [116].

Table 5.1 compares the proposed CPW-fed slot antenna against competing designs. Observe that the designs of [6] and [57] achieve beam steering using phase shifters and beam forming algorithms. However, this adds extra cost and complexity. The design in [21] is a simple monopole antenna that provides wide directivity without the need for beam steering techniques. It, however, has a low total gain. Another drawback of [21] is its deployment mechanism that incurs extra cost and complexity. Also, there is a risk it might not deploy, which contributes to the likelihood of mission failure. In terms of size, the antenna in [117] has the smallest area of 75 mm×75 mm but its main limitation, as pointed out by the authors, is the resulting low gain, i.e., 1.53 dB, because of its bi-directional radiation [118]. To solve this problem, one common approach is to redirect the back radiation pattern forward by placing a backing metallic reflector that is $\lambda_0/4$ away from the antenna [116]. Its main drawback, however, is its large profile structure due to the $\lambda_0/4$ spacing between the

reflector and the antenna. Moreover, the authors of [119] propose to place two S-band patch antennas on two faces of the CanX-4 and CanX-5 CubeSats to achieve omni-directional coverage and a data rate of 10 kbps. In another example, the authors of [6] propose to use a square patch antenna array. The antenna array is fed at four different angles, i.e, 0^0, 90^0, 180^0, and 270^0, to achieve beam steerability using a phase shifter. In contrast, the proposed antenna design achieves a superior gain of 9.71 dB at 2.45 GHz. This is important as it enables long distance communications. Consequently, fewer CubeSats will be required to operate in a swarm. Moreover, it further reduces the cost related to manufacturing and placing a satellite into orbit. Moreover, as the proposed CPW-fed slot antenna design uses a MSS to suppress back radiation, there is less interference with components inside a CubeSat. Note that other types of antennas are not considered because they have a large profile, require deployment mechanisms and occupy a large area [37].

Table 5.1. Comparison between antennas for CubeSat communications and proposed antenna

Ref.	**Type of Antenna**	**CubeSat Type**	**Frequency [GHz]**	**Gain [dB]**	**Volume [mm^3]**	**Beam Steering**
Proposed antenna	*CPW-fed slot antenna*	*3U*	*2.45*	*8.48*	*90×90 ×10.5*	*Not required*
[117]	A square slot antenna	1U	2.45	1.53	75×75 ×1.6	Not required
[6]	Phased patch antenna array with 90^0 hybrid	1U	5.8	5.1	90×90×5	Electronic pointing (using phase shifter)
[119]	Patch antenna	1U	s-band	N/A	N/A	Not required (Omnidirectional)
[57]	Six individual patch antennas placed on different faces of a CubeSat	3U	2.45	4.8	N/A	Beam-forming algorithm
[21]	Four monopole antennas	2U and 3U	0.437	N/A	N/A	Not required (Omnidirectional)

5.1 Antenna Configuration

Figure 5.1 shows the geometry of the proposed CPW-fed slot antenna. The slot and the feed line are etched on a square FR4 substrate with a dielectric constant of 4.4 and a substrate thickness of 1.6 mm. This FR4 substrate is commonly used in antenna designed for CubeSats [6]. The antenna is fed by a 50-Ω CPW with a strip line width W_f = 3.4 mm and is separated from the ground plane by two gaps with width g = 0.45 mm and T = 1.65 mm. The lightening-shaped feedline is formed by extending the signal strip of the CPW in the -y direction to the lower left corner of the slot (the horizontal feed section). This lightening-shaped feed-line has horizontal and slanted (S) feed sections with the same width of W_s = 3.75 mm and an angle of 45^o. It is used to enhance the AR bandwidth. The horizontal feed section is separated from the lower and left edges of the slot by two gaps of width T and g, respectively. Moreover, the tuning stub, with a width of W_n, and a length of L_n, is embedded in the feed-line structure to enhance the impedance bandwidth and to achieve good impedance matching. As shown in Figure 5.1 (a), the vertical tuning stub is formed by extending L_n along the CPW's signal line, whereas the horizontal tuning stub is formed by extending the horizontal feed section to the right by L_t=7.5 mm as measured from the right edge of the centre signal line of the CPW.

Figure 5.1 (b), (c) and (d) show a MSS that is comprised of a 7×6 Double Closed-Square Resonator (DCSR) array. It is printed on an inexpensive 0.8 mm thick (h_2) FR-4 material. This MSS has dimension 90mm×78mm and is placed above the slot antenna. The physical parameters of DCSR are as follows: P = 10 and b = 9 mm. More details about the physical parameters of MSS can be found in reference [115]. The square-shaped metasurface elements have been selected because they provide better performance and results; see reference [120] for details.

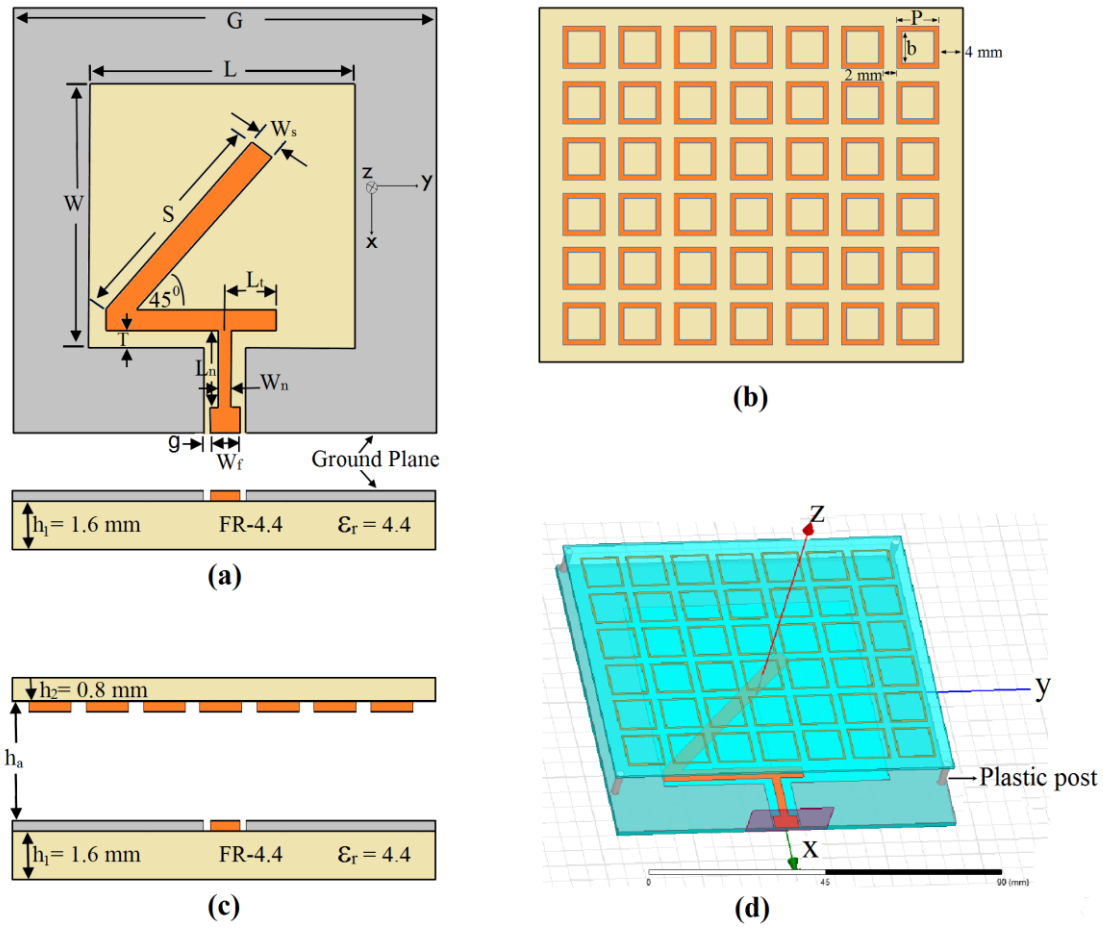

Figure 5.1. Configuration of the proposed CPW-fed slot antenna with a MSS (a) the proposed CPW-fed slot antenna, (b) MSS, (c) a cross section view, and (d) the model in HFSS.

5.2 Results and Discussion

This section outlines a parametric study that aims to identify factors that affect antenna performance; i.e., return loss, impedance bandwidth, gain and radiation pattern. Moreover, Section 5.2.2 compares simulated and experimental results.

5.2.1 Parametric study

This chapter now presents various parametric analyses conducted using HFSS. It focuses on the best return loss, impedance matching, and gain at the operating frequency of 2.45 GHz. Table 5.2 lists the optimal parameters of the proposed antenna.

Table 5.2. Optimal parameters of the proposed antenna

Parameters	Values (mm)
G	90
L	60
W	60.3
W_n	2.15
W_s	3.75
L_n	12.8
L_t	7.5
h_a	8.1
T	1.65
g	0.45
W_f	3.4
S	55.8

- *Design frequency and initial parameters*

  The target operating frequency is f_t=2.45 GHz which is commonly used by the CubeSats community due to its high bit-rate and is within the 2.4-2.5 GHz ISM band [121]. The antenna operating frequency is varied by controlling its size as per $F=f_0/f_t$, where f_0 is the obtained resonant frequency over the specified dimensions. The aim is to achieve a minimum return loss (S_{11}) at the target operating frequency of f_t=2.45 GHz. Therefore, the antenna size needs to be increased (or decreased) by F in order to operate at the desired resonant frequency of f_t. In order to determine the best value of F, the Quasi Network method is used.

- *Effect of W_n and L_t*

  Figure 5.2 (a) illustrates the return loss (S_{11}) with the following widths (W_n): 1.8, 2.15 and 3.15 mm. Other parameters are fixed. It shows that the width W_n of the tuning stub has an effect on impedance matching, operating frequency and impedance bandwidth. When the width W_n increases, e.g., exceeds 2.15 mm, the return loss increases and the impedance bandwidth (BW) improves; it is observed that BW increases proportionally with W_n. Also, the operating frequency is slightly increased when W_n increases and vice-versa; The best value of W_n is 2.15 mm, which gives good impedance matching and hence low reflected power at the target resonant frequency of 2.45 GHz.

Figure 5.2 (b) presents the simulated return loss of the proposed CPW-fed slot antenna for the following L_t lengths: 6.5, 7.5 and 8.5 mm. It shows that L_t also has a significant effect on the operating frequency and return loss. As the length of the horizontal feed section increases, the return loss decreases and the operating frequency increases. The smallest return loss is achieved at L_t = 6.5 mm. However, the operating frequency shifts to 2.55 GHz. The most suitable L_t value is 7.5 mm. This value shifts the operating frequency from 2.55 to 2.45 GHz with a return loss of -27.5 dB and bandwidth of 730 MHz (1.9 – 2.63 GHz).

- *Effect of L_n*

With the width of the tuning stub fixed at W_n = 2.15 mm and the length of the horizontal feed section set to L_t = 7.50 mm, this section presents a study of the following L_n values: 11.80, 12.80 and 13.80 mm. Referring to Figure 5.3, the length L_n has a significant effect on the return loss and the impedance bandwidth. As the value of L_n increases, so does the return loss. This means more power is reflected instead of being radiated into space. Moreover, the BW decreases proportionally with L_n. The smallest return loss is achieved at L_n=11.8 mm. However, the operating frequency is not at the required operating frequency of 2.45 GHz. The most suitable length is L_n= 12.80 mm as it provides small return loss (S_{11} = -27 dB), and wide bandwidth of 750 MHz at the required operating frequency of 2.45 GHz.

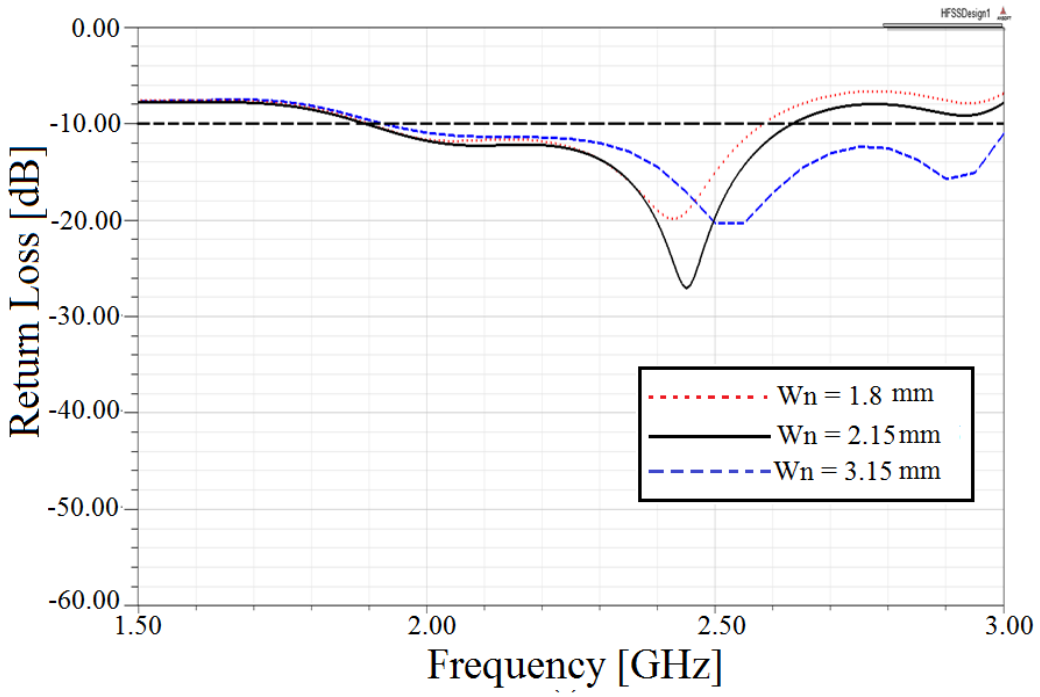

(a)

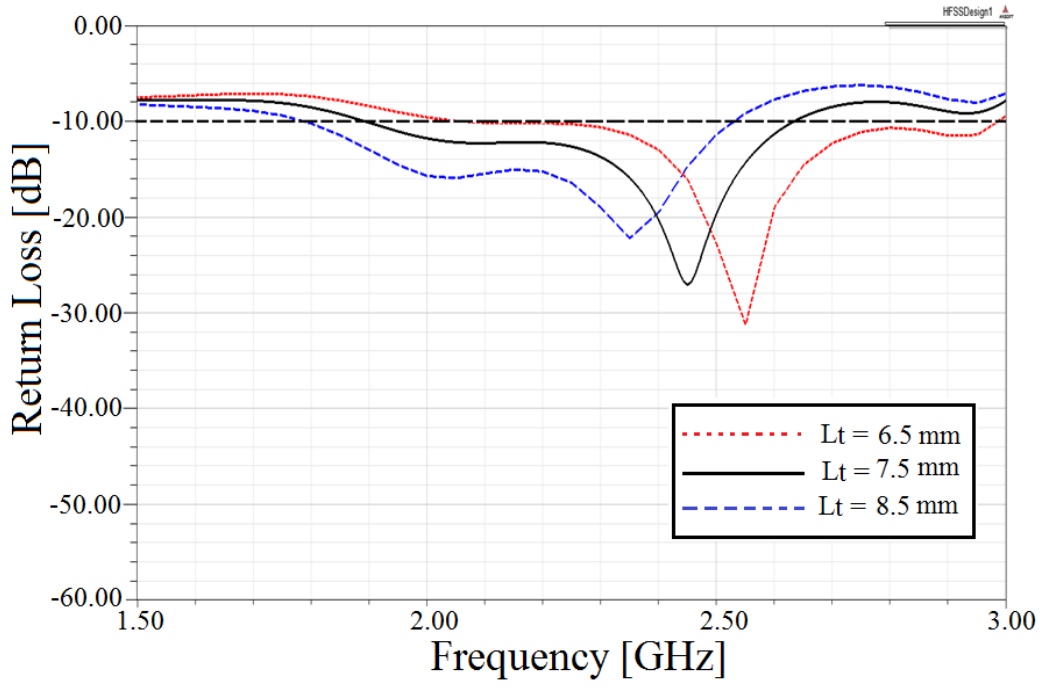

(b)

Figure 5.2. Simulated return loss against frequency for various (a) W_n, and (b) L_t values.

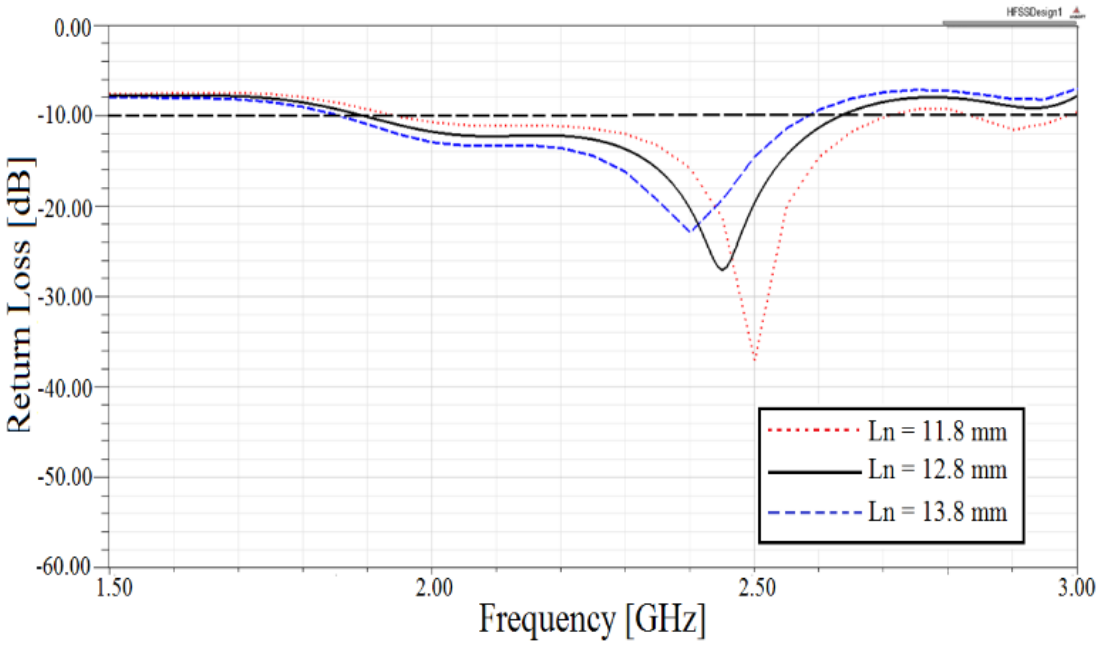

Figure 5.3. Simulated return loss against frequency for various values of L_n.

- *Effect of metasurface starting positions*

  Figure 5.4 shows (a) the simulated return loss (S_{11}) and (b) the simulated 2D gain for the following MSS positions: 0, 6, and 12 mm from the feed line. Other parameters are fixed. MSS positions have a significant effect on the return loss. The return loss (S_{11}) increases and the gain decreases when the MSS starting position is close to the feed line, e.g., 0 and 6 mm. There is almost no change to the resonant frequency of 2.45 GHz. Therefore, the starting position of 12 mm from the feed-line in the -x direction yields the best result. This is because it gives the smallest return loss, e.g., -36.5 dB, and highest gain, e.g., 5.20 dB, at the required operating frequency of 2.45 GHz.

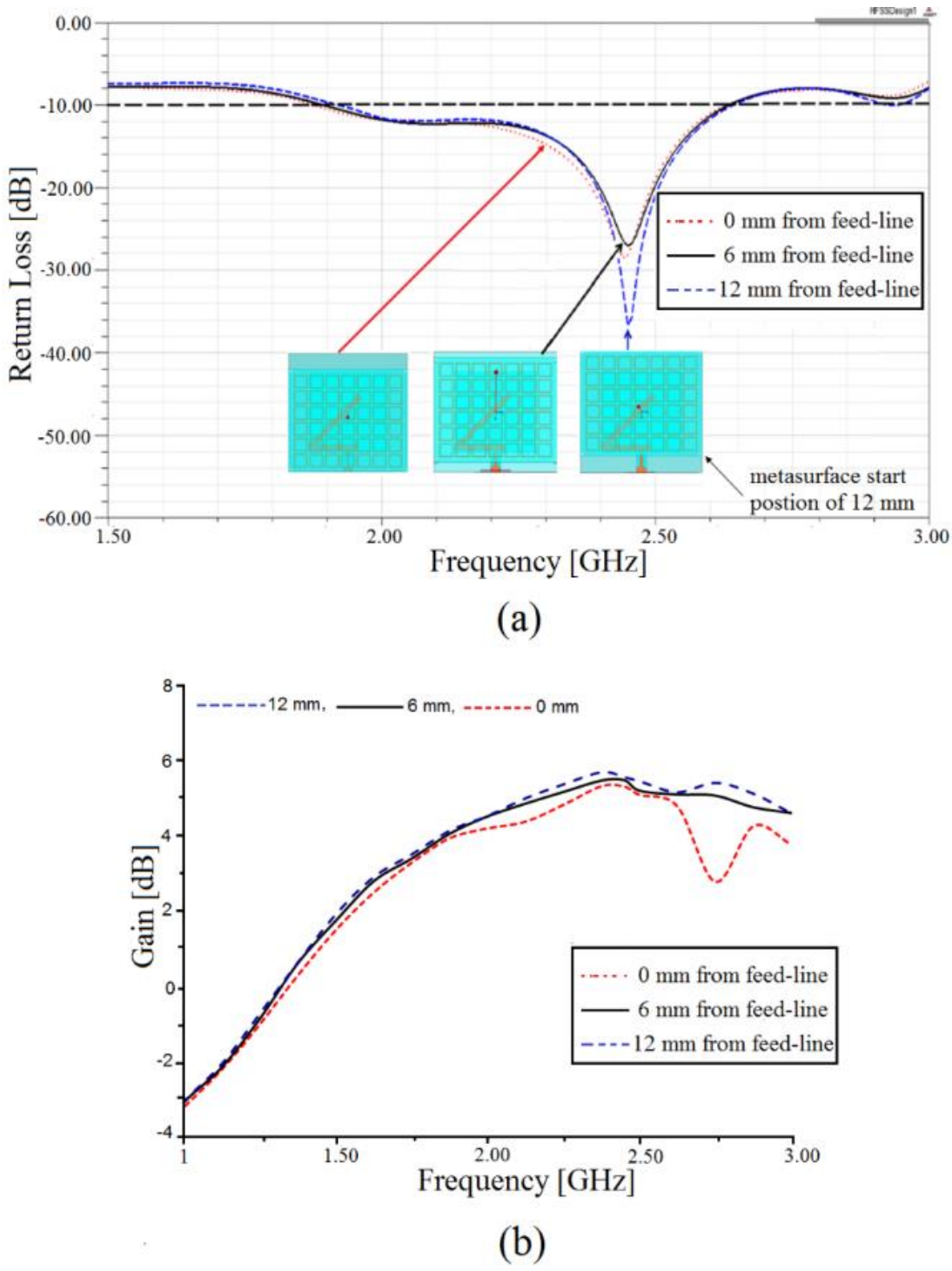

Figure 5.4. The effect of the starting edge of the MSS position on (a) the reflecting coefficient S_{11}, and (b) antenna gain.

- *Effect of metasurface array element sets*

  As shown in Figure 5.5 the array element sets of the MSS have a significant effect on the return loss and hence, impedance matching. As the number of elements increases, the operating frequency approaches the operating frequency of 2.45 GHz and return loss decreases. Different array element sets have been tested. The most important sets that have a significant effect on the return loss are 7x2, 7x4 and 7x6. Thus, these sets are considered from here onwards. Figure 5.5 shows that a 7×6 array element set is ideal because it achieves the smallest return loss; i.e., -36.5 dB at an operating frequency of 2.45 GHz.

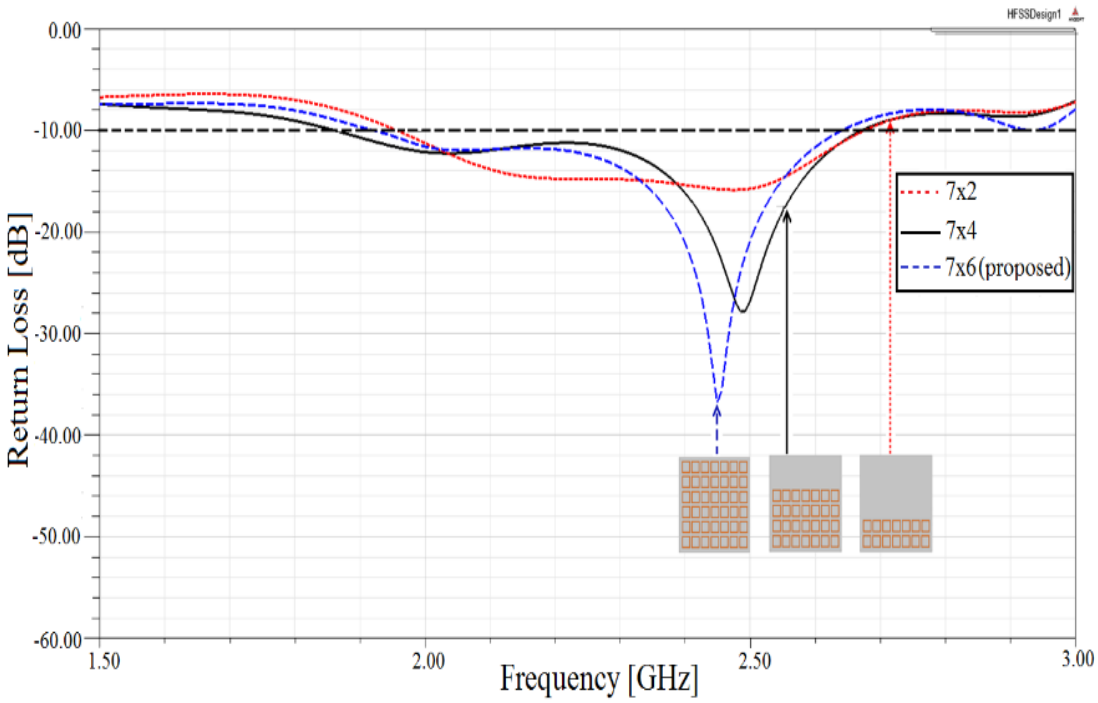

Figure 5.5. The influence of MSS element sets over the return loss (S_{11}) of the proposed antenna.

A. Effect of metasurface height

Next is an evaluation of the effect of MSS height on the impedance matching. The MSS's height is varied from 4.1 to 10.1 mm; see Figure 4.6. Heights of h_a= 4.1 and 6.1 mm result in higher return loss as compared to h_a = 8.1 and 10.1 mm. In the case of h_a = 8.1 mm, the obtained impedance bandwidth (VSWR ≤ 2) is wide, i.e., 130

MHz (2383 – 2513 MHz), and the return loss is very small, i.e., -36.8 dB. This means large bandwidth, low reflected power and good impedance matching.

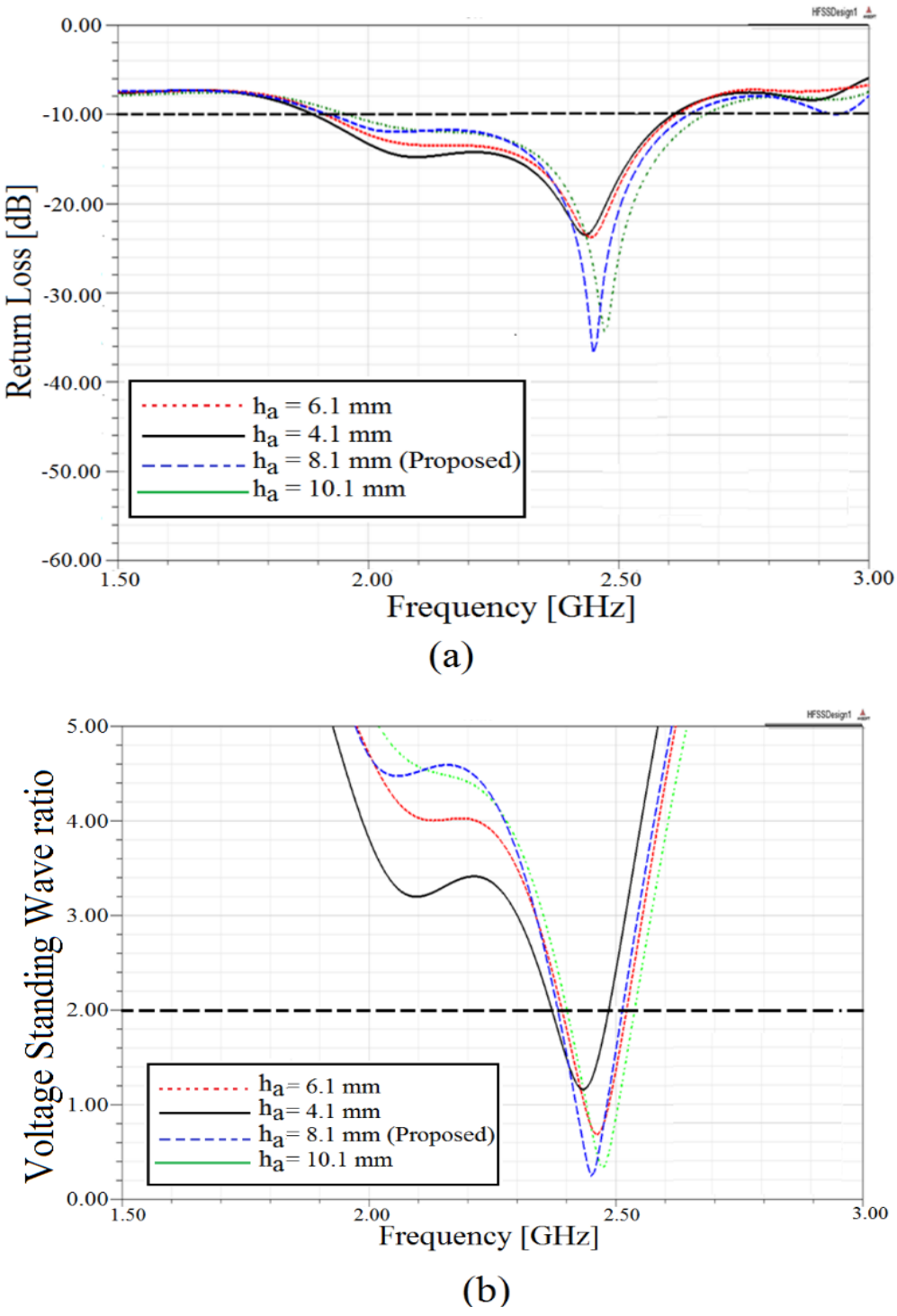

Figure 5.6. The MSS height, i.e., h_a, as a function of (a) the return loss and (b) VSWR of the proposed antenna.

- *Effect of MSS*

This section now studies the effect of MSS on antenna gain. It fixes the width of the tuning stub at W_n = 2.15 mm, the length of the horizontal feed section at L_t = 7.50 mm, the length of the tuning stub at L_n = 12.8 mm, the MSS array set has 7×6 elements and the MSS height is set, i.e., h_a, to 8.1 mm. Figure 5.7 shows the total gain of the CPW-fed slot antenna with and without the use of MSS. It shows that the use of the MSS dramatically increases the antenna's gain from 2.52 to 5.67 dB. Moreover, the amount of back lobe radiation has been further reduced from -9.9 to -8.7 dB. This is important as it increases the total antenna gain. This section concludes that MSS has a significant effect on the antenna gain. The results also indicate decreases in the back lobe pattern. In turn, this dramatically increases (improves) the proposed antenna total gain.

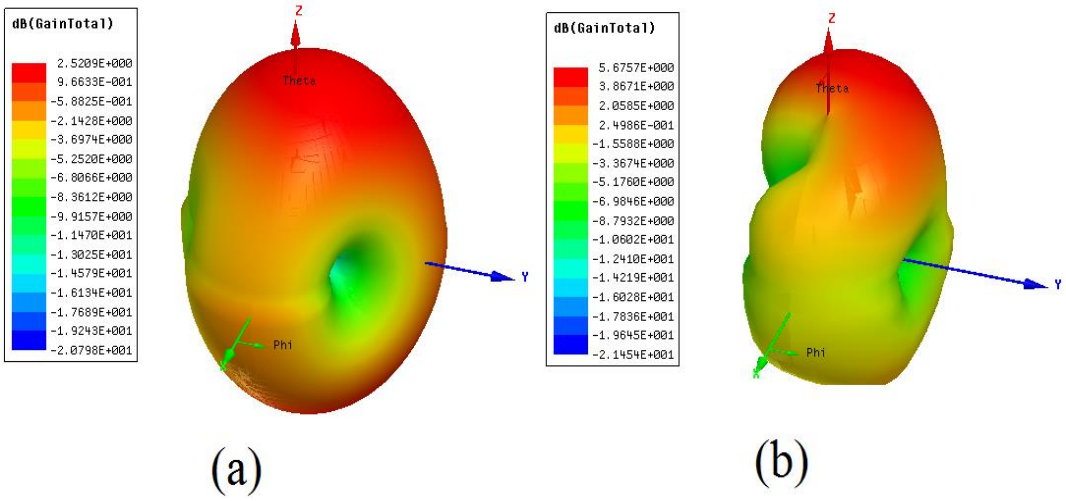

Figure 5.7. The total gain of the proposed CPW-fed slot antenna (a) without MSS, and (b) with the MSS.

- *Effect of CubeSat's body*

The proposed antenna is placed on a 3U CubeSat as shown in Figure 5.8 and Figure 5.11 (b). Note, the antenna can have different placement configurations on a 3U CubeSat. Specifically, for satellite to ground station communications, placing it on only one CubeSat face is sufficient [37]; magnetic torqueing can be

used to ensure it is always pointed at a ground station. For inter-satellite (cross-link) communications, placing an individual antenna on each face of a CubeSat will be required [122].

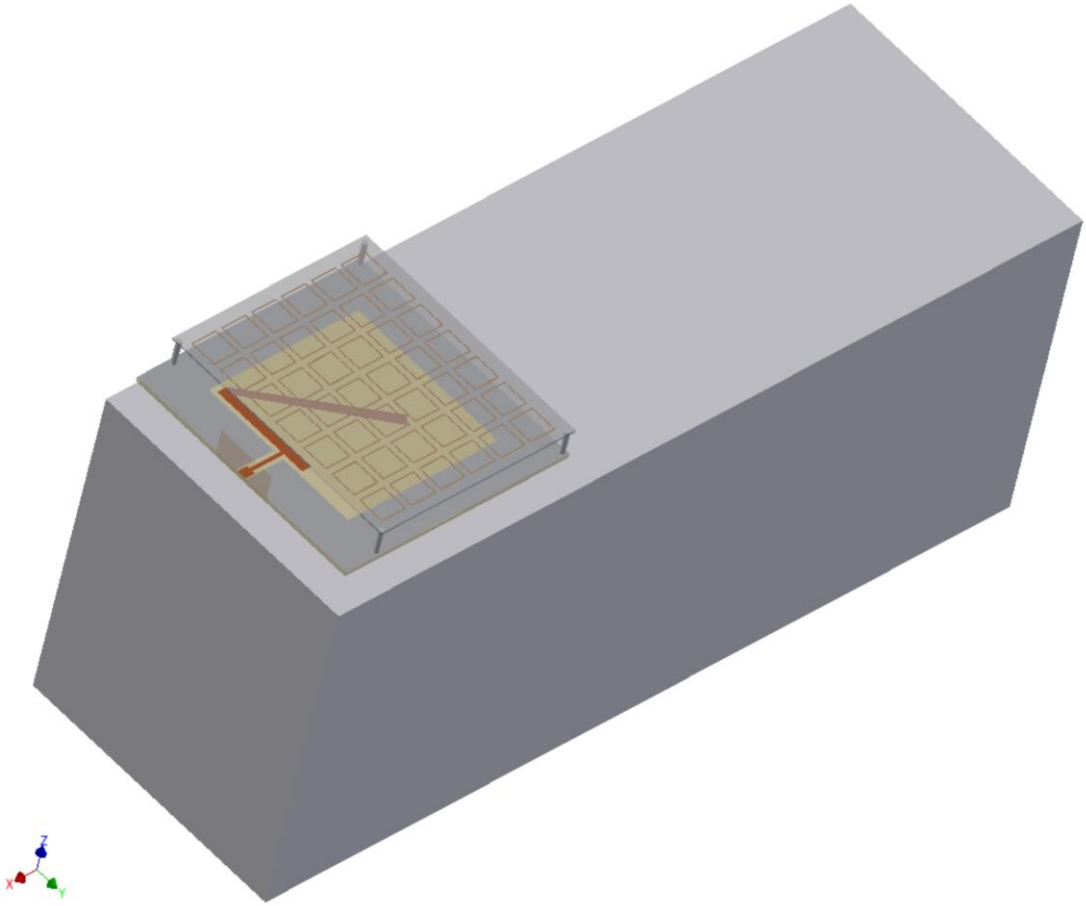

Figure 5.8. A CPW-fed slot antenna on a 3U CubeSat.

To avoid direct contact between the backside (dielectric) of the antenna and the satellite body, a distance (air gap) of 8.5 mm is kept between the antenna and the satellite body. Consequently, the satellite body will act as a reflector that leads to higher gains. The 3U CubeSat body has no effect on the operating frequency. However, the return loss increased from -36.8 to -21.5 dB; see Figure 5.9(a). Moreover, the total antenna gain increased from 5.67 to 9.71 dB; see Figure 5.9 (b). This is because the Aluminium surface of the CubeSat acts as a reflector and reflects some of the back-lobe radiation forward.

Figure 5.10 illustrates the simulated radiation pattern on the xy-plane. It shows that the proposed CPW-fed slot antenna achieves a maximum gain with a 20^0 elevation tilt and Half Power Beamwidth (HPBW) of 33^0 at 2.45 GHz. It also shows that the radiation is in the direction almost normal to the substrate (z-axis).

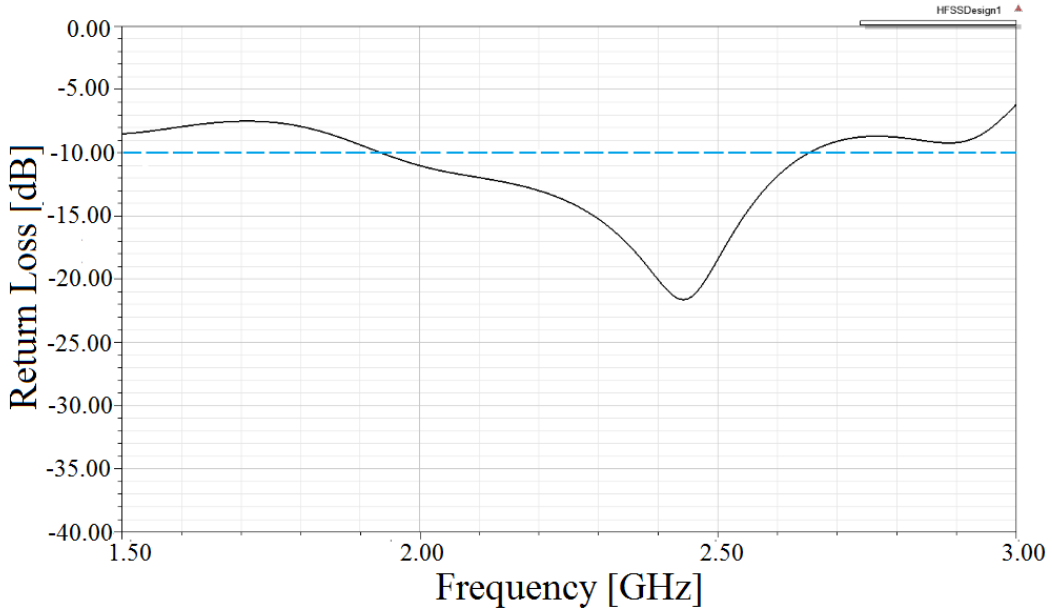

(a)

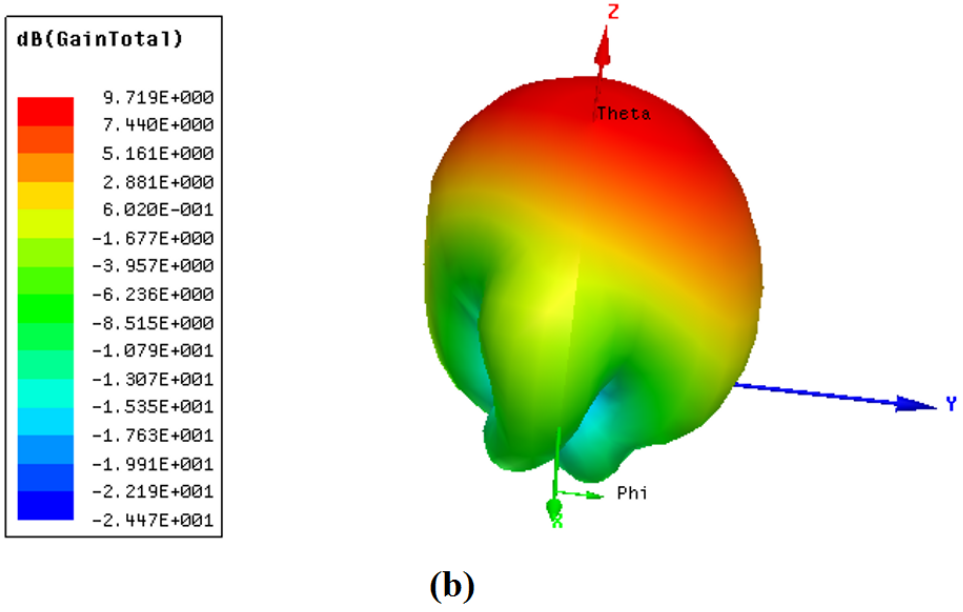

(b)

Figure 5.9. Simulated results of proposed antenna on the CubeSat's body (a) return loss and (b) total gain at 2.45 GHz.

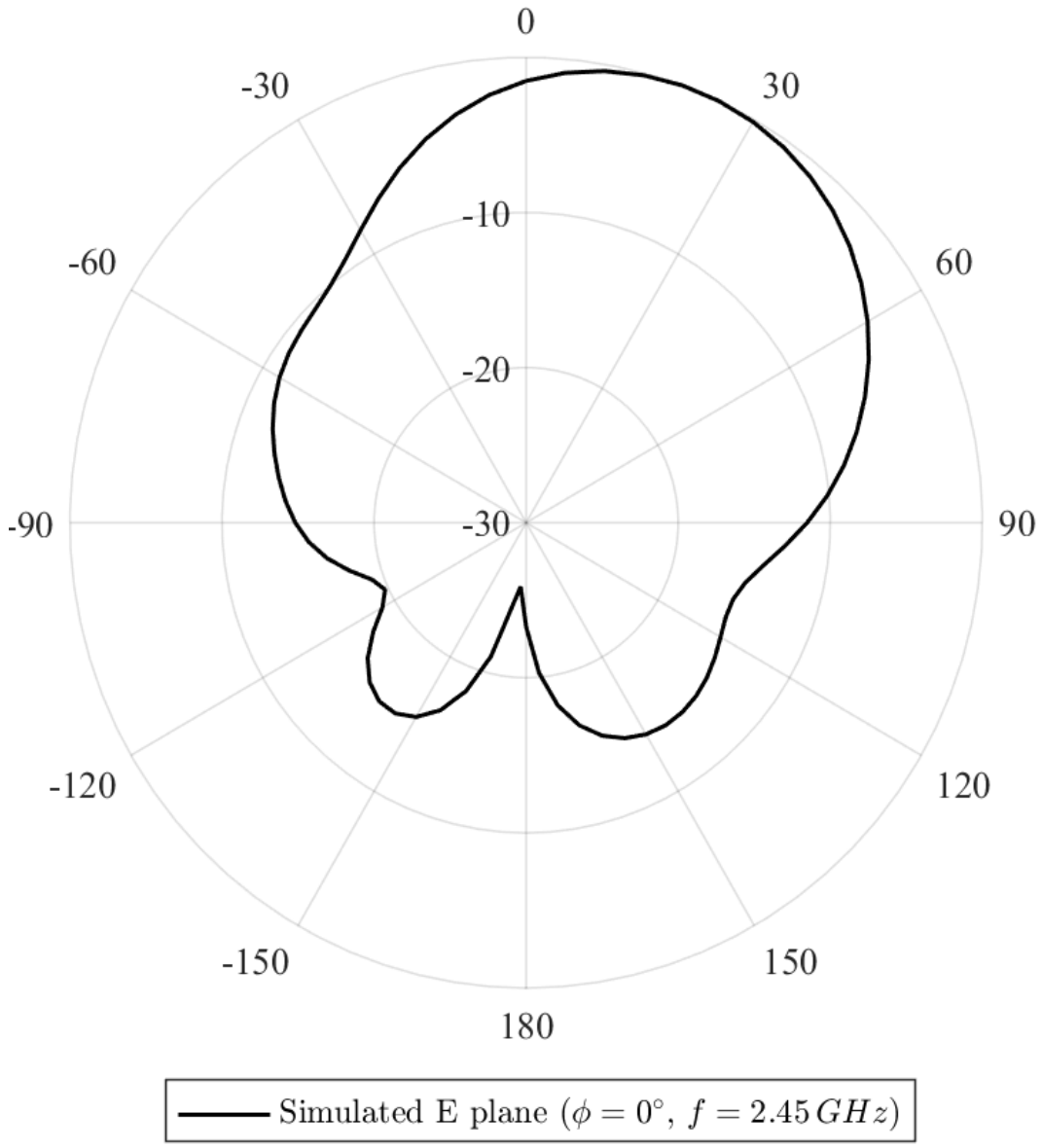

Figure 5.10. Simulated radiation pattern of the proposed antenna on a CubeSat's body at 2.45 GHz.

5.2.2 Experimental verification

In order to verify the simulated results, the proposed CPW-fed slot antenna is fabricated with a MSS array set of 7×6 elements; see Figure 5.11 (a) and (b) for a photograph. The experiments consider the case with and without a 3U CubeSat model. The antenna's characteristics is measured using Keysight's M9370A vector

network analyzer (VNA). The antenna is attached to port one of the VNA using a ridged interconnect featuring male SMA connectors on both ends. The test setup was calibrated with a Rohde & Schwarz ZV-Z270 50Ω calibration kit and a characterized female SMA to male N-connector adapter. The system is de-embedded to the reference plane of the SMA connector on the antenna. The VNA is set to sweep from 1.5 to 3.5 GHz using a resolution bandwidth of 100 kHz and an output power of -5 dBm.

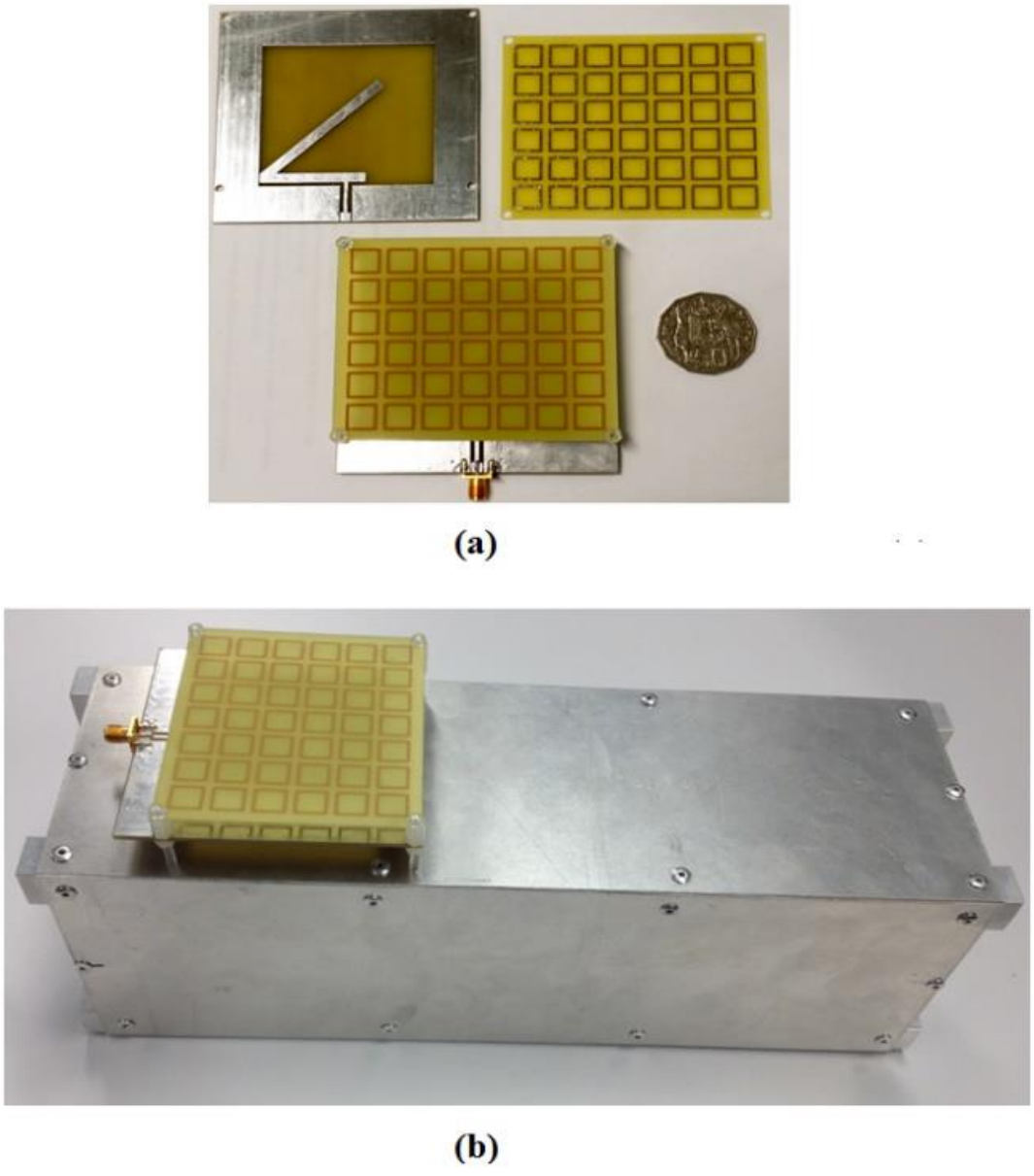

Figure 5.11. A photograph of the fabricated prototype CPW-fed slot antenna: (a) geometry, and (b) its installation on a 3U CubeSat model face.

The simulated and measured return losses (S_{11}) with and without the 3U CubeSat model are depicted in Figure 5.12; all are in agreement with the simulation results from HFSS as they have the same shape and same resonance frequency at their smallest S_{11}. Compared to the simulated return loss of the proposed antenna on the CubeSat's body, the measured and simulated (individual) return losses of the proposed antenna without the CubeSat's body have smaller reflection coefficients. Moreover, both simulation (solid line and long dashed line) and measured (dashed line) results of S_{11} indicate that the CPW-fed slot antenna is well matched at the desired operating frequency; e.g., 2.45 GHz with S_{11} < -10 dB. The simulated and measured fractional impedance bandwidth of the CPW-fed slot antennas is 710 MHz (1940 – 2650 MHz) and 940 MHz (1820 – 2760 MHz) respectively. These negligible discrepancies between the measured and simulated results are caused by the limited accuracy of the etching process used and the antenna testing set up. Figure 5.13 shows the simulated and measured input impedances of the proposed antenna in the frequency bands 1.900 – 2.630 and 1.819 – 2.787 GHz respectively. The simulated and measured input impedance at 2.45 GHz is 43.97Ω and 48.59Ω, respectively.

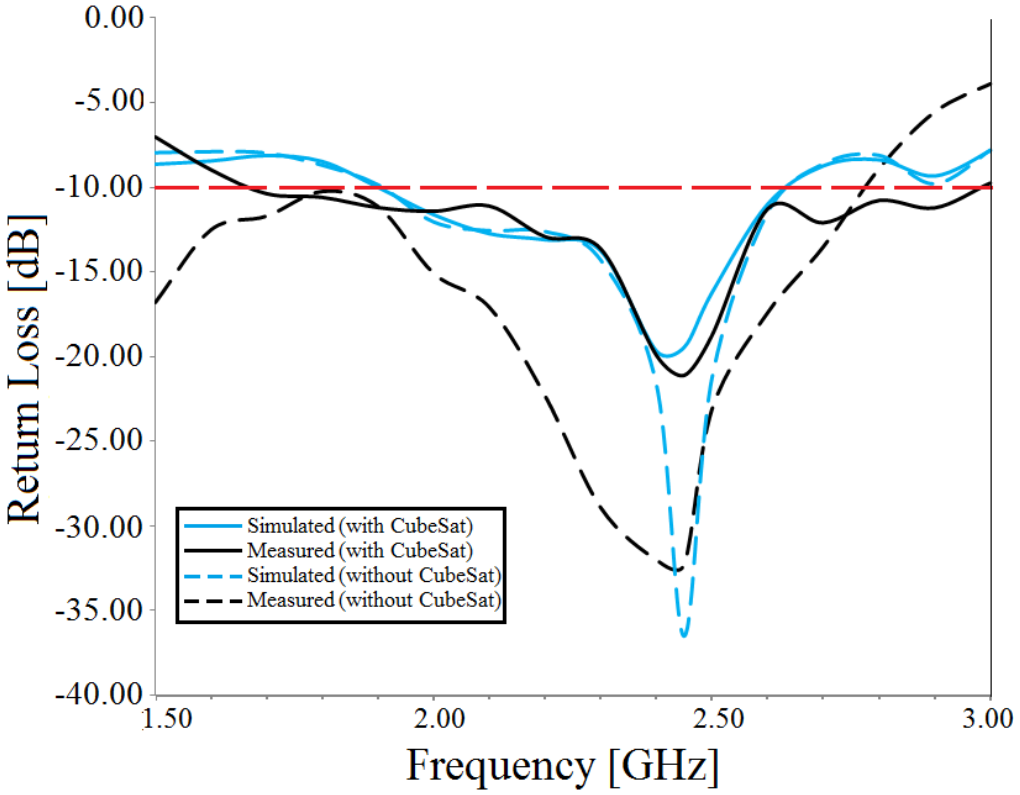

Figure 5.12. Simulated and measured return losses (S_{11}) of the proposed antenna.

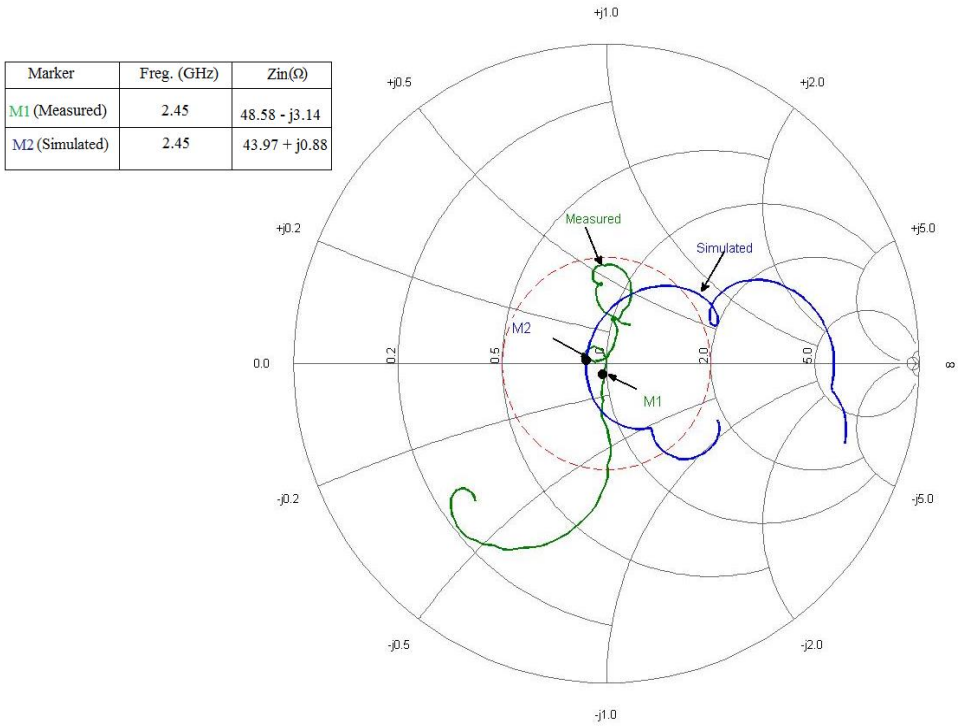

Figure 5.13. Simulated and measured input impedance of the proposed antenna.

Figure 5.14 compares the simulated and measured patterns on the plane parallel to the satellite axis, which contains the antenna itself. The plane includes the direction of the maximum radiation, as discussed earlier in Section 5.2.1. The radiation pattern is quite similar with a small rotation in the pointing angle. This can be due to the mounting of the antenna during measurement, see the inset of Figure 5.14, as the centre of the rotation is different with respect to the phase centre of the antenna.

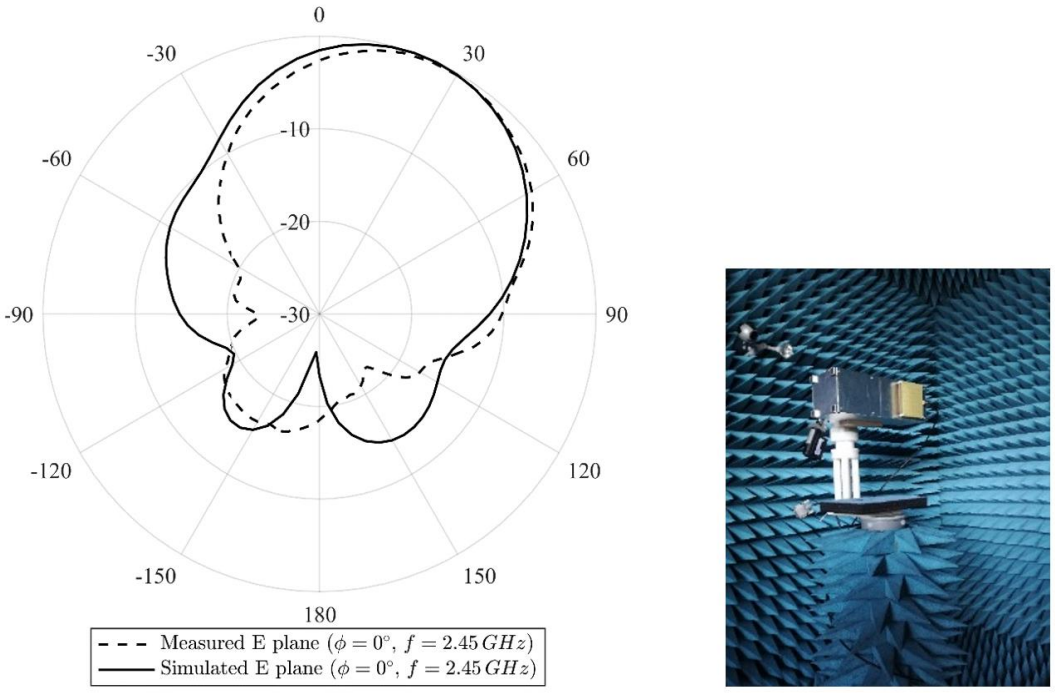

Figure 5.14. Simulated and measured radiation pattern of the proposed antenna on a CubeSat's body at 2.45 GHz (inset: Antenna under measurement).

Figure 5.15 shows the measured and simulated gains versus varying frequencies of the proposed antenna with CubeSat. We see that there is a reasonable agreement through the entire band. The peak gains of simulated and measured gains are 9.71 and 8.8 dBi at 2.45 GHz respectively. The minor discrepancy can be mostly attributed to the fabrication error and measurement uncertainties.

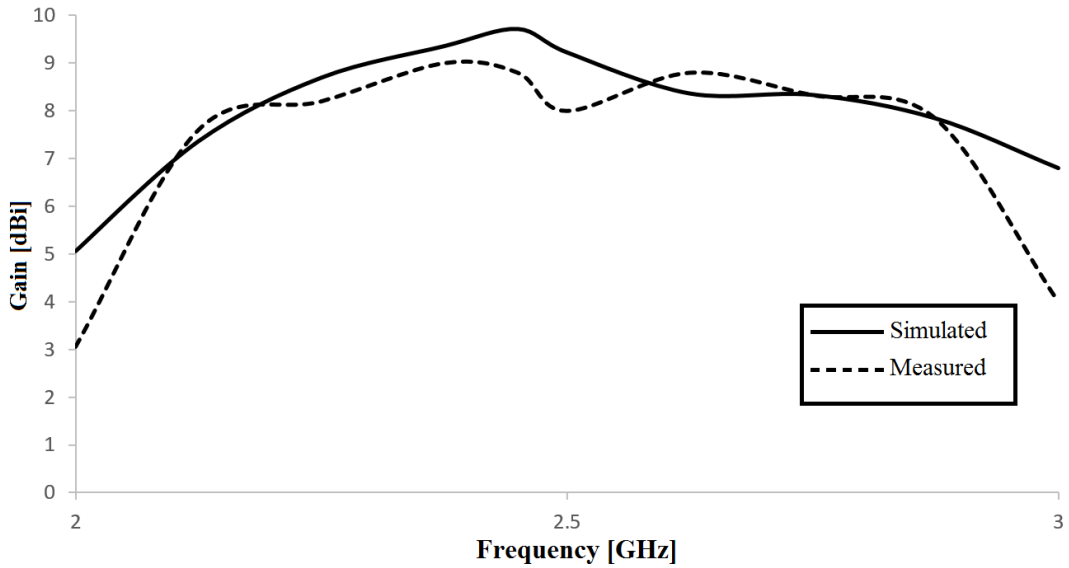

Figure 5.15. Simulated (continuous line) and measured (dashed line) gain of the proposed antenna with CubeSat.

5.3 Conclusion

This chapter has proposed the design and the realization of a high gain CPW-fed slot antenna for CubeSat communications. It also obtained the optimal parameters of the proposed antenna and the optimal element sets of MSS. Moreover, a MSS is designed and used to significantly increase the gain from 2.52 to 5.67 dB. This gain further improved to 9.71 dB when the CPW-fed slot antenna is placed on the Aluminium CubeSat's surface. Simulation and measured results show that the proposed antenna has a return loss that is well below -10 dB at the operational frequency of 2.45 GHz, and achieves an impedance bandwidth of 730 MHz. However, the proposed antenna is only suitable for 3U CubeSats due to its relatively large size and hence it is not suitable for 1U and 2U CubeSats as it occupies a large percentage of a CubeSat's surface area; i.e., 81% for 1U and 40.5% for 2U CubeSats. To this end, the next chapter present a low profile high gain CPW-fed slot antenna using cavity backed technique.

Chapter 6

A LOW PROFILE HIGH GAIN, CAVITY-BACKED CPW-FED SLOT ANTENNA

The main limitation of the proposed high gain CPW-fed slot antenna design in Chapter 5 is its large size, which exceeds 90x90 mm^2. Consequently, it is not suitable for 1U and 2U CubeSats. This chapter proposes a low profile, high gain, cavity-backed CPW-fed slot antenna that operates at 2.45 GHz. The main idea is to use a part of the CubeSat's body as a low profile cavity reflector to redirect the back lobe pattern forward. This proposed antenna design is more robust and occupies less surface area on CubeSats; i.e., 12.96% for 1U and 6.48% for 2U as compared to using a MSS. The proposed CPW-fed cavity backed slot antenna has a small size of 36mm×36mm and a total gain of 8.6 dB; in contrast, amongst all previous S-band planar antennas that are suitable for CubeSats, the best gain is only 5.96 dB and the smallest size is 38×38×3.2 mm^3 at 2.45GHz [37]. In addition, this chapter also proposes a unique configuration of the proposed low profile CPW-fed slot antenna. This is important as it provides communication in all three directions and hence, achieves a cross link communication between CubeSats in a swarm.

6.1 Geometry of the Proposed Antenna

Figure 6.1 (a) shows that the proposed antenna has two parts. One part is the square slot and a 50-Ω CPW-feed line etched on the square Rogers RO3010 substrate with a dielectric constant of 10.2 and thickness of 1.280 mm. Roger substrates are easy to fabricate and have a tight dielectric constant and thickness control. The other part is the metallic cavity reflector with a depth (h_2) of 6.44mm ($\lambda_0/19$). This cavity reflector forms part of the CubeSat's body that helps to redirect the back lobe radiation pattern. The total size of the cavity reflector is 50×50 mm^2. The overall dimension of the antenna is 36×36×6.44 mm^3. The lightening-shaped feed-line is used to enhance the AR bandwidth and to achieve circular polarization. It consists of a horizontal feed section that extends the CPW's strip in the *y* direction and the slanted feed

section (S) with an inclined angle of 45^0 with respect to the x-axis. The strip line of the CPW has a width W_f, gap of P and is extended in the positive *y* axis direction by a horizontal feed section with a length of L_t. This horizontal feed section is used to attain a resonant frequency of 2.45 GHz and to enhance impedance matching. The gap between the strip line and the ground plane is T. In addition, the tuning stub with a width w_n and a length L_n is embedded in the CPW feeding line to widen the impedance bandwidth. Moreover, the matching between the CPW-fed line and the slot antenna is achieved by adjusting the slot width W and substrate thickness h_1. Figure 6.1 (b) shows the proposed antenna on a 2U CubeSat as modelled in HFSS.

The characteristics of the proposed CP antenna have been simulated Using HFSS. In order to design the high performance broadband CP square slot antenna, a detailed parametric study of the antenna is made. The effects of adjusting the length Ln of the tuning stub on return loss are first studied. Fig. 2 exhibits the return loss of the antenna with different Ln. The lengths Ln with four different widths, 7.2, 8.2, 9.2 and 10.2mm, are analyzed while other parameters are fixed. It can be seen from Fig. 2 that the length of the tuning stub Ln has a great effect

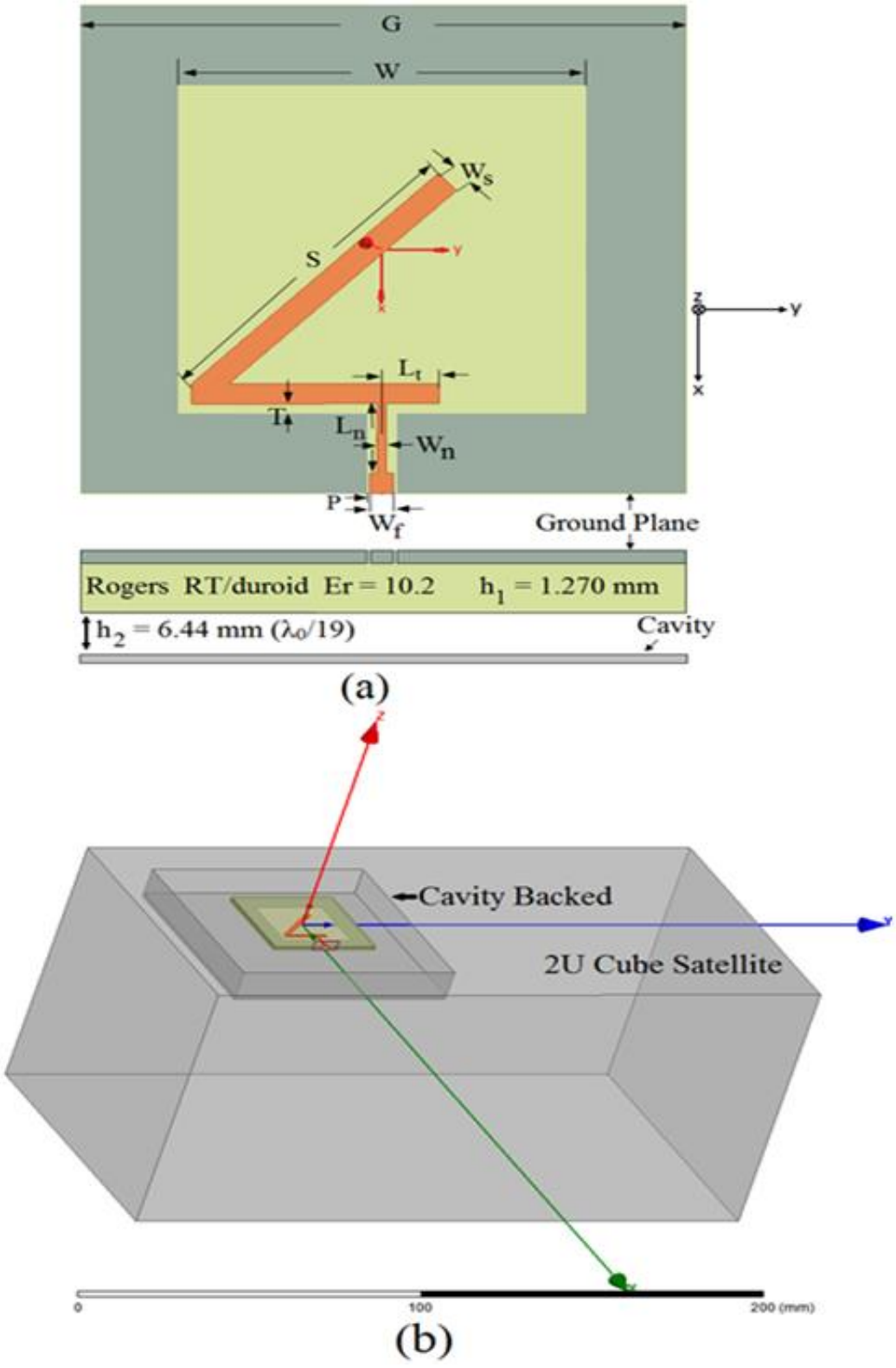

Figure 6.1. Configuration of the CPW-fed slot antenna with a cavity backed reflector. The (a) proposed cavity backed CPW-fed slot antenna, and (b) a 2U CubeSat with the proposed antenna as modelled in HFSS.

6.2 Analysis of the CPW-fed Slot Antenna

This section studies the antenna's resonant frequency, return loss, impedance bandwidth and the total gain in the boresight direction. The optimal parameter values, as found using HFSS, are as follows: G = 36 mm, W= 24 mm, S = 21.29 mm, W_s = 1.68 mm, L_t = 3.27 mm, L_n = 5.12 mm, W_n = 0.51 mm, W_f = 1.36 mm, P= 0.18 mm, T = 0.65 mm, and h_2 = 6.44 mm. It is important to note that when deriving the foregone values, except for the value of interest, other parameter values are fixed.

Figure 6.2 (a) and (b) show the 3D and 2D simulated radiation patterns of the proposed CPW-fed slot antenna with and without the cavity reflector at 2.45 GHz. Without the cavity reflector, the proposed antenna radiates bi-directionally and has a total gain of 3.68 dB; see Figure 6.2 (a). The bidirectional pattern is undesirable as it results in a low total gain and causes interference with the electronics inside the CubeSat. Using a low profile metallic cavity reflector with a depth of h_2= 6.44 mm, see Figure 6.2 (b), it shows that the back lobe radiation pattern is redirected forward. Consequently, there is a dramatic increase in total gain. Specifically, the total gain without cavity is 3.68 dB and with cavity it is 8.62 dB.

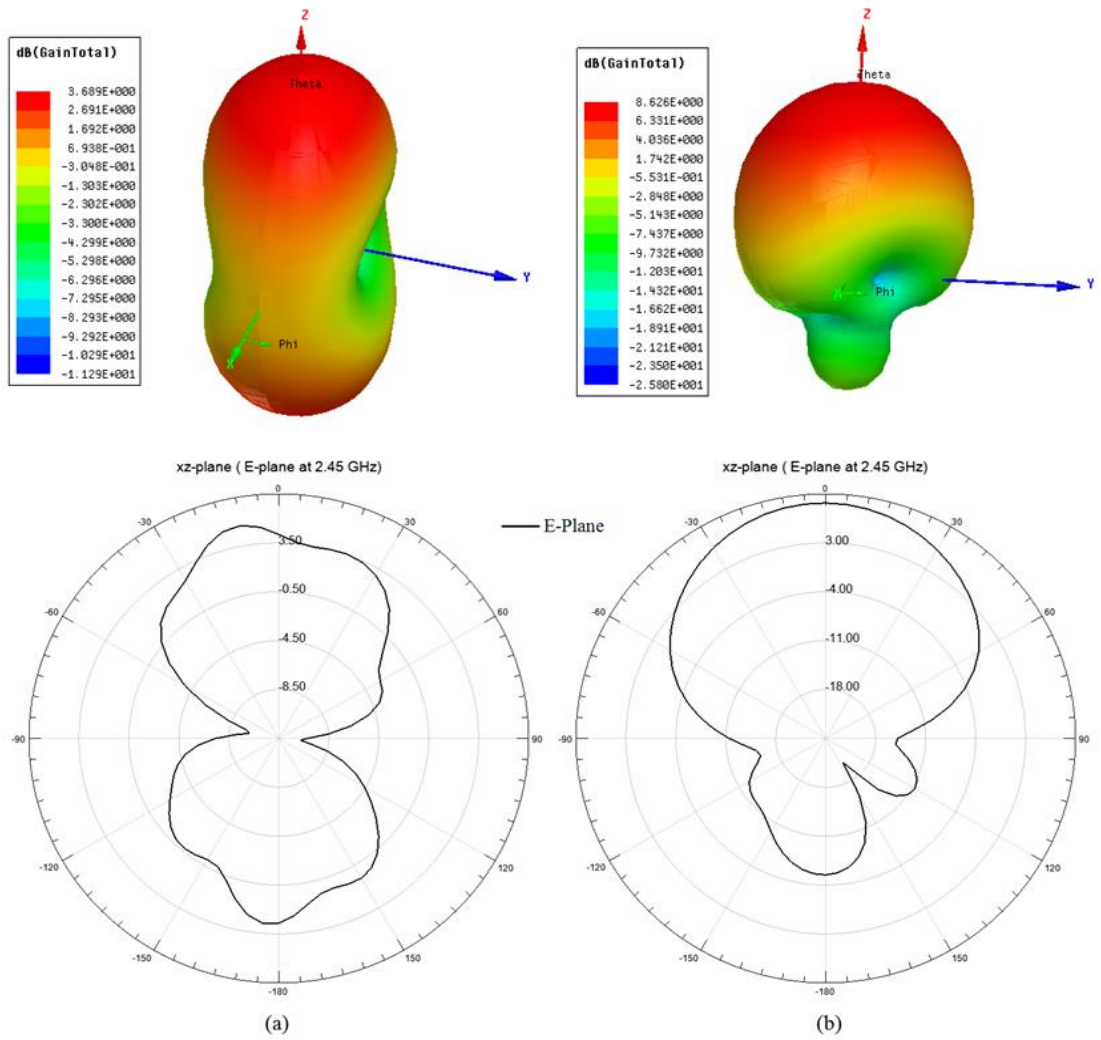

Figure 6.2. Comparison of radiation pattern at 2.45 GHz: (a) without cavity, and (b) with cavity.

- *Cavity Depth*

  The cavity-backed antenna is modelled and designed using HFSS. The proximity of the metallic cavity structure causes parallel-plate capacitance between itself and the ground plane of the antenna. The increased capacitance will decrease the characteristic impedance of the slot dimensions. To decrease the cavity effects on the impedance, the Quasi Newton method which is available in HFSS is used. Figure 6.3 shows the effect of cavity depth on the return loss (S_{11}). With the substrate thickness set to h_1=1.270, the following h_2 values: 4.08 mm (λ_0/30), 5.10 mm ((λ_0/24), 5.56 mm ((λ_0/22), and 6.44 (λ_0/19) are studied. When the depth

is set to 5.56 mm ($\lambda_0/22$), the obtained return loss is -16 dB with a bandwidth of 80 MHz at the resonant frequency of 2.43 GHz. As h_2 becomes less than 6.44 mm, e.g., 4.08 mm, the return loss increases and thus the antenna has poor impedance matching. This is due to the energy and radiation leakage between the reflector and the substrate [123]. In the case of h_2= 4.08 mm ($\lambda_0/30$), the obtained return loss is very high, i.e., -8.5 dB at a resonant frequency of 2.38 GHz. The most suitable depth is h_2= 6.44 mm ($\lambda_0/19$) as it provides the smallest return loss of -30 dB at a resonant frequency of 2.45 GHz. The obtained -10 dB impedance bandwidth is 109 MHz (2.391-2.50 GHz). Moreover, from the radiation pattern measurements for various h_2 depth values, the optimal distance between the cavity and the slot antenna that provides the maximum gain with minimum side lobes and small return loss at 2.45 GHz is 6.44mm ($\lambda_0/19$); see Figure 6.4.

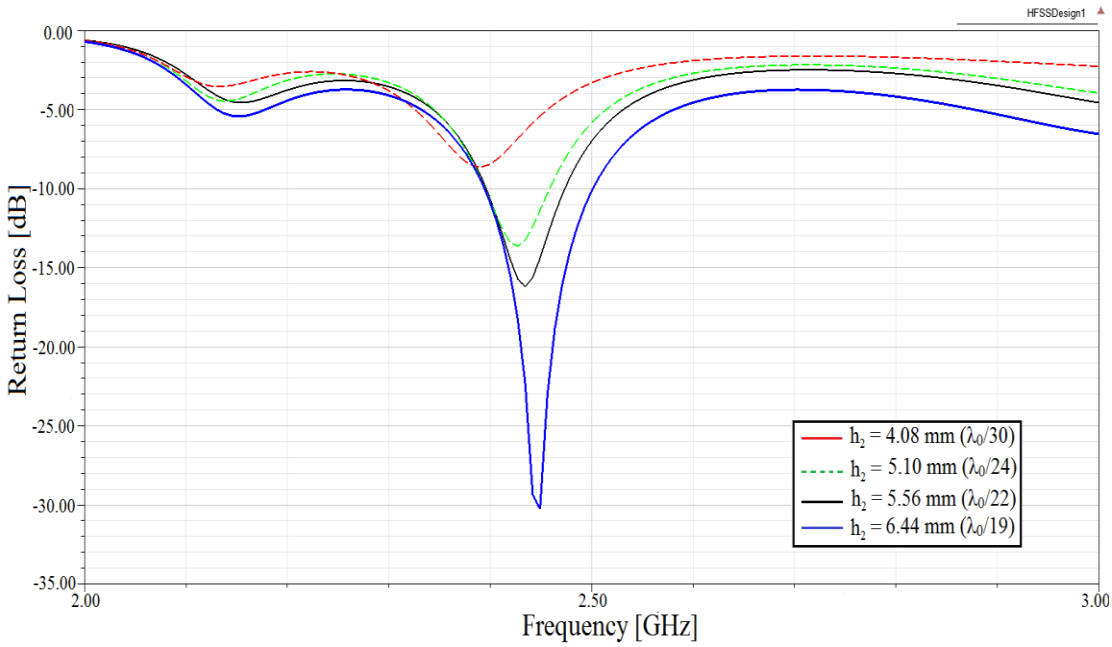

Figure 6.3. Return loss for various depth values.

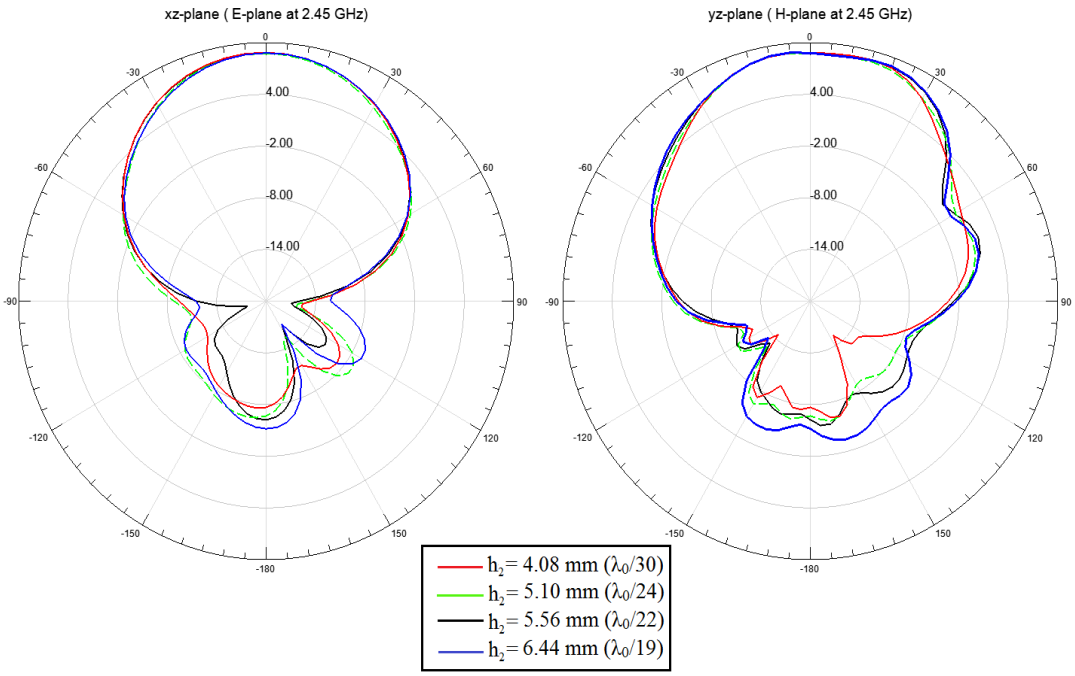

Figure 6.4. Radiation patterns for depths different h_2 values.

- *Substrate Thickness*

  The next concern is the thicknesses of the Rogers RO3010 substrate and its impact on impedance matching and resonant frequency. The available thicknesses are as follows: 0.254, 0.635, 1.270, 1.905 and 2.54 mm. As shown in Figure 6.5, for thicker substrates, resonant frequency decreases and return loss increases. The best h_1 value is 1.27 mm, which gives very good impedance matching with a smallest return loss of -30 dB at 2.45 GHz and an impedance bandwidth of 109 MHz (2.391-2.50 GHz). Moreover, in the case of h_1= 2.540 mm, the obtained return loss is very high, i.e., -7.12 dB at 2.18 GHz.

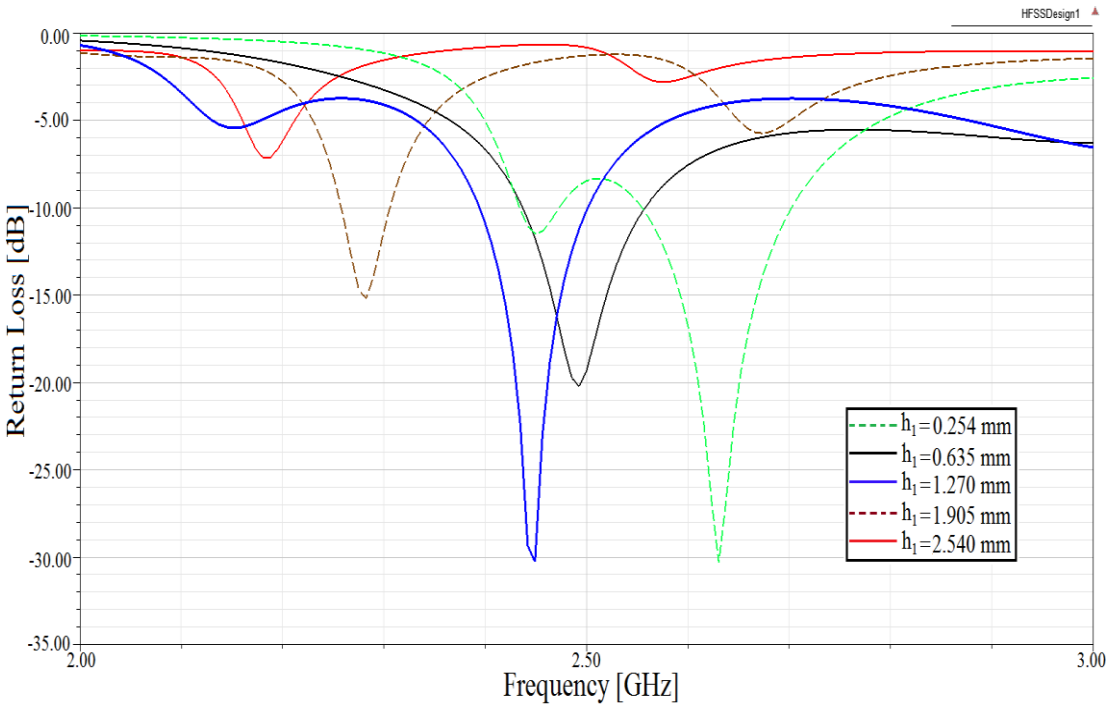

Figure 6.5. Return loss for various substrate thickness h_1.

Figure 6.6 depicts the input impedance (real and imaginary parts) of the CPW-fed slot antenna with a cavity backed reflector. At 2.13 GHz, the real and imaginary parts of the input impedance increase dramatically. The imaginary part of the input impedance has small variation around zero from 2.39 to 2.47 GHz. The real part starts to decrease at 2.5 GHz and drops to very a small value of 11.5 Ω and hence achieves very high reflection at frequencies ranging from 2.70 to 2.80 GHz. The input impedance (real and imaginary parts) is 50+j1.9 Ω at the resonant frequency of 2.45 GHz; see Figure 6.6. This means good impedance matching. The inductance of the CPW-fed line is compensated by the capacitance between the antenna and the cavity reflector. Hence, good impedance matching is achieved. Moreover, the simulated axial ratio of the proposed antenna is shown in Figure 6.7. It has a CP 3-dB AR bandwidth of 160 MHz from 2.38 to 2.52 GHz. Very small axial ratio of 0.18 dB is obtained at a resonant frequency of 2.45 GHz.

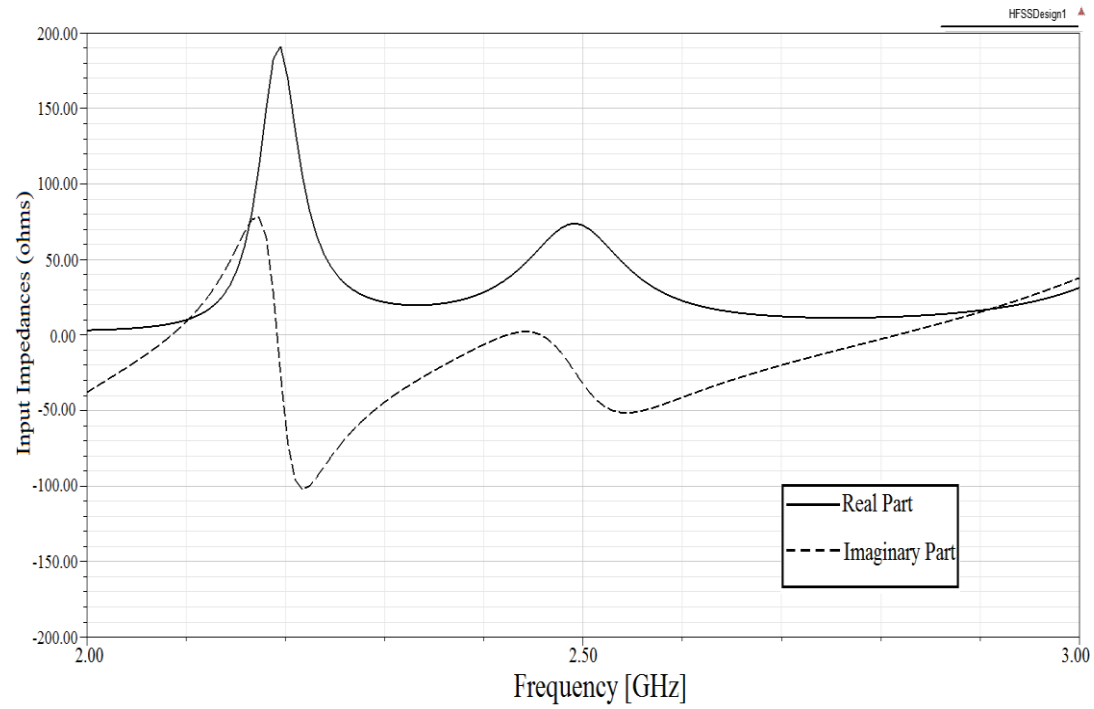

Figure 6.6 Input impedance.

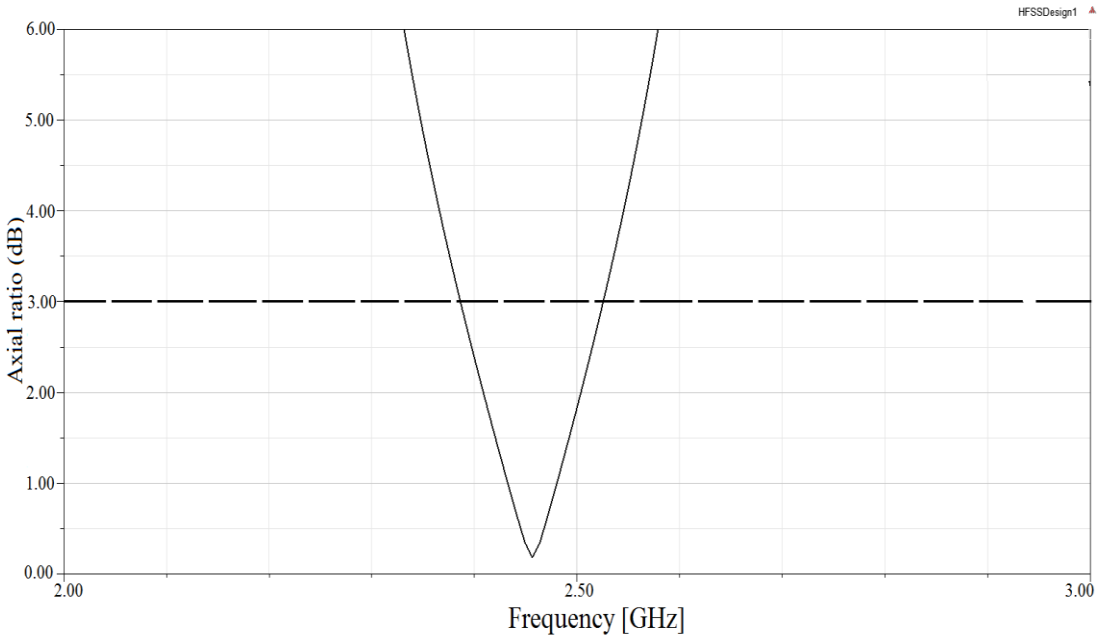

Figure 6.7. Axial ratio.

6.3 CPW-fed Slot Antenna array

This section now presents a unique configuration of three small CPW-fed slot antennas. Each individual CPW-fed slot antenna is placed at the top corner of each face of a 2U CubeSat. The placed antennas thus provide communication in all three directions; see Figure 6.8. Moreover, they only occupy 6.48% of the total surface area on each CubeSat's face. Hence, the remaining real estate, i.e., 93.52%, is sufficient to mount solar cells.

By changing the phase of the input feeding signals of each antenna, different radiation patterns can be achieved and the direction of these radiation patterns can be controlled. The antenna thus facilitates cross-link communications amongst CubeSats operating in a swarm.

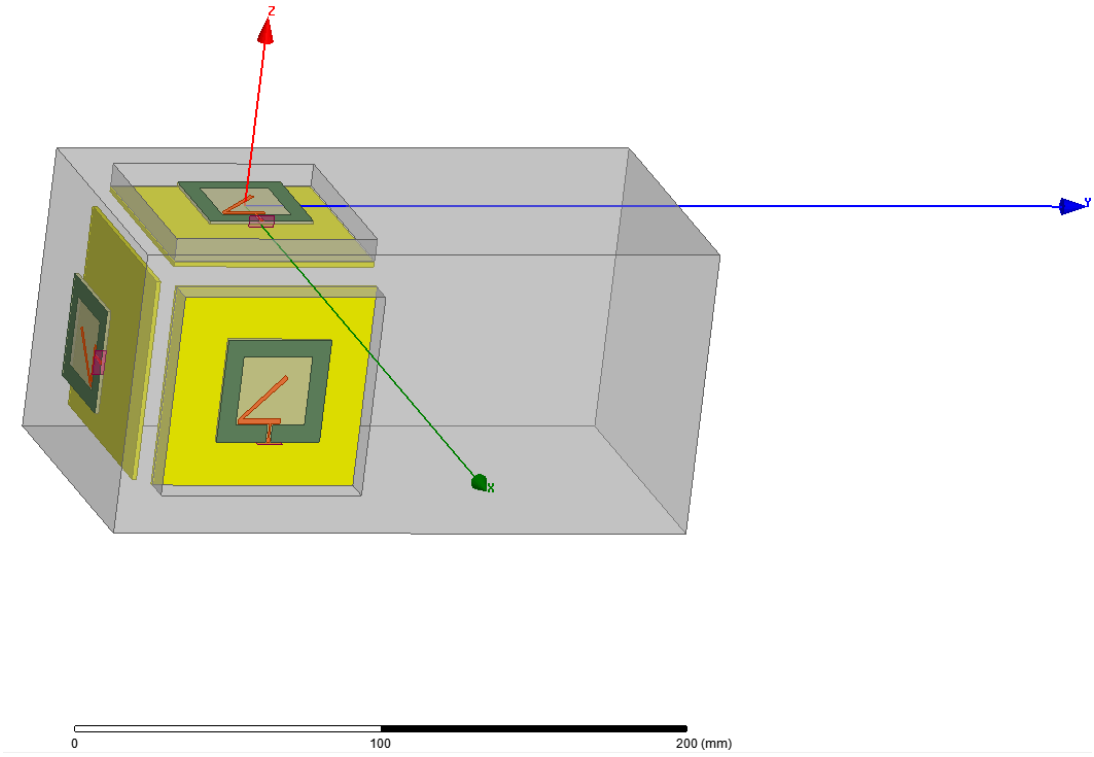

Figure 6.8. Proposed ACM antenna configuration.

6.4 Conclusion

This chapter has described a low profile, high gain CubeSat antenna. Advantageously, it uses part of the CubeSat body as a cavity reflector to dramatically increase the total gain from 3.68 dB (without cavity reflector) to 8.62 dB (with cavity reflector). The space between the antenna and the cavity reflector is small, e.g., 6.44 mm and hence, giving the antenna a reasonably low profile. The total antenna size including the cavity reflector has dimension 36×36×6.44 mm^3. Moreover, simulation results show that the proposed antenna has a return loss of -30 dB at a resonant frequency of 2.45 GHz, -10 dB impedance bandwidth of 109 MHz (2.391-2.50 GHz) and a CP bandwidth of 160 MHz.

Chapter 7

CONCLUSIONS

CubeSats require antennas that are small, have high gains and wide bandwidth. These features help maximize space for solar panels and ensure the communication links with ground stations and other CubeSats have high data rates. In addition, CubeSats require antennas that operate in the unlicensed ISM band. Henceforth, this thesis presents the first comprehensive study and survey of existing micro-strip and patch antennas for CubeSats. Critically, among micro-strip patch and slot antennas that are suitable for use on CubeSats, they have low gains and narrow bandwidth. Moreover, this thesis has conducted a comprehensive quantitative evaluation of the most suitable micro-strip and patch antennas on a common platform; i.e., HFSS. These antennas include shorted patch [46], CPW-feed square slot [45] and asymmetric E-shaped [56] antennas. The evaluation metrics include their volume, gain, bandwidth, return loss, robustness, beam steerability and cost. The key findings are that the most suitable shorted patch [46], CPW-fed square slot [45] and asymmetric E-shaped antennas operate at a resonant frequency higher than the desired CubeSat ISM operating frequency of 2.4-2.5 GHz band. This means to lower their operating frequency to 2.45 GHz, their overall size needs to be increased, meaning they will occupy a larger area; a key concern as CubeSats have limited real estate. Other findings are that the tested shorted patch and CPW-fed square slot antennas have low gains. Consequently, they can only be used for short distance communications; this means in a swarm, more CubeSats will be required. Lastly, a CubeSat's body has a significant impact on the gain, return loss and bandwidth; a key factor neglected by prior works.

Based on the said findings, Chapter 4 first reports two new antennas that operate at 2.45 GHz (S-band). In particular, the said antennas are based on the shorted patch antenna in [46] and the CPW-feed square slot antenna in [45]. A key change is that

the F-shapes of the new S-band CPW-feed square slot antenna are replaced with a square slot to improve its gain. HFSS simulation results show that the gain of the modified CPW-feed square slot antenna is improved by 0.6 dB. Moreover, the new S-band shorted patch and CPW-fed square slot antennas have small -10 dB return losses of -27.5 and 20.5 dB at 2.45 GHz, respectively. However, the main limitation of the modified shorted patch antenna is its narrow bandwidth and low gain. To address the aforementioned problems, this chapter also presented a novel high gain wideband F-shaped patch antenna design that operates at 2.45 GHz. It achieves a high gain; i.e., 8.51 dB and a wide bandwidth of 1121 MHz. On the other hand, the repurposed CPW-fed square slot antenna has very low gains due to its bidirectional radiation pattern.

Chapter 5 outlines the design and the realization of a high gain CPW-fed slot antenna that is suitable for use on a 3U CubeSat. The main idea is to use MSS to redirect the back radiation pattern lobe forward, resulting in gain enhancement. The simulation and measured results show that the proposed CPW-fed slot antenna achieved a superior gain of 9.71 dB and a wide bandwidth of 730 MHz. However, the proposed antenna is only suitable for 3U CubeSats because of its relatively large size.

Lastly, Chapter 6 presents a small size, high-gain, cavity-backed, CPW-fed slot antenna for use on 2U CubeSats. It operates in the unlicensed ISM band (2.45 GHz). A key feature is to use a part of a CubeSat's body to redirect the back radiation forward. The proposed antenna has a small size; i.e., 36×36 mm^2 and it occupies only 12.96% of a 1U CubeSat's surface and 6.48% of a 2U CubeSat's surface. The simulation results show that the proposed antenna achieves a superior gain of 8.62 dB and a -10 dB impedance bandwidth of 109 MHz. This chapter also proposes a unique configuration to facilitate cross-link communications between CubeSats in a swarm.

All proposed antenna designs are cheap, easy to fabricate and do not require a deployment mechanism. Moreover, the proposed CPW-fed square slot and F-shaped patch antennas have high gains and wide bandwidth. However, their radiation patterns are not steerable. This is important to CubeSats as they are not able to re-

orient themselves after deployment. Thus, a key future research direction is to design antenna arrays to facilitate steerable radiation patterns. Of particular interest is its feeding network. An example is the corporate feed network, which is used for passive antenna arrays. However, it occupies a large area. Another example is to combine phase shifters with a feed network; a common approach used by active antenna arrays. This approach, however, adds cost and complexity. To this end, a promising future research direction is to design a simple and feeding network for the proposed antenna array in Chapter 6.

BIBLIOGRAPHY

[1] D. K. Van Keuren, "Moon in their eyes: Moon communication Relay at the Naval Research Laboratory, 1951-1961," *Beyond the Ionosphere: Fifty years of satellite communication*, pp. 9-18.

[2] T. Pratt and C. W. Bostian, *Satellite communications*: John Wiley & Sons, 1986.

[3] I. V. Gorbach, R. I. Gorbach, and M. G. Duma, "Earth Segment of National Satellite Communication System Providing Operation of Ukrainian Telecommunication Network for Digital TV and Radiobroadcasting," *17th International Crimean Conference on Microwave & Telecommunication Technology*, 2007, pp. 305-306.

[4] C. Underwood, V. Lappas, A. D. S. Curiel, M. Unwin, A. Baker, and M. Sweeting, "Science mission mcenarios using “palmsat” pico-patellite technology," *in Proc. 18th Annual AIAA/USU Conference on Small Satellites*, Logan, UT, USA, 2004, pp. 1-11.

[5] R. Sandau, "Status and trends of small satellite missions for Earth observation," *Acta Astronautica*, vol. 66, pp. 1-12, 2010.

[6] R. M. Rodriguez-Osorio and E. F. Ramirez, "A hands-on education project: Antenna design for Inter-CubeSat communications [education column]," *IEEE Antennas and Propagation Magazine*, vol. 54, pp. 211-224, Oct. 2012.

[7] *National Aeronautics and Space Administration (NASA) [online] available: http://www.nasa.gov/index.html*.

[8] L. J. DeLucas, "International Space Station," *Acta Astronautica*, vol. 38, pp. 613-619, April 1996.

[9] A. Scholz, W. Ley, B. Dachwald, J. J. Miau, and J. C. Juang, "Flight results of the COMPASS-1 picosatellite mission," *Acta Astronautica*, vol. 67, pp. 1289-1298, 2010.

[10] R. Nugent, R. Munakata, A. Chin, R. Coelho, and J. Puig-Suari, "The cubesat: The picosatellite standard for research and education," *Aerospace Engineering*, vol. 805, pp. 756-5087, 2008.

[11] C. Pinciroli, M. Birattari, E. Tuci, M. Dorigo, M. D. R. Zapatero, T. Vinko, *et al.*, "Self-organizing and scalable shape formation for a swarm of pico satellites," *NASA/ESA Conference on Adaptive Hardware and Systems*, Noordwijk, Netherlands, Jun. 2008, pp. 57-61.

[12] C. A. Rouff, M. G. Hinchey, J. Pena, and A. Ruiz-Cortes, "Using formal methods and agent-oriented software engineering for modeling NASA swarm-based systems," *IEEE Conference Swarm Intelligence Symposium*, Honolulu, HI, United State, Apr. 2007, pp. 348-355.

[13] R. Fdhila, T. M. Hamdani, and A. M. Alimi, "A multi objective particles swarm optimization algorithm for solving the routing pico-satellites problem," *IEEE International Conference on Systems, Man, and Cybernetics* Seoul, Korea, October 2012., pp. 1402-1407.

[14] H. Heidt, J.P. Suari, A.S. Moore, S. Nakasuka, and a. R. J. Twiggs, "CubeSat: A new Generation of Picosatellite for Education and Industry Low-Cost Space Experimentation," *14th Annual/USU Conference on Small Satellites*, Logan, Utah, 2000.

[15] J. P. Suari, C. Turner, and and R.J. Twiggs, "The Development and launch Support Infrastructure for Eighteen Different Satellite Customers On One Launch," *15th Annual/USU Conference on Small Satellites*, Logan, Utah, 2001.

[16] (Surrey Satellite technology Ltd. Home page:). *http://www.sstl.co.uk*.

[17] B. Yost, "EDSN-Edison Demonstration for SmallSat Networks Overview," 2013.

[18] L. Reyneri, C. Sansoè, D. Del Corso, C. Passerone, S. Speretta, and M. Tranchero, "PicPot: a small satellite with educational goals,," *18th EAEEIE Conference on innovation in education for electrical and information engineering*, Praha, Italy, July 2007.

[19] R. Sandau and K. Brieb, "Potential for Advancement in Remote Sensing Using Small Satellite," *The international Archives of the photogrammetry, Remote Sensing and Spatial Information Science*, Beijing, 2008.

[20] (Surrey Space Centre. Home page:). *http://www.ee.surrey.ac.uk/SSC/*.

[21] *An international network of 50 CubeSats Project [online]. available: https://www.qb50.eu/, accessed Oct. 24, 2015*.

[22] H. Bedon, C. Negron, J. Llantoy, C. M. Nieto, and C. O. Asma, "Preliminary internetworking simulation of the QB50 cubesat constellation," *IEEE Latin-American Conference on Communications (LATINCOM)*, Bogota, Colombia, September 2010, pp. 1-6.

[23] H. Jyun-Hau, L. Ting-Yang, L. Chieh-Min, and J. Jyh-Ching, "Design and evaluation of the attitude control system of the PHOENIX CubeSat," *CACS International Conference on Automatic Control*, Sun Moon Lake, Taiwan, December 2013, pp. 47-51.

[24] G. Mantzouris, "Micro and Pico Satellites in Maritime Security Operations," *Journal of Naval Science and Engineering*, vol. 8, pp. 1-30, 2012.

[25] K. Woellert, P. Ehrenfreund, A. J. Ricco, and H. Hertzfeld, "Cubesats: Cost-effective science and technology platforms for emerging and developing nations," *Advances in Space Research*, vol. 47, pp. 663-684, 2011.

[26] J. A. King, J. Ness, G. Bonin, M. Brett, and D. Faber, "Nanosat Ka-Band Communications - A Paradigm Shift in Small Satellite Data Throughput," *26th Annual AIAA/Utah State University Conference on Small Satellites*, Logan, UT, August 2012.

[27] S. Gao, G. Amendola, G. Massa, C. Underwood, M. Brenchley, M. Pointer, *et al.*, "Antennas for Modern Small Satellites," *IEEE Antennas and Propagation Magazine*, vol. 51, pp. 40-56, 2009.

[28] X. Chen, C. G. Parini, B. Collins, Y. Yao, and M. U. Rehman, *Antennas for Global NavigationSatellite Systems*: John Wiley & Sons, 2012.

[29] P. Muri, O. Challa, and Janise. McNair, "Enhancing small satellite communication through effective antenna system design," *Conference on Military Communications,* San Jose, CA, 2010, pp. 347-352.

[30] B. Murakami, A. Ohta, M. Tamamoto, G. Shiroma, R. Miyamoto, and W. Shiroma, "Self-steering antenna arrays for distributed picosatellite networks," *17th Annual AIAA/Utah State University Conference on Small Satellites*, Logan, UT, United State, August 2003.

[31] W. Alomar, J. Degnan, S. Mancewicz, M. Sidley, J. Cutler, and B. Gilchrist, "An extendable solar array integrated Yagi-Uda UHF antenna for CubeSat platforms," *IEEE International Symposium on Antennas and Propagation (APSURSI)*, 2011, pp. 3022-3024.

[32] J. Costantine, Y. Tawk, C. G. Christodoulou, J. Banik, and S. Lane, "CubeSat Deployable Antenna Using Bistable Composite Tape-Springs," *IEEE Antennas and Wireless Propagation Letters,* vol. 11, pp. 285-288, 2012.

[33] J. Costantine, Y. Tawk, I. Maqueda, M. Sakovsky, G. Olson, S. Pellegrino, *et al.*, "UHF Deployable Helical Antennas for CubeSats," *IEEE Transactions on Antennas and Propagation,* vol. 64, pp. 3752-3759, 2016.

[34] M. A. Saporetti, A. Giacomini, L. J. Foged, G. Galagani, G. Scozza, C. Occhiuzzi, *et al.*, "Modular, customisable, accomodation-friendly antenna system for satellite avionics: Development, prototyping and validation," *IEEE Conference on Metrology for Aerospace (MetroAeroSpace)*, 2014, pp. 555-559.

[35] A. Thurn, S. Huynh, S. Koss, P. Oppenheimer, S. Butcher, J. Schlater, *et al.*, "A Nichrome burn wire release mechanism for CubeSats," *41st Aerospace Mechanisms Symposium*, Pasadena, California, USA, 2012.

[36] F. M. Andreas, "Antennas," in *Wireless Communications*, ed: Wiley-IEEE Press, 2011, pp. 165-178.

[37] F. EM. Tubbal, R. Raad, and K-W. Chin, "A survey and study of planar antennas for pico-satellites," *IEEE Access*, vol. 3, pp. 2590-2612, Dec. 2015.

[38] I. Singh and D. VS. Tripathi, "Micro strip Patch Antenna and its Applications: a Survey," *International Journal of Computer Technology and . Applications*, vol. 2, pp. 1595-1599, 2011.

[39] S. Shrestha, M. Agarwal, P. Ghane, and K. Varahramyan, "Flexible microstrip antenna for skin contact application," *International Journal of Antennas and Propagation,* vol. 2012, 2012.

[40] A. Nascetti, E. Pittella, P. Teofilatto, and S. Pisa, "High-Gain S-band Patch Antenna System for Earth-Observation CubeSat Satellites," *IEEE Antennas and Wireless Propagation Letters,* vol. 14, pp. 434-437, February 2015.

[41] C. Y. Chiu, K. M. Shum, C. H. Chan, and K. M. Luk, "Bandwidth enhancement technique for quarter-wave patch antennas," *IEEE Antennas and Wireless Propagation Letters,* vol. 2, pp. 130-132, 2003.

[42] F. Ferrero, C. Luxey, R. Staraj, G. Jacquemod, M. Yedlin, and V. Fusco, "A Novel Quad-Polarization Agile Patch Antenna," *IEEE Transactions on Antennas and Propagation,* vol. 57, pp. 1563-1567, May 2009.

[43] F. Rahmadani and A. Munir, "Microstrip Patch Antenna Miniaturization Using Artificial Magnetic Conductor," *IEEE 6th International Conference on Telecommunication Systems, Services, and Applications,* Kuta, Bali, Indonesia, October 2011, pp. 219-223.

[44] A. Holub and M. Palivka, "A Novel Microstrip Patch Antenna Miniaturization Technique: A meanderly Folded Shorted- Patch Antenna," *24th IEEE Conference on Microwave Techniques*, Prague, April 2008.

[45] W. Liao and Q. X. Chu, "CPW-feed Square Slot Antenna With Lightening-Shaped Feed line For Broadband Circularly Polarized Radiation," *Progress In Electromagnetics Research,* vol. 18, pp. 61-69, 2010.

[46] H. Malekpoor and S. Jam, "Enhanced Bandwidth of Shorted Patch Antennas Using Folded-Patch Techniques," *IEEE Antennas and Wireless Propagation Letters,* vol. 12, pp. 198-201, 2013.

[47] N. Behdad and K. Sarabandi, "Bandwidth enhancement and future size reduction of a class of miniaturized slot antennas," *IEEE Transactions on Antenna and Propagation,* vol. 52, no. 8, pp. 1928-1935, August 2004.

[48] R. Addaci, A. Diallo, P. L. thuc, and R. Staraj, "Efficient miniaturization technique for wire patch antennas," *Microwave and Optical Technology Letters,* vol. 54, no. 5, pp. 1325-1327, May 2012.

[49] R. Azadegan and K. Sarabandi, "Design of Miniaturized Slot Antennas," *Antennas and Propagation Society International Symposium,* vol. 4, pp. 565-568, July 2001.

[50] R. Azadegan and K. Sarabandi, "Miniaturized Folded-Slot: An Approach to Increase the Bandwidth and Efficiency of Miniaturized Slot Antennas," *Antennas and Propagation Society International Symposium,* vol. 4, pp. 14-17, 2002.

[51] R. O. Ouedraogo, E. J. Rothwell, A. R. Diaz, K. Fuchi, and A. Temme, "Miniaturization of patch antennas using a metamaterial- inspired technique," *IEEE Transactions on Antennas and Propagation,* vol. 60, no. 5, pp. 2175-2182, May 2012.

[52] S. A. Razavi and M. H. Neshati, "Development of a Low-Profile Circularly Polarized Cavity-Backed Antenna Using HMSIW Technique," *IEEE Transactions on Antennas and Propagation,* vol. 61, pp. 1041-1047, March 2013.

[53] J. S. Row, "The design of a squarer-ring slot antenna for circular polarization," *IEEE Transactions on Antennas and Propagation,* vol. 53, no. 6, pp. 1967-1972, June 2005.

[54] D. Sievenpiper, H. Hui-Pin, and R. M. Riley, "Low-profile cavity-backed crossed-slot antenna with a single-probe feed designed for 2.34-GHz satellite radio applications," *IEEE Transactions on Antennas and Propagation,* vol. 52, pp. 873-879, 2004.

[55] W. Hong, N. Behdad, and K. Sarabandi, "Size Reduction of Cavity-Backed Slot Antennas," *IEEE Transactions on Antennas and Propagation,* vol. 54, pp. 1461-1466, May 2006.

[56] H. Malekpoor and S. Jam, "Miniaturised asymmetric E-shaped microstrip patch antenna with folded-patch feed," *Microwaves, Antennas & Propagation, IET,* vol. 7, pp. 85-91, 2013.

[57] A. Budianu, T. J. W. Castro, A. Meijerink, and M. J. Bentum, "Inter-satellite links for cubesats," *IEEE Conference on Aerospace,* Big Sky, MT, USA, Mar. 2013, pp. 1-10.

[58] G. Di Massa and G. Mazzarella, "Shorted annular patch antenna," *Microwave and Optical Technology Letters,* vol. 8, pp. 222-226, 1995.

[59] H. Iwasaki, "A Circularly Polarized Small-Size Microstrip Antenna with a Cross Slot," *IEEE Transactions on Antennas and Propagation,* vol. 44, pp. 1399-1401, October 1996.

[60] K-L. Wong, C-C. Huang, and W-S. Chen, "Printed ring slot antenna for circular polarization," *IEEE Transactions on Antennas and Propagation,* vol. 50, pp. 75-77, January 2002.

[61] S-L. Ma, C.J. Shih, and J-S. Row, "Four-element microstrip array with polarization diversity," *Microwave and Optical Technology Letters,* vol. 55, pp. 1653-1657, July 2013.

[62] T. J. Mizuno, J. D. Roque, B. T. Murakami, L. K. Yoneshige, G. S. Shiroma, R. Y. Miyamoto, *et al.*, "Antennas for distributed nanosatellite networks," *IEEE/ACES. International Conference on Wireless Communications and Applied Computational Electromagnetics*, Hawaii, HI, USA, Apr. 2005, pp. 606-609.

[63] R. Azadegan and K. Sarabandi, "Bandwidth Enhancement of Miniaturized Slot Antennas Using Folded, Complementary, and Self-Complementary Realizations," *IEEE Transactions on Antenna and Propagation,* vol. 55, no. 9, pp. 2435-2444, September 2007.

[64] J. S. Row and S. Chuang-Jiashih, "Polarization-Diversity Ring Slot Antenna With Frequency Agility," *IEEE Transactions on Antennas and Propagation,,* vol. 60, pp. 3953-3957, 2012.

[65] Y. J. Hu, W. P. Ding, and W. Q. Cao, "Broadband Circularly Polarized Microstrip Antenna Array Using Sequentially Rotated Technique," *IEEE Antennas and Wireless Propagation Letters,* vol. 10, pp. 1358-1361, 2011.

[66] Y. Qian, D. Sievenpiper, V. Radisic, E. Yablonovitch, and T. Itoh, "A novel approach for gain and bandwidth enhancement of patch antennas," *IEEE Conference on Radio and Wireless* Colorado Springs, United State, August 1998, pp. 221-224.

[67] R. Montaño, N. Neveu, S. Palacio, E. Martinez, D. R. Jackson, J. Chen, *et al.*, "Development of low-profile antennas for cubesats," *Conference on Small Satellites*, Logan, UT, United State, August 2014.

[68] B. Ghosh, S.K. M. Haque, and N. R. Yenduri, "Miniaturization of Slot Antennas Using Wire Loading," *IEEE Antennas and Wireless Propagation Letters*, vol. 12, pp. 488-491, April 2013.

[69] T. Y. Lee and J. S. Row, "Frequency Reconfigurable Circularly Polarized Slot Antennas with Wide Tuning Range," *Microwave and Optical Technology Letters*, vol. 53, no. 7, pp. 1501-1505, July 2011.

[70] Z. H. Tu, Q. X. Chu, and Q. Y. Zhang, "High-gain Slot Antenna with Parasiticpatch and Windowed metallic Superstrate," *Progress In Electromagnetics Research Letters*, vol. 15, pp. 27-36, 2010.

[71] J. Lange, "Interdigitated Stripline Quadrature Hybrid (Correspondence)," *IEEE Transactions on Microwave Theory and Techniques*, vol. 17, pp. 1150-1151, December 1969.

[72] H. Oraizi and A. R. Sharifi, "Design and optimization of broadband asymmetrical multisection wilkinson power divider," *IEEE Transactions on Microwave Theory and Techniques*, vol. 54, pp. 2220-2231, May 2006.

[73] E. J. Wilkinson, "An N-Way Hybrid Power Divider," *IRE Transactions on Microwave Theory and Techniques*, vol. 8, pp. 116-118, January 1960.

[74] D. S. Goshi, K. M. K. H. Leong, and T. Itoh, "Recent advances in retrodirective system technology," *IEEE Conference on Radio and Wireless Symposium*, San Diego, CA, United Sate, October 2006, pp. 459-462.

[75] K. M. K. H. Leong, R. Y. Miyamoto, and T. Itoh, "Moving forward in retrodirective antenna arrays," *IEEE Potentials*, vol. 22, pp. 16-21, September 2003.

[76] R. Y. Miyamoto and T. Itoh, "Retrodirective arrays for wireless communications," *IEEE Microwave Magazine*, vol. 3, pp. 71-79, March 2002.

[77] R. Coccioli, Y. Fei-Ran, M. Kuang-Ping, and T. Itoh, "Aperture-coupled patch antenna on UC-PBG substrate," *IEEE Transactions on Microwave Theory and Techniques*, vol. 47, pp. 2123-2130, November 1999.

[78] R. Gonzalo, P. De Maagt, and M. Sorolla, "Enhanced patch-antenna performance by suppressing surface waves using photonic-bandgap substrates," *IEEE Transactions on Microwave Theory and Techniques*, vol. 47, no. 11, pp. 2131-2138, November 1999.

[79] M. Rahman and M. A. Stuchly, "Circularly polarised patch antenna with periodic structure," *IEE Proceedings - Microwaves, Antennas and Propagation*, vol. 149, pp. 141-146, 2002.

[80] M. J. Vaughan, K. Y. Hur, and R. C. Compton, "Improvement of microstrip patch antenna radiation patterns," *IEEE Transactions on Antennas and Propagation*, vol. 42, pp. 882-885, June 1994.

[81] H-Y. D. Yang and J. Wang, "Surface waves of printed antennas on planar artificial periodic dielectric structures," *IEEE Transactions on Antennas and Propagation,* vol. 49, pp. 444-450, March 2001.

[82] E. Yablonovitch, "Photonic band-gap structures," *Journal of the Optical Society of America B,* vol. 10, pp. 283-295, 1993.

[83] K-F. Tong and J. Huang, "New Proximity Coupled Feeding Method for Reconfigurable Circularly Polarized Microstrip Ring Antennas," *IEEE Transactions on Antennas and Propagation,* vol. 56, pp. 1860-1866, July 2008.

[84] S. Gao, A. Sambell, and S. S. Zhong, "Polarization-agile antennas," *IEEE Antennas and Propagation Magazine,* vol. 48, pp. 28-37, June 2006.

[85] W. Richards, L. Yuen, and D. Harrison, "An improved theory for microstrip antennas and applications," *IEEE Transactions on Antennas and Propagation,* vol. 29, pp. 38-46, 1981.

[86] P. Salonen, M. Keskilammi, and M. Kivikoski, "New slot configurations for dual-band planar inverted-F antenna," *Microwave and Optical Technology Letters,* vol. 28, pp. 293-298, March 2001.

[87] C. Y. Chiu, C. H. Chan, and K. M. Luk, "Study of a small wide-band patch antenna with double shorting walls," *IEEE Antennas and Wireless Propagation Letters,* vol. 1, pp. 230-231, December 2004.

[88] C. Y. Chiu, H. Wong, and C. H. Chan, "Study of small wideband folded-patch-feed antennas," *IET Microwaves, Antennas and Propagation,* vol. 1, pp. 501-505, April 2007.

[89] F. Jolani, A. M. Dadgarpour, and H. R. Hassani, "Compact M-slot Folded Patch Antenna for WLAN," *Progress In Electromagnetics Research Letters* vol. 3, pp. 35-42, 2008.

[90] A. Tiburcio-Silver, A. Sanchez-Juarez, and A. Avila-Garcia, "Properties of gallium-doped ZnO deposited onto glass by spray pyrolysis," *Solar Energy Materials and Solar Cells,* vol. 55, pp. 3-10, July 1998.

[91] K. Schilling, "Earth observation by distributed networks of small satellites," *IEEE International Conference on Instrumentation, Communications, Information Technology, and Biomedical Engineering (ICICI-BME)* Bandung, Indonesia, November 2009.

[92] A. Alù, F. Bilotti, N. Engheta, and L. Vegni, "Subwavelength, compact, resonant patch antennas loaded with metamaterials," *IEEE Transactions on Antennas and Propagation,* vol. 55, pp. 13-25, January 2007.

[93] F. Bilotti, A. Alu, and L. Vegni, "Design of miniaturized metamaterial patch antennas with-negative loading," *IEEE Transactions on Antennas and Propagation,* vol. 56, pp. 1640-1647, 2008.

[94] A. Erentok, "Antenna performance near a volumetric metamaterial realization of an artificial magnetic conductor," *IEEE Transactions on Antennas and Propagation,* vol. 53, pp. 160-172, 2005.

[95] H. Mosallaei, H. Mosallaei, K. Sarabandi, and K. Sarabandi, "Design and Modeling of Patch Antenna Printed on Magneto-Dielectric Embedded-Circuit Metasubstrate," *IEEE Transactions on Antennas and Propagation*, vol. 55, pp. 45-52, January 2007.

[96] G. A. Conway and W. G. Scanlon, "Antennas for Over-Body-Surface Communication at 2.45 GHz," *IEEE Transactions on Antennas and Propagation*, vol. 57, pp. 844-855, 2009.

[97] J. W. Philps, "Zigbee light link and its applicationss," *IEEE Wireless Communications*, vol. 20, August 2013.

[98] A. P. Feresidis, G. Goussetis, W. Shenhong, and J. C. Vardaxoglou, "Artificial magnetic conductor surfaces and their application to low-profile high-gain planar antennas," *IEEE Transactions on Antennas and Propagation*, vol. 53, pp. 209-215, 2005.

[99] L. K. Fong and R. Chair, "On the Use of Shorting Pins in the Design of Microstrip Patch Antennas," *Hong Kong Institution of Engineer Transactions* vol. 11, pp. 31-38, June 2004.

[100] L. C. Kempel, "Radiation by cavity-backed antennas on a circular cylinder," *IEE Proceedings - Microwaves, Antennas and Propagation*, vol. 142, pp. 233-239, January 1995.

[101] B. Liu, W. Hong, Y-Q. Wang, Q-H. Lai, and K. Wu, "Half Mode Substrate Integrated Waveguide (HMSIW) 3-dB Coupler," *IEEE Microwave and Wireless Components Letters*, vol. 17, pp. 22-24, January 2007.

[102] F. Ferrero, C. Luxey, R. Staraj, G. Jacquemod, M. Yedlin, and V. Fusco, "Theory and design of a tunable Quasi-Lumped Quadrature Coupler," *Microwave and Optical Technology Letters*, vol. 51, pp. 2219-2222, September 2009.

[103] A. U. Bhobe, C. L. Holloway, M. Piket-May, and R. Hall, "Wide-band slot antennas with CPW feed lines: hybrid and log-periodic designs," *IEEE Transactions on Antennas and Propagation*, vol. 52, pp. 2545-2554, October 2004.

[104] J-S. Chen, "Dual-frequency annular-ring slot antennas fed by CPW feed and microstrip line feed," *IEEE Transactions on Antennas and Propagation*, vol. 53, pp. 569-573, January 2005.

[105] X-C. Lin and C-Ch. Yu, "A Dual-Band CPW-Fed Inductive Slot-Monopole Hybrid Antenna," *IEEE Transactions on Antennas and Propagation*, vol. 56, pp. 282-285, January 2008.

[106] Z. C. Ioannidis, Z. C. Ioannidis, O. Dumbrajs, and I. G. Tigelis, "Eigenvalues and Ohmic Losses in Coaxial Gyrotron Cavity," *IEEE Transactions on Plasma Science*, vol. 34, pp. 1516-1522, 2006.

[107] *High Frequency Structure Simulator (HFSS) [online] available: http://www.ansys.com/*.

[108] K. Arunachalam, P. Maccarini, T. Juang, C. Gaeta, and P. R. Stauffer, "Performance evaluation of a conformal thermal monitoring sheet sensor array for measurement of surface temperature distributions during superficial hyperthermia treatments," *International Journal of Hyperthermia,* vol. 24, pp. 313-325, 2008.

[109] S. Oren, "Quasi-Newton algorithms: Approaches and motivations," *IEEE Conference on Decision and Control Including the 12th Symposuim on Adaptive Processes, vol. 12,* , 1973, pp. 422-427.

[110] R. W. Ziolkowski, "Design, fabrication, and testing of double negative metamaterials," *IEEE Transactions on Antennas and Propagation,* vol. 51, pp. 1516-1529, July 2003.

[111] C. Rakluea, S. Chaimool, P. Rakluea, and P. Akkaraekthalin, "Unidirectional CPW-fed slot antenna using metasurface," *8th International Conference on Electrical Engineering/Electronics, Computer, Telecommunications and Information Technology (ECTI-CON),* Khon Kaen, Thailand, May 2011, pp. 184-187.

[112] S. Chaimool, K. L. Chung, and P. Akkaraekthalin, "Bandwidth and gain enhancement of microstrip patch antennas using reflective metasurface," *IEICE transactions on communications,* vol. 93, pp. 2496-2503, October 2010.

[113] F. Em. Tubbal, R. Raad, K.-W. Chin, and B. Butters, "S-band shorted patch antenna for inter pico satellite communications," *IEEE 8th International Conference on Telecommunication System, Services and Application,* Kuta, Bali, Indonesia, , October 2014, pp. 1-4.

[114] R. W. Ziolkowski, "Design, fabrication, and testing of double negative metamaterials," *IEEE Transactions on Antennas and Propagation,* vol. 51, pp. 1516-1529, Jul. 2003.

[115] S. Chaimool, K. L. Chung, and P. Akkaraekthalin, "Bandwidth and gain enhancement of microstrip patch antennas using reflective metasurface," *IEICE transactions on Communications,* vol. 93, pp. 2496-2503, Oct. 2010.

[116] Y. Yoshimura, "A microstripline slot antenna (short papers)," *IEEE Transactions on Microwave Theory and Techniques,* vol. 20, pp. 760-762, Nov. 1972.

[117] F. Em . Tubbal, R. Raad, K.-W. Chin, and B. Butters, "S-band shorted patch antenna for inter pico satellite communications," *8th International Conference on Telecommunications, Systems, Services and applications (TSSA),* Kuta, Bali, Indonesia Oct. 2014, pp. 1-4.

[118] C. Rakluea, S. Chaimool, P. Rakluea, and P. Akkaraekthalin, "Unidirectional CPW-fed slot antenna using metasurface," *8th International Conference on E Electrical Engineering/Electronics, Computer, Telecommunications and Information Technology. (ECTI-CON),* Khon Kaen, Thailand, May 2011, pp. 184-187.

[119] N. Orr, J. Eyer, B. Larouche, and R. Zee, "Precision formation flight: the CanX-4 and CanX-5 dual nanosatellite mission," *21st Annual AIAA/USU Conference on Small Satellites,* Logan, UT, USA, Aug. 2007, pp. 1-10.

[120] T-K. Wu. *Frequency Selective Surfaces: Wiley online library, 1995.* .

[121] F. EM. Tubbal, R. Raad, and K-W. Chin, "A Wideband F-shaped Patch Antenna for S-band CubeSats Communications " *10th International Conference on Signal Processing and Communication Systems (ICSPCS),* Surfers Paradise, Gold Coast, Australia Dec. 2016.

[122] F. Em . Tubbal, ER. Raad, K-W. Chin, and M. Madni, "Low profile aperture coupled microstrip antenna for inter cubesat communications," *4th International CubeSat Workshop,* London, United kingdom, May 2015, pp. 1-2.

[123] L. Dussopt and J. M. Laheurte, "Parasitic effects of parallel-plate modes in planar antennas fed by conductor-backed coplanar waveguides," IEE National *Conference on Antennas and Propagation,* 1999, pp. 363-366.